VILNIUS UNIVERSITY
NATURE RESEARCH CENTER

VIKTORIJA GRAJEVSKAJA

STUDYING THE MECHANISMS OF CARDIOVASCULAR DEVELOPMENT AND REGENERATION IN DANIO RERIO (HAMILTON, 1822)

Doctoral (PhD) Thesis
Biomedical sciences, zoology (05 B)

Vilnius, 2017

Doctoral thesis was prepared while studing for a PhD at Vilnius University in 2010 - 2014. Dissertation is defended extramurally.

Scientific consultant - dr. Darius Balčiūnas (Temple University, biomedical sciences, biology - 01 B)

List of abrreviations

Ac/Ds - Activator/Dissociation

AER - Apical Ectodermal Ridge

aldh1a2 - aldehyde dehydrogenase 1 family, member A2

ALPM - Anterior Lateral Plate Mesoderm

ANF - Atrial Natriuretic Factor

ASDs - Atrial Septal Defects

AV block - Atrio-Ventricular block

ba - before amputation

ba - branchial arches

BAC - Bacterial Artificial Chromosome

BFP - Blue Fluorescent protein

Bmp - Bone morphogenetic protein

Bmp2 - Bone morphogenetic protein 2

bp - base pair

CHD - Coronary Heart Disease

cHS4 - chicken Hypersensitive Site-4

cmlc2 - cardiac myosin light chain-2

Cre - Cyclization recombination protein

CreER^{T2} - Cyclization recombination protein fused to a triple mutant of the human *Estrogen Receptor, Tamoxifen*-inducible

cx40 - connexin40

cxcl12a - chemokine (C-X-C motif) ligand 12

cxcr4b - chemokine receptor 4b

CRISPR/Cas9 system - Clustered Regularly Interspaced Short Palindromic Repeats/ CRISPR associated protein 9

crygc - crytallin, gamma c

DAPI - 4',6-Diamidino-2-Phenylindole

DMSO - Dimethyl sulfoxide

dlx2 - distal-less homeobox 2

DNA - Deoxyribonucleic Acid

dpa - days post amputation

dpc - days post coitum

dpf - days post fertilization

dpi - days post injury

DTA - Diphtheria Toxin A chain

e - eye

EMS - Ethyl Methanesulfonate

EMT - Epithelial to Mesenchymal Transition

Ensembl - ENS European Molecular Biology Laboratory (genome browser)

ENU - *N*-Ethyl-*N*-nitrosourea

EPDCs - Epicardium-Derived Cells

ESCs - Embryonic Stem cells

Evi-1 – Ectopic viral integration site 1

fb - forebrain

Fgf - Fibroblast growth factor

fli1a - friend leukemia integration 1a

fli1b - friend leukemia integration 1b

fli1b^{tpl50} - *tpl50* mutation in *fli1b* gene

flk1 - fetal liver kinase 1

Flp^{o} - *Flip*, codon optimized

Fn - fibronectin

FRT - Flp Recombinase Recognition Target

FT1 - FLExTrap gene trap

gata-1 - GATA binding protein 1

gata-2 - GATA binding protein 2

gata4 - GATA binding protein 4

gata-X - GATA binding protein X

GFP - Green Fluorescent Protein

h - heart

Hand2 - Heart and neural crest derivatives expressed 2

hb - hindbrain

Hh - Hedgehog

HIF1/2α - Hypoxia-Inducible Factor 1/2-alpha

HOS - Holt Oram Syndrome

hoxa - homeobox a cluster

hoxd - homeobox d cluster

hpf - hours post fertilization

Hsmar1 - Homo sapiens mariner-1

hsp - heatshock

hst - heartstrings

Igf - Insulin-like growth factor

indels - insertions/deletions

INS - chicken β-globin Insulator

iPCR - inverse Polymerase Chain Reaction

ISH - In Situ Hybridization

IVF - In Vitro Fertilization

Jak/Stat - Janus kinase/signal transducers and activators of transcription

loxP - locus of crossing-over X of P1

LMZ - Lateral Marginal Zone

LPM - Lateral Plate Mesoderm

kdrl - kinase insert domain receptor like

MAPK - Mitogen-Activated Protein Kinase

mb - midbrain

Mef2c - Myocyte enhancer factor 2C

ml - mililiters

MLV - Moloney Murine Leukemia Virus

mRFP - monomeric Red Fluorescent Protein

MS222 - Tricane Methanesulfonate

msxB - muscle segment homeobox B

msxC - muscle segment homeobox C

Mzf1 – Myeloid Zinc Finger 1

Nrg1/ Errb2 - Neuregulin/ Erb-b2 receptor tyrosine kinase

nkx2.5 - NK2 homeobox 5

PAM - Protospacer-Adjacent Motif

PBS - Phosphate-Buffered Saline

Pbx1 - Pre-B-cell leukemia transcription factor 1

PCR - Polymerase Chain Reaction

PDGF - Platelet-Derived Growth Factor

pdlim7 - PDZ and LIM domain 7

PFA - Paraformaldehyde

Plk1 - Polo like kinase 1

pre-mRNA - precursor messenger Ribonucleic Acid

polβ - DNA polymerase gene β

poly(A) - polyadenylation sequence

pp(A) - ocean pout antifreeze protein polyadenylation sequence

RA - Retinoic Acid

raldh2 - retinaldehyde dehydrogenase 2

RNA - Ribonucleic Acid

RT PCR - Reverse Transcription Polymerase Chain Reaction

S1 - Switchblade 1

SA - Splice Acceptor

SB - Sleeping Beauty

sc - spinal cord

SD - Splice Donor

sgRNA - single guide RNA

shh - sonic hedgehog

smndc1 – survival motor neuron domain containing 1

Sox-5 - Sex determining region Y-box 5

SSR - Site-Specific Recombinase

TALENs - Transcription Activator-Like Effector Nucleases

TAM - Tamoxifen

TF - Transcription Factor

tbx3a - T-box transcription factor 3a

tbx5a - T-box transcription factor 5a

tbx5a^{hst} - *heartsrings* mutation in *tbx5a* gene

tbx5a^{tpl58} - *tpl58* mutation in *tbx5a* gene

tbx5a^{tpl58R} - revertion of *tpl58* mutation in *tbx5a* gene

tbx18 - T-box transcription factor 18

tcf21 - transcription factor 21

tnc - tenascin-C

Tgfβ - Transforming growth factor β

TILLING - Targeting Induced Local Lesions in Genomes

tnnt2a - troponin T type 2a

tagln - transgelin

UAS - Upstream Activating Sequence

UCSC - University of California, Santa Cruz (genome browser)

VSDs - Ventricular Septal Defects

VSV-G - Vesicular Stomatitis Virus Envelope Glycoprotein

Wnt - Wingless type MMTV integration site family

wt1b - Wilms tumor suppressor gene 1b

YFP - Yellow Fluorescent Protein

Z-CAT - Zebrafish Cardiomyocyte Ablation Transgene

ZFNs - Zinc-Finger Nucleases

ZPA - Zone of Polarizing Activity

zp(A) - zebrafish β-actin transcription termination sequence

4-HT - 4-Hydroxytamoxifen

5’RACE - Rapid Amplification of cDNA Ends

5’UTR - 5’ Untranslated Region

Introduction

Nowadays cardiovascular disease remains a major health issue responsible for human death worldwide. According to the World Health Organization, in 2011, a coronary heart disease (CHD) had killed approximately 7.3 million people all over the world (2013), and the highest death rates have been observed in Asia and Eastern Europe. Unfortunately, Lithuania is ranked as a fourteenth country in the world facing mortality due to cardiac failure. As has been reported by European Cardiovascular Disease Statistics, in 2009, 14,417 Lithuanians had lost their lives because of the coronary heart disease (Roger et al. 2012). In comparison to Lithuania, the United States experiences relatively low mortality rate due to CHD; however, the heart disease still remains a leading cause of the death. Every year about 785,000 Americans are expected to experience a new coronary attack, while about 470,000 people are likely to have a recurrent heart attack (Roger et al. 2012).

Providing cardiac patients with a new heart tissue is a goal of the regenerative cardiology. Importantly, developing strategies and tools for regenerative medicine in the heart is based on the information collected from the model organisms for cardiogenesis and heart regeneration. So far, a significant amount of knowledge has been obtained from research done on the vertebrate animal heart development (Bakkers 2011; Brand 2003; Bruneau 2002; Srivastava et al. 2006). As for the heart regeneration studies, for a long time they were limited due to the lack of a good model system. In 2002, Poss and colleagues have demonstrated that zebrafish is able to regenerate a partially amputated ventricle, and this discovery brought a new prospective to the entire field. Thereafter, other zebrafish cardiac injury methods such as genetic ablation (Wang et al. 2011) and cryoinjury (Gonzales-Rosa et al. 2011; Schnabel et al. 2011; Chablais et al. 2012) have been developed. Although there are plenty of the genetic tools available to study regeneration (reviewed in Gemberling et al. 2013), the lack of adult

zebrafish conditional mutants still remains an important disadvantage of the system, and complicates the analysis of a function of the developmentally essential genes during regeneration. So far, developmentally critical signaling pathways were uncovered to be important for heart regeneration using either an induced transgenic inhibition of dominant-negative proteins (Fgf (Lepilina et al. 2006), RA (Kikuchi et al. 2011), MAPK (Jopling et al. 2012), HIF1/2α (Jopling et al. 2012), Fn (Wang et al. 2013), Jak1/Stat3 (Fang et al. 2013), Igf (Huang et al. 2013), Gata4 (Gupta et al. 2013), Notch (Zhao et al. 2014)) or pharmacological inhibition (Pdgf (Lien et al. 2006), Tgfβ/Activin (Chablais and Jaźwińska 2012), Plk1 (Jopling et al. 2010), Igf (Choi et al. 2013; Huang et al. 2013), Hh (Choi et al. 2013)). However, for further detail analysis more elegant strategies such as conditional manipulations of the gene activity are absolutely necessary.

Research aim:

Use insertional gene trap alleles, *tbx5a*^{tpl58} and *fli1b*^{tpl50}, to study cardiovascular development and regeneration in *Danio rerio* (Hamilton, 1822).

Research objectives:

1. Identify eight insertional gene trap lines in zebrafish.
2. Test regeneration of the blood vessels in *fli1b*^{tpl50} insertional zebrafish mutant.
3. Examine if *-3.3nkx2.5* and *-6.1nkx2.5* promoter regions contain heart-specific enhancers that are active during normal heart development.
4. Check if chicken β-globin insulation sequences can protect transgene from chromosomal position effect in *D. rerio* genome during normal cardiogenesis.
5. Determine if *tbx5a*^{tpl58R} allele can be conditionally re-mutated in embryonic and adult zebrafish heart.

6. Test heart regeneration in conditional *tbx5a*^{tpl58R}*;tnnt2a:CreER*^{T2} mutants.
7. Identify a minimal *tbx5a* cardiac regulatory sequence using deletion analysis.

Thesis statements:

1. Insertional gene trap lines in zebrafish can be effectively identified using inverse PCR and 5'RACE methods.
2. In response to injury, GFP that is driven by endogenous promoter of the insertionally mutated *fli1b*^{tpl50} allele becomes overexpressed in the caudal fin, but regeneration of the blood vessels proceeds normally.
3. Both *-3.3nkx2.5* and *-6.1nkx2.5* promoter regions contain heart-specific enhancers, which activate mRFP expression during normal zebrafish heart development.
4. Chicken β-globin insulator sequences fail to protect *-3.3nkx2.5:RFP /INS* and *-6.1nkx2.5:RFP/INS* transgenes from chromosomal position effect in zebrafish genome during normal cardiogenesis.
5. Administration of 4-hydroxytamoxifen induces a conditional re-mutation of *tbx5a*^{tpl58R} allele in embryonic and adult zebrafish heart.
6. Heart regeneration in conditional *tbx5a*^{tpl58R}*;tnnt2a:CreER*^{T2} mutants is impaired.
7. A minimal 177 bp *tbx5a* enhancer drives a heart-specific mRFP expression in the developing and adult zebrafish.

The novelty and significance of the project

Studies performed during this research project are novel and highly significant for different fields of the biomedical science (for example, zoology, genetics, gene engineering, developmental biology, and regenerative medicine).

Genes mutated in six new insertional genetrap mutant lines were identified. All of them are available to zebrafish research community and can be used to investigate a variety of biological processes. One of the identified gene trap lines (*fli1b*^{tpl50}) that has a mutation in *fli1b* gene was found to exhibit GFP overexpression in vasculature and blood at 7 days after partial amputation of the caudal fin. The observed regrowth proceeded unevenly, but, finally, the regenerated tail appeared normal. These findings provide important information about *fli1b* expression as well as morphological changes in the regrowing caudal fin during first four weeks after injury and can be useful for further regeneration studies of vertebrate vascular system.

For the first time, the functional analysis of chicken β-globin insulation sequences was performed in F1 ire F2 zebrafish embryos. The obtained data provide valuable information for the generation of transgenic constructs. Moreover, a revealed positive effect of the insulators on the transgene expression pattern, intensity and variagation is important for the future investigations of the gene regulation in the eukaryotes. The results of the *-3.3nkx2.5* ire *-6.1nkx2.5* analysis in the developing zebrafish heart are useful for future identification of *nkx2.5* enhancers and repressors in vertebrates during development.

The determined heart specific *tnnt2a:CreER*^{T2} expression provides a new Cre driver that can be used for conditional manipulations of the *loxP*-based recombination events in the developing and adult zebrafish heart. Importantly, the first conditional induction of the mutation was performed in the adult fish. Mutations that can be controlled in a spatial and temporal manner are absolutely necessary to study a role of the developmentally critical genes in the regeneration mechanisms. Moreover, the conditional mutations are very important for determination of the gene secondary functions. The obtained results uncovered for the first time that *tbx5a* gene plays a critical role during zebrafish heart regeneration.

Although many laboratories have demonstrated an importance of *tbx5* in vertebrate development, the regulation of the gene still remains unknown. During this research project, a novel minimal *tbx5a* enhancer that drives mRFP expression in the embryonic and adult zebrafish heart was identified. This finding is an important contribution for the investigation of the *tbx5a* regulatory basics that could help to understand the details and specificities of the regenerative mechanisms in the vertebrate heart.

1. Literature review

1. 1. Zebrafish as a model system to study vertebrate heart development and regeneration

In the last two decades zebrafish became an important model system to study cellular and molecular events underlying normal formation of the vertebrate heart. Zebrafish embryos provide a unique combination of advantages that are important for an investigation of cardiogenesis process. First, due to *ex utero* development and optical transparency of embryos, cardiac formation can be observed and examined through all developmental stages in a living organism. Second, even in the absence of functional heart (weak or no blood circulation), through a mean of passive diffusion oxygen can still reach cells in a small-size embryo meaning that severe heart defects can be detected and analyzed. Third, a large number of progeny makes zebrafish suitable for genetic screens (Streisinger et al. 1981) allowing for identification of the genes essential for normal vertebrate cardiac development. In addition, adult zebrafish is a powerful model system to study vertebrate heart regeneration (Poss et al. 2002).

1. 1. 1. Zebrafish heart formation

The heart is the first organ to form in vertebrate organism. Zebrafish heart development proceeds extremely fast (Stainier 2001). At 20 hours post fertilization (hpf) individual cardiomyocytes begin to contract, and at 22 hpf the regular heart beating is observed (Scott and Yelon, 2010). The blood circulation is being detected from 24 hpf (Scott and Yelon 2010). Importantly, at 2 days post fertilization (dpf) zebrafish developing heart is comparable to 12 days *post coitum* (dpc) mouse embryonic heart as well as 35 days human embryonic heart (Stainier 2001).

In 5 hpf zebrafish embryo, the cardiac progenitors consisting of atrial and ventricular precursors are symmetrically located on the both sides of the lateral marginal zone (LMZ hereafter) (Fig. 1a) (Bakkers 2011). During gastrulation, starting at 6 hpf, due to the convergent extension movements mediated by mesoderm and endoderm collective cell migration and intercalation (reviewed in Tada and Helsenberg 2012), cardiac progenitors from the LMZ are relocated to the anterior lateral plate mesoderm (ALPM hereafter) (Fig. 1b). By 12 hpf three types of cardiac cells are present in ALPM: atrial, ventricular and endocardial precursors. Three hours later, at 15 hpf, atrial and ventricular progenitors start to differentiate resulting in the expansion of myocardium that is critical for later migration (Reiter et al. 2001; Yelon et al. 2000).

Endocardial cells are the first cardiac cells migrating from the ALPM to the midline, and can be found there at 17 hpf (Fig. 1c). Myocardium precursors start moving towards the midline and migrate as a coherent population of cells (Trinh and Stainier 2004). When cardiac cells reach the midline, they fuse forming a disc-like structure (Fig. 1d). The cardiac disk consists of the three layers. The endocardium is situated in the center of the disk and surrounded by ventricular myocytes, while the outside layer of the disk is composed of atrial myocytes.

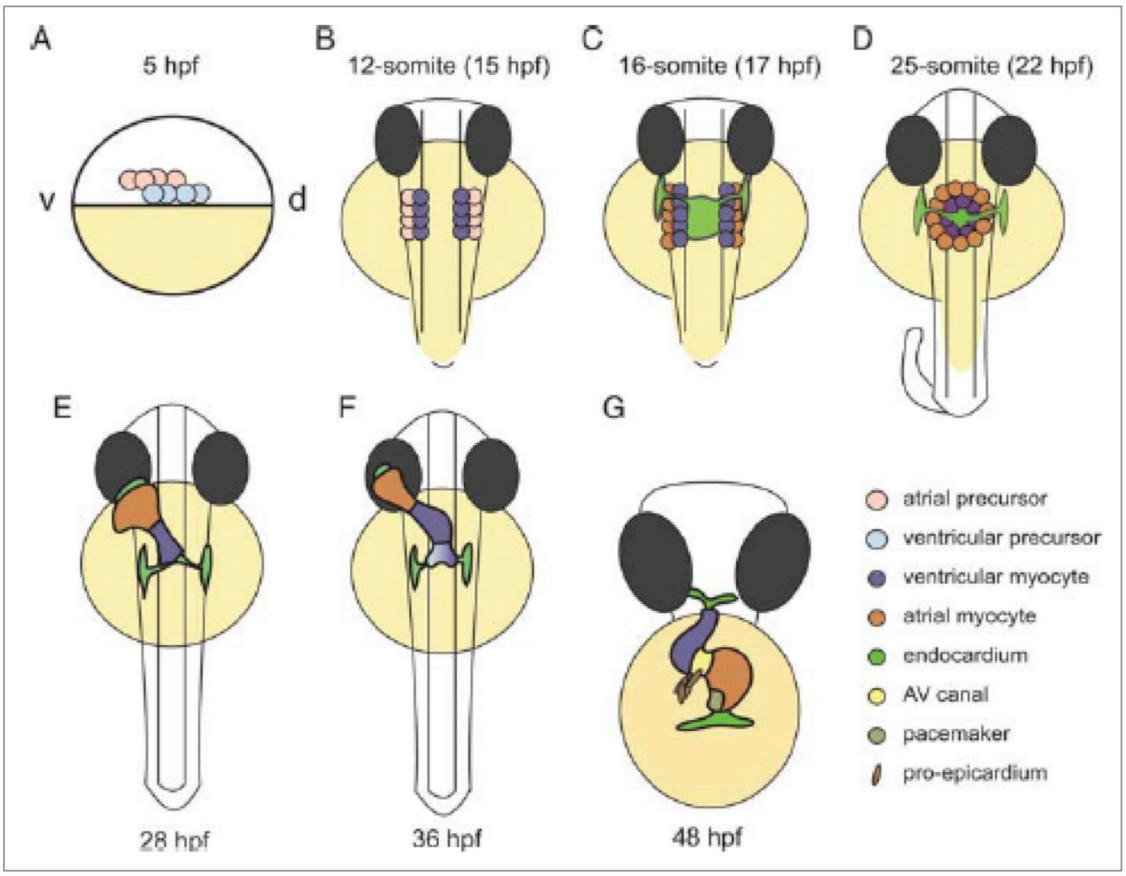

Figure 1. A functional zebrafish heart develops in 2 days (from Bakkers 2011).

During morphogenesis a symmetrical cardiac disk is being transformed into the asymmetrical linear heart tube (Bakkers 2011). The cardiac disk telescopes into a cardiac cone that will elongate to form a heart tube (Stainier 2001). The ventricular part of the heart tube (arterial pole) undergoes assembly first and is formed by 22 hpf, while atrial part is developed by 24 hpf (Fig 2e, 2f). By 28 hpf, a venous pole of the tube is positioned anteriorly to the left, whereas an arterial pole is arranged at the midline (Fig. 1 e). Heart looping starts at 30 hpf (Lohr and Yost 2000) and results in a formation of two cardiac chambers, ventricle and atrium, that are morphologically easily distinguishable by 36 hpf (Fig. 2g).

Endocardial cells located between the two chambers differ morphologically (Beis et al. 2005). These cells receive a signal from myocardium and undergo epithelial to mesenchymal transition (EMT hereafter) (Fig. 3a). Consequently,

endocardial cells migrate into the cardiac jelly (an extracellular matrix between endocardium and myocardium) (Fig. 3b), where they form the endocardial cushions that later will be remodeled into valves (Fig. 3c). By 5 dpf, the heart valves are formed (Hu et al. 2000) and embryonic zebrafish heart exhibits adult heart configuration (Lohr and Yost 2000). However, Martin and Bartman (2009) uncovered two distinct cardiac valve morphogenesis stages in zebrafish larvae: elongation (6 - 16 dpf) and maturation (16 - 28 dpf).

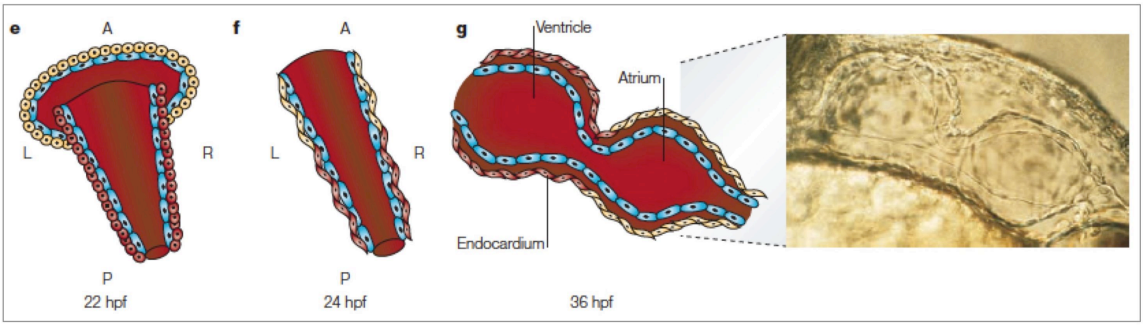

Figure 2. Asymmetrical development of the zebrafish heart tube begins from the formation of the ventricular part of the tube (from Stainier 2001).

The last zebrafish heart layer to form, epicardium, develops from the pro-epicardial organ that is located close to the venous pole (Liu and Stainier 2010; Bakkers 2011). After heart looping is completed, pro-epicardium cells migrate to the heart and form the third and the outermost cardiac layer, epicardium. Some of the epicardial cells undergo EMT, enter the heart and differentiate into coronary vasculature and fibroblasts (Liu and Stainier 2010).

Adult zebrafish heart consists of four compartments: sinus venosus (connected with anterior and posterior cardinal veins, and hepatic portal veins), atrium, ventricle, and bulbus arteriosus (connected with ventral aorta) (Hu et al. 2000). There are three cardiac valves in the mature zebrafish heart: sino-atrial, atrio-ventricular, ventricular-bulbar (Hu et al. 2001; Menke et al. 2011); they ensure the directed circulation and prevent blood backflow.

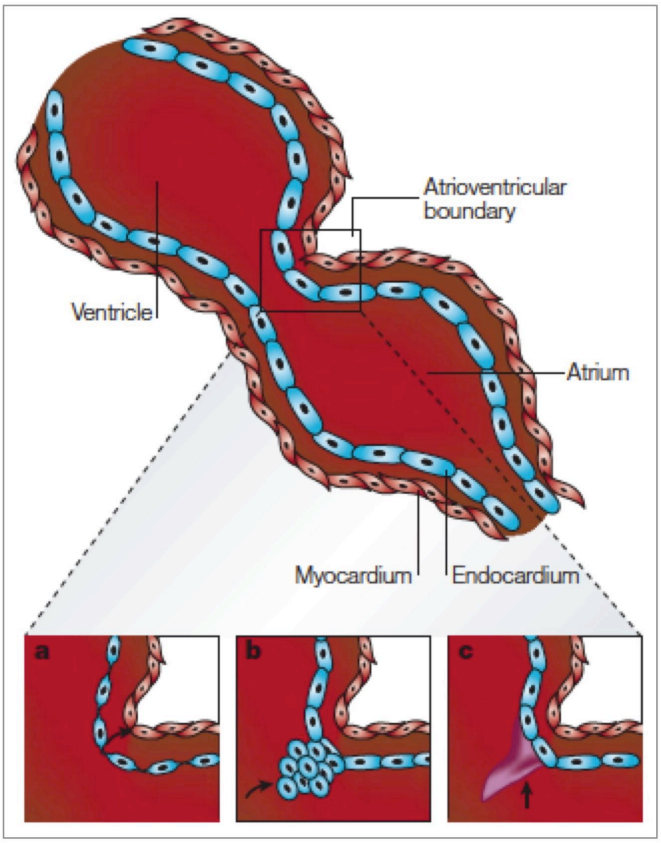

Figure 3. Endocardium cells give rise to the zebrafish heart valves (from Stainier 2001).

The mature atrial as well as ventricular wall is comprised of endocardium, myocardium, and epicardium (Hu et al. 2001). The heart muscle consists of three layers: trabecular, primordial and cortical (Gupta and Poss 2012). The last layer had been recently discovered and was shown to forms at 6 weeks post fertilization from approximately eight cardiomyocytes that originated in the trabecular layer (Gupta and Poss 2012).

1. 1. 2. Zebrafish heart regeneration after different types of injury

Zebrafish is a vertebrate model that even in the adult stage possesses a high regenerative capacity. Upon injury zebrafish regenerate a variety of organs and

tissues such as retina (Bernhardt et al. 1996), optic nerve (Becker and Becker 2002), lateral line (Lopez-Schier and Hudspeth 2006), spinal cord (Becker et al. 1997), liver (Sadler et al. 2007), fins (Johnson and Weston 1995), and the heart (both ventricle and atrium) (Poss et al. 2002; Raya et al. 2003). To study zebrafish cardiac regeneration, heart ventricle can be injured by one of the three established methods: partial ventricular resection (Poss et al. 2002; Raya et al. 2003), cryoinjury (Gonzales-Rosa et al. 2011; Schnabel et al. 2011; Chablais et al. 2011) or genetic ablation (Wang et al. 2011) (Fig. 4). Interestingly, the last technique has been also successfully used to induce tissue damage in the heart atrium (Wang et al. 2011).

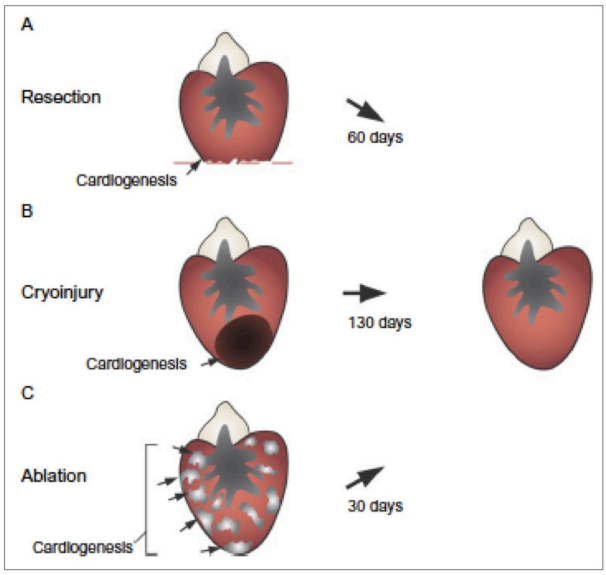

Figure 4. Zebrafish heart regenerates after different types of injury (from Choi and Poss 2012).

During partial resection, a ventricular apex (about 20 % of the heart ventricle) is mechanically removed with small scissors resulting in a short bleeding followed by a blood clot formation (Poss et al. 2002; Raya et al. 2003) (Fig. 5). Cryoinjury technique involves damaging the tip of the cardiac ventricle (approximately 20 %) through an exposure to the cold temperatures, and can be

achieved via physical contact (1-2 s) of the ventricular apex with dry ice (Schnabel et al. 2011) or copper cryoprobe previously immersed in liquid nitrogen (Gonzales-Rosa et al. 2011; Chablais et al. 2011) (Fig. 5). Schnabel and others (2011) performed a comparative analysis of cardiac regeneration after ventricular resection versus cryoinjury and concluded that similar cellular mechanisms underlie regenerative process in response to different type of injury.

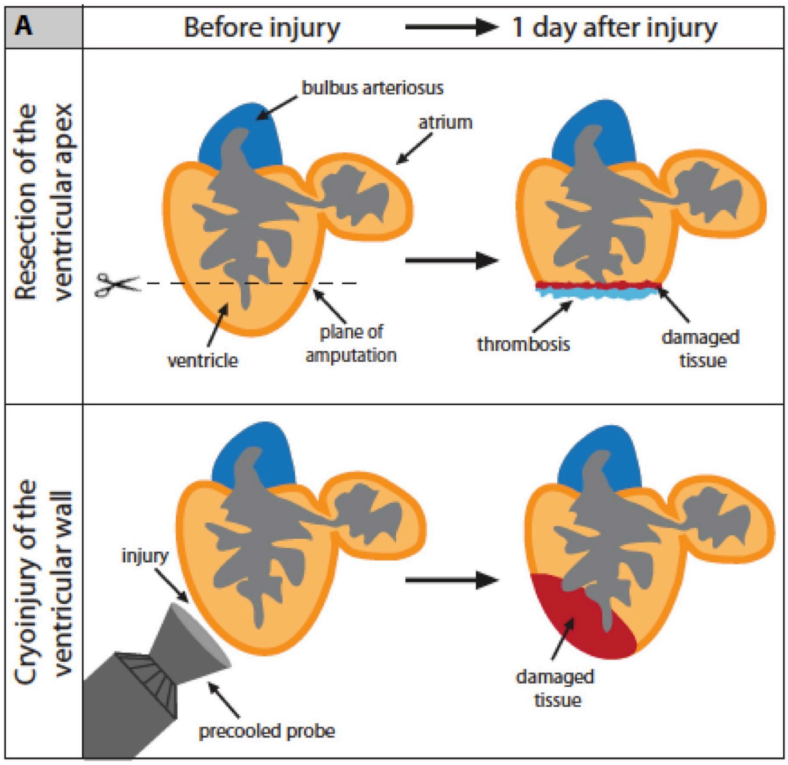

Figure 5. Comparison of two injury methods: ventricular resection and cryoinjury (from Chablais et al. 2011).

In order to genetically ablate cardiac myocardium, Wang and others (2011) have generated a Z-CAT system (zebrafish cardiomyocyte ablation transgene) (Fig. 6), a double transgenic zebrafish line carrying one copy of the cardiomyocyte-specific 4-hydroxytamoxifen inducible Cre driver, *cmlc2:CreER*, and one copy of the reporter construct containing *β-actin* promoter driving *mCherry* and STOP sequences that are flanked with *loxP* sites oriented in the same

direction and followed by diphtheria toxin A chain sequence, DTA. Wang and others (2011) have shown that an intraperitoneal injections of 4-HT induces recombination between *loxP* sites resulting in the deletion of *mCherry* and initiation of the expression of DTA that causes cardiomyocyte-specific death. It was found that adult zebrafish regenerates up to 60% of the ablated cardiac muscle (Wang et al. 2011).

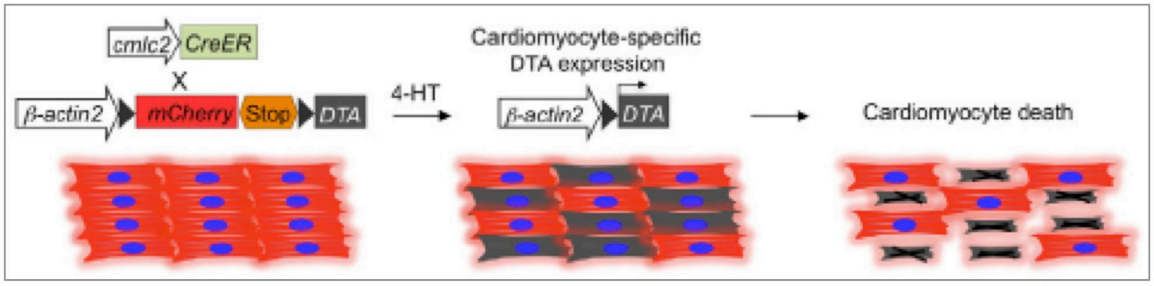

Figure 6. Working principle of cardiomyocyte-specific genetic ablation in adult zebrafish (from Wang et al. 2011).

In adult zebrafish, heart regeneration process was shown to take approximately 1-2.5 months after injury (reviewed in Choi and Poss 2012) (Fig. 4). The shortest time for the completion of ventricular regeneration (30 days) was observed after genetic ablation of the ventricular and atrial cardiomyocytes (Wang et al. 2011), and this can be explained by the fact that only one type of cells was ablated. Meanwhile, a complete ventricular regeneration after partial resection was reported in 30-60 days after injury (Poss et al. 2002; Raya et al. 2003), meaning that it takes twice more time to growth back 20 % of amputated ventricular apex than to restore up to 60 % of all ventricular cardiomyocytes after ablation. In comparison to the ventricles injured by partial resection or genetic ablation, cryoinjured ventricular apex regenerates the longest period of time (60-130 days) (Chablais et al. 2011; Gonzales-Rosa et al. 2011). In case of cryoinjury, longer regeneration time is related to additional step of the necrotic tissues removal that

takes about 3 weeks, and is followed by generating of the scar that subsequently is replaced with new myocardium (Gonzales-Rosa et al. 2011).

1. 1. 3. The cellular and molecular basis of zebrafish cardiac regeneration

A series of studies performed in the past thirteen years have brought a rough chronological sketch for the events occurring during zebrafish cardiac regeneration on both cellular and molecular level. In response to injury, normal zebrafish ventricle undergoes a step-wise regeneration process that consists of the following stages: inflammation, induction of endocardium, activation of epicardium, reparation/remodeling of the damaged area, regeneration of cardiac muscle via proliferation of spared cardiomyocytes, vascularization of the regenerate (Fig. 7).

The initiating stage of the zebrafish heart regeneration was shown to be composed of three main processes that are overlapping in time. First, as any other injury (Martin and Leibovich 2005) ventricular damage triggers an inflammatory response (Chablais et al. 2011). At 1 dpi a cryoinjured part of the ventricle is infiltrated with leukocytes indicating an inflammation (Schnabel et al. 2011). Moreover, a microarray analysis of adult zebrafish ventricles at 3, 7 and 14 days after partial resection revealed that 13 out of 662 differentially expressed genes encoding for the wound response/ inflammatory/anti-inflammatory factors are overexpressed at 3 dpa. This study included 14,900 zebrafish transcripts corresponding to 10,318 genes (Lien et al. 2006). Consistent with microarray results, Wang and others (2011) detected an infiltration of macrophages (3 and 5 dpi) and neutrophils (5 dpi) in zebrafish ventricle after genetic ablation indicating the inflammation.

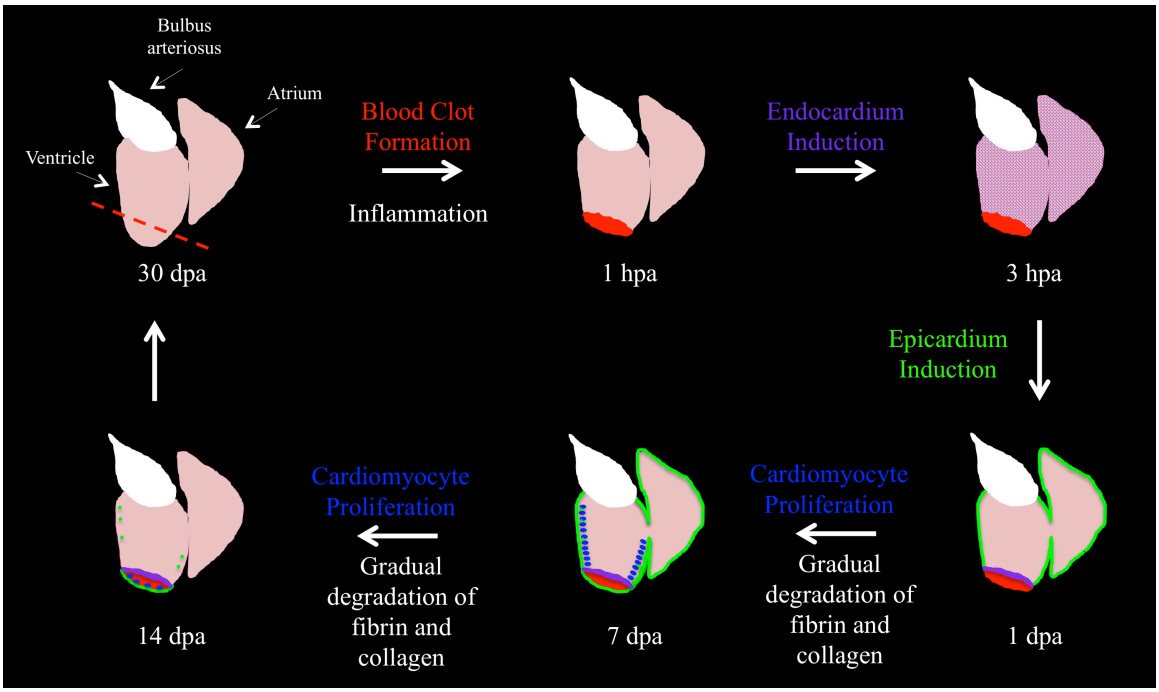

Figure 7. The main stages of adult zebrafish heart regeneration in response to ventricular resection: blood clot formation, inflammation, endocardium induction, epicardium induction, cardiomyocyte proliferation, gradual degradation of fibrin and collagen.

1. 1. 3. 1. An inflammatory response, endocardial and epicardial activation

Another process that was uncovered to proceed early during cardiac regeneration is an induction of endocardium. In response to heart injury and inflammation, RA synthesis is induced in the endocardium (Kikuchi et al. 2011b). At 3 hpa *aldehyde dehydrogenase 1 family, member A2, aldh1a2* (previously called *raldh2*), is expressed in the entire endocardium, and by 1 dpa localizes to the endocardium in the injured area (Kikuchi et al. 2011b).

Another important process occurring during the initiating stage of zebrafish heart regeneration is an induction of outer cardiac layer, epicardium, (Lepilina et al. 2006) which involves an up-regulation of the epicardium-specific embryonic genes. For example, at 3 days post amputation (Lepilina et al. 2006; Lien et al.

2006; Schnabel et al. 2011) as well as post cryoinjury (Schnabel et al. 2011) an epicardium marker *T-box 18* (*tbx18* hereafter) was found to be overexpressed in both atrium and ventricle. Moreover, several research groups (Gonzalez-Rosa et al. 2011; Schnabel et al. 2011) have demonstrated that another epicardium-specific developmental gene, *Wilms tumor suppressor gene 1b* (*wt1b* hereafter), is significantly upregulated at 1-3 days after cryoinjury. Schabel and others (2011) analyzed the epicardium-specific markers expression in both resection and cryoinjury cardiac injury models and concluded that it is comparable.

Induction of the epicardium promotes its expansion (Lepilina et al. 2006) resulting in a full coverage of the injured area. Schnabel and others (2011) discovered that, in contrast to cryoinjured ventricles that are already covered with epicardial cells by 3 dpi, in resected ventricles the wound is completely enclosed within epicardium only by 7 dpa. Expansion of epicardium proceeds due to proliferation (Schnabel et al. 2011) and migration of epicardial cells (Gonzales-Rosa et al. 2012).

In response to ventricular resection as well as cryoinjury, epicardium was shown to proliferate at 3 and 7 dpa/dpi (Schnabel et al. 2011). In case of genetic ablation, epicardial cells proliferation results in a multilayer epicardium at 7 dpi (Wang et al. 2011). Kim and others (2010) found that proliferation of epicardium depends on *Platelet-derived growth factor* (*PDGF* hereafter) signaling pathway. Inhibition of *PDGF* deteriorates proliferation of epicardial cells and results in the loss of epithelial phenotype (Kim et al. 2010).

Gonzales-Rosa and colleagues demonstrated that transplanted *wt1b:GFP+* epicardium-derived cells (EPDCs hereafter) exhibit high migration in the regenerating (cryoinjury) host ventricle and contribute to the expanded epicardium (2012). Interestingly, some *wt1b: GFP+* EPDCs extended protrusions to myocardium or migrated inside the myocardium (Gonzales-Rosa et al. 2012). The Fgf signaling was the first pathway shown to be important in initiating EMT of

epicardial cells into myocardium during zebrafish heart regeneration (Lepilina et al. 2006).

In order to examine the cellular contributions of epicardial cells during zebrafish heart regeneration, Kikuchi and others (2011) analyzed the expression of the transcription factor 21 (*tcf21* hereafter) that, in comparison to previously used markers, *tbx18* and *wt1b,* was found to be more specific to epicardium. During zebrafish heart development as well as regeneration cells expressing *tcf21* were shown to contribute to the formation of perivascular cells and were never detected to give rise to myocardium indicating that *tcf21*-positive epicardial cells are not a source of new cardiomyocytes (Kikuchi et al. 2011). However, there remains a possibility that *tcf21* is not expressed in all epicardial-derived cells (EPDCs hereafter) and thus do not label all epicardium descendants (Gonzales-Rosa et al. 2012). In order to ensure that all EPDCs are labeled, Gonzales-Rosa and others (2012) adapted cell transplantation technique to engraft 3 dpi fluorescent cardiac tissue containing EPDCs into **γ**-irradiated non-fluorescent host heart immediately after cryoinjury. Researchers found that EPDCs contribute to regeneration by differentiating into myofibroblasts and perivascular fibroblasts (Gonzales-Rosa et al. 2012), but not to cardiomyocytes. Thus, obtained data suggest that epicardium is not a source of new cardiomyocytes. Similarly, Gonzales-Rosa and others (2012) did not detected EPDCs differentiation into cardiac muscle cells in the irradiated zebrafish that exhibited compromised proliferation of cardiomyocytes.

To sum up, epicardium was found to play significant roles in cardiac regeneration. Epicardial cells produce paracrine signaling molecules, participate in inflammatory responses, and provide cellular contributions through undergoing EMT and subsequently giving rise to several types of fibroblasts: myofibroblasts and perivascular cells.

1. 1. 3. 2. Reparation of the damaged ventricular apex

The second stage of zebrafish cardiac regeneration is reparation that involves such processes as wound sealing, accumulation of fibroblasts and collagen deposition (Chablais et al. 2011). In case of ventricular resection, a blood clot covering a wound is reorganized into a fibrin clot (Poss et al. 2000; Raya et al. 2003). Similarly, in cryoinjured ventricle a deposition of fibrin was reported (Chablais et al. 2011; Schnabel et al. 2011). In both resected and cryoinjured ventricles, fibroblasts accumulate in the injured area (Chablais et al. 2011; Gonzales-Rosa et al. 2011) and synthesize a structural protein, collagen, that is deposited in the extracellular matrix resulting in a scar formation that functions as a temporary scaffold (Chablais and Jaźwińska 2012). De Preux Charles and others (2016) showed that inflammation is very important for transient scar deposition. According to Gonzales-Rosa and others (2011), resected ventricles exhibit less collagen deposition than cryoinjured at 7 dpa (Gonzales-Rosa et al. 2011). Interestingly, no significant scarring was detected in ventricles after genetic cardiomyocyte ablation (Wang et al. 2011).

Chablais and Jaźwińska (2012) demonstrated that Tgfβ/Activin signaling is essential for collagen deposition in cryoinjured zebrafish heart. The chemical inhibition of Tgfβ/Activin pathway had no effect on fibrin formation, but resulted in the absence of scarring and subsequently lack of cardiac regeneration. Chablais and Jaźwińska (2012) concluded that scar provides a mechanical support for the injured ventricular wall. Disruption of Tgfβ/ Activin signaling was also found to result in the reduction of fibronectin that was detected on the border between healthy and injured myocardium in cryoinjured zebrafish hearts (Chablais and Jaźwińska 2012). Interestingly, fibronectin is known to play an important role in wound healing and exist in two forms: plasma and cellular. Plasma fibronectin contributes to the early repair events: upon injury, circulates in the blood stream and is incorporated into fibrin clots where is involved in clot stabilization, platelet

adhesion, spreading and segregation. Meanwhile, a cellular form of fibronectin is produced in the cells migrating to the clots and functions in the late repair events such as cells adhesion, spreading, proliferation, migration, protein deposition into ECM, growth factor sequestration (reviewed in To and Midwood 2011). Lien and colleagues (2006) found that fibronectin is upregulated in the resected zebrafish ventricle. Wang and others (2013) demonstrated epicardial cells produce fibronectin in response to ventricular injury (resection and genetic ablation), and deposition of this protein in the extracellular matrix is critical for heart regeneration in zebrafish.

1. 1. 3. 3. Regeneration of cardiac muscle via proliferation of spared cardiomyocytes

The third stage of cardiac regenerative process is the actual regeneration that includes a proliferation of the spared cardiomyocytes within the compact layer of the heart myocardium (Poss et al. 2002; Raya et al. 2003; Jopling et al. 2010; Kikuchi et al. 2010; Chablais et al. 2011; Chablais and Jaźwińska 2012; Gonzales-Rosa et al. 2011; Kikuchi et al. 2011; Wang et al. 2011; Schnabel et al. 2011; Gupta et al. 2013; Schindler et al. 2014), an invasion of the new cardiac muscle cells into the infarcted tissue (Chablais et al. 2011; Schnabel et al. 2011; Chablais and Jaźwińska 2012; Itou et al. 2012), and a gradual degradation of the fibrin and collagen (Poss et al. 2002; Chablais et al. 2011; Gonzales-Rosa et al. 2011; Schnabel et al. 2011; Chablais and Jaźwińska 2012). So far, research data suggest that the majority or all new cardiomyocytes are derived from pre-existing ones (Poss et al. 2002; Raya et al. 2003; Jopling et al. 2010; Kikuchi et al. 2010; Chablais et al. 2011; Wang et al. 2011; Kikuchi et al. 2011) that possibly undergo a dedifferentiation resulting in a disorganization of the sarcomeric structures (Jopling et al. 2010; Wang et al. 2011; Jopling et al. 2012) and down-regulation of

sarcomeric genes (Jopling et al. 2010; Sleep et al. 2010) followed by a re-activated expression of the embryonic markers (Lepilina et al. 2006; Schnabel et al. 2011).

In all injury models, the highest proliferation of cardiac muscle cells has been detected at 7 days after damage (Poss et al. 2002; Schanbel et al. 2011; Wang et al. 2011). At this time point, 10-15% of cardiomyocytes were found to be proliferating at the amputation plane of the partially resected ventricles (Poss et al. 2002; Kikuchi et al. 2011). In comparison, 42% of cardiac muscle cells were detected to be proliferating in the whole ventricle after cardiomyocyte-specific genetic ablation at 7 dpi (Wang et al. 2011). Similarly, 43% of atrial muscle cells exhibited proliferation in response to genetic ablation of cardiomyocytes in atrium at 7dpi (Wang et al. 2011). Interestingly, Schnabel and others (2011) reported proliferation of 12% of all ventricular cardiomyocytes in non-lesioned myocardium at 3dpi.

So far, developmental pathways such as Platelet-derived growth factor (PDGF) (Lien et al. 2006), Retinoic acid (RA) (Kikuchi et al. 2011), Hedgehog (Hh) (Choi et al. 2013), Insulin-like growth factor (Igf) (Choi et al. 2013; Huang et al. 2013), Jak1/Stat3 (Fang et al. 2013), Transforming growth factor β (Tgfβ) (Chablais and Jaźwińska 2012; Choi et al. 2013), heart and neural crest derivatives expressed 2 (Hand2) (Schindler et al. 2014), Neuregulin/ erb-b2 receptor tyrosine kinase (Nrg1/ Errb2) (Gemberling et al. 2015), Notch (Zhao et al. 2014) have been shown to positively affect cardiomyocyte proliferation during zebrafish heart regeneration. On the other hand, p38α MAPK activity (Jopling et al. 2012) as well as elevation of miR-133 (Yin et al. 2012) negatively affects proliferation of cardiac muscle cells in regenerating zebrafish ventricle.

The exact source of the mitogens inducing proliferation of spared cardiomyocytes remains to be determined. Recently, Xiao and others (2016) had successfully generated functional zebrafish cardiomyocyte subtypes *in vitro* via differentiation of pluripotent embryonic cells. Currently, research data suggest that cardiac muscle proliferation could potentially be stimulated by epicardium and

endocardium. Eid and other (1992) discovered that culturing cardiomyocytes in the presence of epicardium-derived cells (EPDCs) results in maintaining a cardiomyocyte-specific cell morphology characterized by elongated shape of the cells with longitudinal arrays of myofibrils. Later on, Weeke-Klimp and others (2010) uncovered that EPDCs enhance contraction proliferation, alignment in cellular arrays, mature sarcomeres and contraction of the heart muscle cells. In response to cardiac injury, zebrafish epicardium and endocardium were reported to up-regulate components of developmental pathways that are required for cardiomyocyte proliferation. PDGF, Tgfβ and Hh signaling is reactivated in epicardium (Lien et al. 2006; Kim et al. 2010; Chablais and Jaźwińska 2012; Choi et al. 2013), while RA, Igf, and Notch - in both epicardium and endocardium (Kikuchi et al. 2011; Choi et al. 2013; Huang et al. 2013; Zhao et al. 2014). Interestingly, Kikuchi and colleagues (2011) detected morphological changes of endocardial layer in the area of injury that remained up to 7 dpa.

Proliferating cardiomyocytes were reported to invade the injured part of the ventricle (Chablais et al. 2011; Schnabel et al. 2011; Chablais and Jaźwińska 2012; Itou et al. 2012). Itou and others (2012) found that the migration of cardiomyocytes to the injury area during heart regeneration is controlled independently from proliferation (Itou et al. 2012). Chablais and Jaźwińska (2012) demonstrated that Tgfβ/Activin pathway promotes invasion into post-infracted area of ventricle. A target of Tgfβ/Activin signaling, *tenascin-C (tnc),* that encodes for an extracellular de-adhesive protein Tenascin-C (TNC), was detected in fibroblasts located on the boarder between uninjured myocardium and post-infarct at 7 dpci (Chablais et al. 2011). Schnabel and others (2011) reported that cardiomyocytes begin to invade the lesion as early as 7 dpi, while Chablais and colleagues (2011) observed the protrusions of cardiomyocytes along the TNC expressing fibroblasts at 14 dpci. Thus, data suggest that TNC is one of the molecular modulators controlling the cardiac muscle cells attachments during zebrafish heart regeneration (Chablais et al. 2011). Itou and others (2012) showed

that migration of cardiomyocytes to the site of injury in the partially resected ventricle is required for cardiac regeneration and depends on the expression of *chemokine receptor 4b (cxcr4b)* in cardiomyocytes. Since a ligand for *cxcr4b* receptor, *chemokine (C-X-C motif) ligand 12 a (cxcl12a),* is produced by epicardial cells, epicardium plays an important role in coordinating migration of cardiomyocytes.

While proliferating cardiomyocytes are invading regenerate, fibrin-collagen scaffold accumulated in the extracellular matrix is being gradually degraded (Poss et al. 2002; Chablais et al. 2011; Gonzales-Rosa et al. 2011; Schnabel et al. 2011; Chablais and Jaźwińska 2012). Chablais and colleagues (2011) reported that in cryoinjured ventricle a primary fibrin-based matrix is lysed by 7 dpci, and starting from that time point two distinct layers can be detected: the fibrin layer surrounding a post-infarct, and a scar inside it. The degradation of fibrin layer was observed from 14 dpci resulting in a complete disappearance by 30 dpi (Chablais et al. 2011). In contrast, collagen deposition was finally resolved by 60 dpci (Chablais et al. 2011). According to Gonzales-Rosa and others (2011), scar was completely absent in regenerated heart by 130 dpi. The fastest recovery and resolution of fibrin and collagen was found in resected ventricle (Poss et al. 2002; Raya et al. 2003; Gonzales-Rosa et al. 2011).

1. 1. 3. 4. Vascularization of regenerated myocardium

Another important stage of zebrafish cardiac regeneration is neovascularization of the restored myocardium. Marin-Juez and colleagues (2016) demonstrated that angiogenic sprouting into the injured part of ventricle starts at 15h after cryoinjury, and following revascularization is critical for cardiomyocyte proliferation. Lepilina and others (2006) reported that in response to ventricular resection epicardial cells undergo epithelial-to-mesenchymal transition (EMT), invade the regenerate, and give rise to new vasculature. Overexpression of

embryonic cardiovascular markers such as *fli1a, flk1, hand2* and *gata4* in resected ventricle was detected close to regenerating area at 7 dpa (Lepilina et al. 2006; Kikuchi et al. 2011). A new network of coronary vessels positive for *fli1a* and *flk1* was observed at 14 dpa (Lepilina et al. 2006). Kim and colleagues (2010) detected a significant overexpression of mural cell markers, *sm22αb/transgelin (tagln)* and *α-smooth muscle actin (αSMA)/acta2*, in the fibrin clot at 14 dpa. Later, Kikuchi and others (2011) found that epicardial-derived cells expressing *tcf21* give rise to perivascular cells that support vasculature. So far, Fgf and PDGF signaling pathways were found to be required for formation of coronary vasculature in regenerating zebrafish heart (Lepilina et al. 2006; Kim et al. 2010).

Proliferation in endocardium and coronary blood vessels was detected during cardiac regeneration (Gonzales-Rosa et al. 2011; Schnabel et al. 2011). Gonzales-Rosa and others (2011) found proliferating endothelial throughout the ventricle. This finding suggests that angiogenesis maybe induced in a paracrine manner. No *fli:eGFP*-positive angioblast precursors were detected (Gonzales-Rosa et al. 2011). Invasion of *fli1a: eGFP*-positive vessel sprouts from healthy myocardium into the regenerating area was detected at 3dpi (Gonzales-Rosa et al. 2011). However, transplantation experiments showed that *fli1a: GFP*-positive endothelial cells do not exhibit significant contribution to regenerating host heart. These experimental results suggest that previously observed vascular sprouts towards regenerate are not a main source of coronary blood vessels in regenerating zebrafish heart. Most likely detected vascular sprouts serve as connections between vasculature of non-injured and regenerating area rather than undergo migration and give rise to new vasculature in the regenerate (is not a main resource of coronary vasculature) (Gonzales-Rosa et al. 2012).

1. 1. 4. Does zebrafish heart regeneration recapitulate cardiogenesis?

Developmental signaling pathways such as Fibroblast growth factors (Fgf) (Lepilina et al. 2006; Kikuchi et al. 2010), Retinoic acid (RA) (Kikuchi et al. 2011), Chemokine (Itou et al. 2012), Mitogen-activated protein kinase (MAPK) (Jopling et al. 2012), Hedgehog (Hh), Insulin-like growth factor (Igf) (Choi et al. 2013), Transforming growth factor β (Tgfβ) (Chablais and Jaźwińska 2012; Choi et al. 2013) and Janus kinase/signal transducers and activators of transcription (Jak/Stat) (Fang et al. 2013) were found to be required for zebrafish ventricular regeneration. In addition, developmentally essential cardiac transcription factor GATA binding protein 4, *Gata4*, (Gupta et al. 2013), a microRNA, mir-133 (Yin et al. 2012), and an extracellular matrix protein Fibronectin (Fn) (Wang et al. 2013) were also shown to play a critical role during zebrafish cardiac regeneration. All together, these findings suggest that the genetic program controlling the heart regenerative process in adult zebrafish is similar to if not the same as the genetic program guiding the heart development in zebrafish embryos.

Controversially, Raya and others (2003) reported that zebrafish cardiac regeneration involves a re-activation of the genes that are not expressed in the heart during development, and proposed that regeneration is regulated by a unique genetic program that is different from the developmental. For example, it was found that *Msx* family members, *muscle segment homeobox B (msxB)* and *muscle segment homeobox C (msxC),* are upregulated in cardiomyocytes around the injury site in zebrafish hearts at 3 dpa. Importantly, none of these genes was detected in the uninjured ventricles. Strikingly, the analyzed transcription factors were not expressed in the heart during development (Raya et al. 2003). However, a functional role of Msx genes during heart regeneration was never tested.

Other genes proposed to be unique for zebrafish heart regeneration are the components of Notch signaling pathway (Raya et al. 2003). In response to injury, overexpression of receptor, *notch1b,* and ligand, *deltaC,* was detected in

ventricular endocardium at 1 dpa. In contrast to *msxB* and *msxC,* transcripts of *notch1b* and *deltaC* were also detected in endocardium of uninjured zebrafish ventricle. Recently, Zhao and others (2014) showed that other Notch receptors, *notch1a, notch2* and *notch3* are also expressed in the endocardium and, in addition, in the epicardium of the uninjured adult heart. Moreover, a significant upregulation of *notch1a, notch1b* and *notch2* was observed in the endocardium at 7 dpa. Interestingly, two of these receptors, *notch1a* and *notch2,* were also overexpressed in the epicardium covering the wound at 7 dpa.

Although Notch pathway components are upregulated in the endocardium and epicardium upon injury, the signaling was found to be unessential for the activation of both cardiac layers and the induction of the coronary arteries regeneration in response to ventricular resection (Zhao et al. 2014). Furthermore, Zhao and others (2014) discovered that Notch pathway plays a critical role in cardiomyocyte proliferation; both suppression as well as hyperactivation of the Notch signaling disrupts cardiac regeneration in zebrafish. Zhao and others (2014) findings complement earlier observations of Notch overexpression during heart regeneration described by Raya and others (2003).

However, the hypothesis proposed by Raya and others (2013) suggesting that Notch signaling might be specific to regenerative program, but not to developmental seems to be incorrect because previously Walsh and Stainier (2001) demonstrated that *notch1b* is expressed in the developing zebrafish heart, and by 45 hpf localizes in the enodocardium specifically at the atrio-ventricular boundary. Moreover, later, Milan and colleagues (2006) showed that Notch pathway is essential for the specification of conduction system in zebrafish embryo. Therefore, Notch signaling is rather common than specific module for both regenerative and developmental mechanisms in the zebrafish heart.

To sum up, published data imply that genetic programs similar to the ones regulating cardiogenesis might control heart regeneration; nonetheless, an existence of regeneration-unique mechanisms cannot be excluded. In order to

further understand cellular and molecular mechanisms that guide regeneration, more players need to be uncovered. According to the current findings, developmentally essential genes (mutations result in phenotypes or premature death) are important candidates for being functionally significant during regeneration. So far, the only technique that had successfully been used to test a role of developmental genes during cardiac regeneration in adult zebrafish was a heat-shock inducible dominant-negative approach. However, more elegant methods such as conditional manipulations of the mutations are required to enable a detail functional analysis of the roles of key molecules throughout cardiac regeneration in specific cells and tissues.

1. 2. Classical conditional mutagenesis in a mouse model system

Conditional mutagenesis is an advanced mutagenesis type that allows for a tissue-specific and temporally controlled disruption of a particular gene activity *in vivo*. This powerful technique provides a solution for several extremely important obstacles faced by researchers when studying gene function (Rajewsky et al. 1996). First, function of genes that are essential for development (mutations result in lethal phenotype) can be elucidated. Second, different functions of the same gene that plays roles at several developmental stages and/or in different cell types can be accurately analyzed (avoiding complex phenotypes). Third, somatically acquired diseases can be modeled and studied.

The first conditional mutation in a vertebrate organism was generated by Rajewsky laboratory using mouse model system (Gu et al. 1994). Gu and colleagues created a T cell-specific conditional knockout for *DNA polymerase gene β, polβ,* and demonstrated that conditional inactivation of gene activity on DNA level in specific cell type can be successfully used to avoid a lethal phenotype in vertebrate organism (1994). The developed strategy relied on using a Cre/loxP site-specific recombination system consisting of two main components:

the cyclization recombination protein (Cre) and a pair of two 34 bp length locus of crossing-over X of P1 (loxP) DNA recombination sites. Target sequence was flanked by head-to-tail oriented loxP sites (floxed) and precisely introduced into embryonic stem cells (ESCs) via homologous recombination (Thomas and Capecchi, 1987). This gene targeting technique made mouse an unrivalled vertebrate model system for several decades. According to Kwan review, by 2002, 101 conditional mice alleles for 91 genes have been published.

1. 3. Mutagenesis strategies in zebrafish

Mutagenesis is an extremely powerful genetic technique that is widely used to study gene functions. The principle of mutagenesis process relies on a genetic material being modified in a stable manner. The resulting change in DNA, called a mutation, is transmitted to the next generations (Ennis 2001). Huge efforts invested into the establishment of genetic tools allowing for dissection of vertebrate development brought a variety of mutagenesis techniques that are now available. All mutagenesis methods can be classified into two main categories: forward or reverse genetic approaches. The forward genetics involves a phenotypic analysis as a starting point and aims to uncover a mutated gene that causes the observed phenotype (Solnica-Krezel et al. 1994; Mullins et al. 1994; Gaiano et al. 1996; Amsterdam et al. 1999; Kawakami et al. 2004; Parinov et al. 2004). In contrast, the reverse genetics implicates an analysis of particular gene of interest; therefore, a specific sequence is modified and, subsequently, resulted phenotypes are examined (Wienholds et al. 2002; Doyon et al. 2008; Meng et al. 2008; Huang et al. 2012; Sander et al. 2011; Hwang et al. 2013).

In zebrafish, mutagenesis techniques considered to be the forward genetic approaches include classical chemical mutagenesis, EMS- (Solnica-Krezel et al. 1994) or ENU-induced (Mullins et al. 1994), and insertional mutagenesis, retrovirus- (Gaiano et al. 1996; Amsterdam et al. 1999) or transposon-mediated

(Kawakami et al. 2004; Clark et al. 2004; Parinov et al. 2004). These methods were revolutionizing because for the first time they allowed for uncovering hundreds of novel genes that are essential to form a vertebrate organism. Now the collections of the generated mutants can be used to dissect a functional role of the mutated genes in detail.

For comprehensive analysis of the gene functions, a series of tools allowing for the targeted mutagenesis have been created in the past twelve years. Currently, the reverse genetic approaches available in zebrafish encompass such genetic tools as TILLING (Targeting Induced Local Lesions in Genomes) (Wienholds et al. 2002), ZFNs (Zinc-finger nucleases) (Doyon et al. 2008; Meng et al. 2008), TALENs (Transcription Activator-like Effector Nucleases) (Huang et al. 2012; Sander et al. 2011) and CRISPR/Cas9 system (Clustered Regularly Interspaced Short Palindromic Repeats/ CRISPR associated protein 9) (Hwang et al. 2013; Hruscha et al. 2013; Jao et al. 2013), the last technique being be the most versatile and efficient (Jao et al. 2013). Moreover, in contrast to other reverse genetic approaches, CRISPR/Cas9 system can be successfully used for targeted site-specific insertions of exogenous DNA (Hruscha et al. 2013). For example, site-specific recombinase sequences can be introduced to create conditional alleles in similar manner as being done in mice. The other possibility could be an insertion of phiC31 site into the desired genetic location and introduction of the sophisticated gene trap via site-specific recombination.

To conclude, in the past twenty years, a variety of mutagenesis approaches ranging from random to directed gene modifications were developed. At the same time, zebrafish has been established as an advantageous vertebrate model organism for the genetic experiments. Mutagenesis screens performed in zebrafish resulted in a tremendous amount of information about genetic basis of vertebrate biology. Currently, with the tools available, many efforts are being directed to understand development, disease and regeneration processes in more detail.

1. 3. 1. ENU mutagenesis

ENU induced chemical mutagenesis is a highly efficient method for introducing random point mutations in the eukaryote genome (Russell et al. 1979; Mullins et al. 1994). ENU stands for *N*-ethyl-*N*-nitrosourea ($C_3H_7N_3O_2$) that is an alkylating agent capable to produce DNA lesions predominantly resulting in single-nucleotide substitutions (Mullins et al. 1994). In case of nonsynonymous substitution, either missense or nonsense mutations leading to a codon that codes for different amino acid or a premature stop codon, respectively, can be produced. The missense mutation reduces, abolishes or changes protein activity, while the nonsense mutation prematurely truncates a protein.

The ENU mutagen was successfully used to mutate the genes in the first large-scale genetic screens in vertebrates, and a zebrafish was used as a model organism (Mullins et al. 1994; Driever et al. 1996; Haffter and Nüsslein-Volhard, 1996). In zebrafish, this type of mutagenesis relies on treating of adult male with sublethal dose of the ENU chemical compound. Hereby, the point mutations are being efficiently induced in the premeiotic germ cells, spermatogonia, and that helps to avoid a mosaicism in the F1 generation. According to Mullins and others estimations (1994), approximately 1-3 mutations per gene can be found in 1000 mutagenized haploid genomes. Theoretically, ENU can be used to uncover all genes in the zebrafish genome meaning that the screen is saturated. However, the important limitation of ENU mutagenesis remains a difficulty of mapping the mutations. In contrast, another type of random mutagenesis, an insertional approach, resolves this issue and provides an efficient method for identification of the mutated genes because the mutagenic insert serves as a molecular tag (Gaiano et al. 1996; Kawakami et al. 2004; Clark et al. 2004); nonetheless, the mutagenesis rate is 7-10 times lower than when using the ENU (Mullins et al. 1994; Solnica-Krezel et al. 1994; Driever et al. 1996; Haffter et al. 1996; Amsterdam et al. 2012),

and approximately one out of 80-100 provirus insertions is mutagenic (Amsterdam et al. 1999).

1. 3. 2. Insertional mutagenesis

The principle of the insertional mutagenesis relies on the random introduction into the genome of an exogenous DNA sequence that acts as a mutagen. Based on the techniques used to deliver the mutagen, there are two insertional mutagenesis approaches: retrovirus- (Gaiano et al. 1996; Amsterdam et al. 1999) or transposon-mediated (Kawakami et al. 2004; Clark et al. 2004). In case of the retrovirus-mediated mutagenesis, a pseudotyped retrovirus composed of a Moloney murine leukemia virus (MLV) DNA and a vesicular stomatitis virus envelope glycoprotein (VSV-G) is used to produce random insertions of the mutagenic sequence into the genome. The proviral DNA sequence itself can serve as a mutagen and disrupt normal gene activity by one of the several mechanisms (reviewed in Ranzani et al. 2013).

For example, upon integration of a retrovirus upstream of the endogenous gene, an exogenous enhancer can change normal activity of the gene that is still driven by endogenous promoter. On the other hand, retrovirus can incorporate into the actual promoter sequence resulting in the disconnection of the endogenous gene transcription from the endogenous promoter and placing it under retroviral promoter. Alternatively, retrovirus can integrate into the intron of the gene. In that situation, the upstream endogenous splice donor can be spliced to the internal retroviral splice acceptor. The generated fusion transcript then can be terminated via retroviral poly(A) resulting in a production of a truncated fusion protein. Finally, retrovirus can also hit an exon of the endogenous gene and cause premature termination of the endogenous transcript by the retroviral poly(A) (reviewed in Ranzani et al. 2013).

Although there is a variety of ways how retroviral vectors can disrupt gene activity, the majority of over 500 mutations isolated from a large-scale retrovirus-mediated screen performed in Nancy Hopkins lab (Gaiano et al. 1996; Amsterdam et al. 1999; Golling et al. 2002; Amsterdam and Hopkins 2004; Amsterdam and Hopkins 2006) were generated by using pseudotyped retroviral vectors containing a gene trap because that would provide an additional feature allowing for he analysis of the expression patterns of the mutated genes (Chen et al. 2002; Amsterdam et al. 2003). The gene trap encompasses a splice acceptor followed by an exonic sequence, a splice enhancer, an epitope tag, and a splice donor (Chen et al. 2002). In case of an intronic integration in a sense orietantation, a splice donor of the upstream endogenous exon will splice to a gene trap and then splice out to the downstream exon resulting in a frame shift. Interestingly, a half of the mutations generated with provirus containing gene trap are located in the first intron of the trapped genes suggesting an existence of a bias toward a 5'end of the genes that can be beneficial because may decrease a chance of generating dominant negative alleles. Therefore, a pseudotyped retroviral- mutagenesis is an efficient mutagenesis method that is based on either provirus sequence acting as a mutagen or a delivered gene trap possessing mutagenic features.

Another genetic technique that is successfully used in zebrafish for gene trapping involves a delivery of the gene trap through the transposons that are capable of moving a genetic material via a "copy-paste" transposition mechanism (Kawakami et al. 2004; Clark et al. 2004). In comparison to transposons, the retrovirus-based mutagenesis is more efficient; nonetheless, the mutations caused by retroviruses may be a result of different mutagenesis mechanisms. In addition, retroviruses are not suitable to carry the large size cargos (more than 8 kb) that can be efficiently conveyed by transposons (Balciunas et al. 2006). Therefore, transposons are more likely to be right candidates for the delivery of the large sophisticated next generation gene traps (for example, conditional gene traps) that would provide more tools for the precise functional studies of the trapped genes.

1. 3. 3. Gene trapping with transposons

The ability of the transposons to carry long DNA sequences makes them a unique genetic tool for both transgenesis and mutagenesis (Balciunas et al. 2006). To date, 9 transposons have been demonstrated to work in zebrafish *in vivo* (reviewed in Ni et al. 2008). Some of these transposable elements were identified in fish. For example, a *Tol2* that is the most efficient transposon was discovered as an autonomous element from the medaka fish genome (Kawakami et al. 1998, 2000; Kawakami and Shima 1999). Another transposon active in zebrafish (Davidson et al. 2003) that was also isolated from the fish genome is a *Sleeping Beauty (SB)*. In contrast to *Tol2,* the *SB* has naturally lost its transpositional activity due to accumulated mutations. Interestingly, on the basis of molecular phylogenetic analysis, the *SB* was successfully reconstructed resulting in a restored function (Ivics et al. 1997). Several research groups tested in zebrafish a functionality of the transposons that were previously characterized in the invertebrate species. For example, Raz and others (1998) showed that *Tc3* transposon identified in *Ceanorhabditis elegans* is active in zebrafish germ line. Meanwhile, Fadool and others (1998) demonstrated that *Drosophila melanogaster* transposable element, *mariner,* is also functional in zebrafish and can integrate into the germ cells. Other transposons that were found to be active in zebrafish are *Hsmar1, Tol1, Ac/Ds, Harbinger3-DR,* and *piggyBac* (reviewed in Ni et al. 2008). So far, only two transposons, *SB* (and *SB10*) and *Tol2,* were successfully used for insertional mutagenesis in zebrafish (Clark et al. 2004; Sivasubbu et al. 2006; Song et al. 2012a, 2012b; Kawakami et al. 2004; Asakawa and Kawakami 2009).

The transposon-mediated mutagenesis relies on the insertion of the gene trap that disrupts gene activity. The classical gene trap that is also known as a promoter trap or 5' gene trap usually contains a slice-acceptor, reporter and polyadenylation sequence (poly(A)) (Sivasubbu et al. 2006) (Fig. 8). Upon successful integration of the gene trap into the intron of a gene (in a sense

orientation and correct reading frame), the upstream exons of the gene will be fused with the reporter sequence. In this way, normal spicing of wild type pre-mRNA will be disrupted. In addition, the gene trap poly(A) sequence located downstream of the reporter will prematurely terminate the transcription of the fusion transcript (Sivasubbu et al. 2006). Thus, a 5' end of the gene will be trapped, and a 3' ends will not be expressed. As a result, a fusion protein containing the N-terminus of the wild type protein that is attached to the reporter protein will be produced. This gene trapping approach is very valuable because it allows for a mutation of the gene and analysis of the gene-specific expression pattern to be carried in the same embryo and at the same time. The limitation of this method is inability to select for the mutations in the genes that are not expressed at the time of the screening.

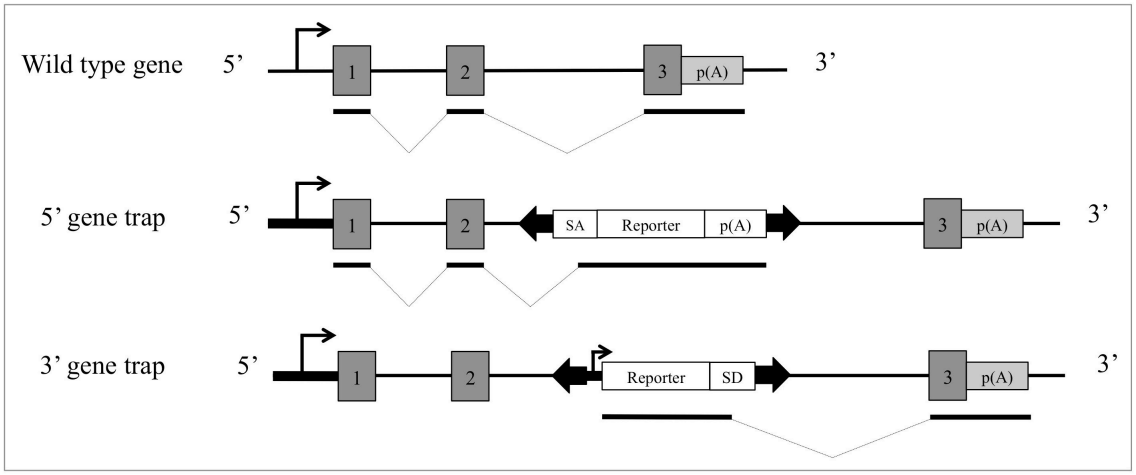

Figure 8. Insertional mutagenesis with 5' and 3' gene traps relies on trapping upstream or downstream exons of the endogenous gene, respectively. The 5' gene trap contains a spice acceptor (SA) that allows for "catching" the upstream exon and formation of reporter fusion transcript that it is terminated by exogenous polyadenylation sequence (p(A)). The 3' gene trap mutagenicity relies on the presence of exogenous splice donor (SD) that permits for formation of reporter fusion transcript with downstream endogenous exons.

There is another gene trapping strategy that allows for the detection of the mutated genes that are not transcriptionally active at the time of the selection. This approach involves a poly(A) trap or a 3' gene trap (Sivasubbu et al. 2006) that usually encompasses a ubiquitous promoter, reporter and splice-donor (Fig. 8). Upon successful intronic integration, a splice donor in the gene trap is spliced to an exogenous splice-acceptor. Thus, a reporter sequence is fused with the downstream exons of the trapped gene, and a transcription of the fusion mRNA is terminated by the endogenous poly(A). The ubiquitous promoter located before the reporter sequence drives the expression of the fusion transcript. A 5' end of the gene is transcribed; however, due to the absence of poly(A) signal the transcript composed of upstream exons is unstable and therefore will be degraded. Meanwhile, a 3' end is trapped and fused to a reporter resulting in a production of a fusion protein consisting of the reporter domain and C-terminus of the wild type protein. Because of the exogenous promoter driving the expression of the fusion transcript, the fusion protein will be constitutively produced. Therefore, genes that are not active during embryonic stages or are active only at specific point during development can still be uncovered.

A "gene-breaking" trap that combines advantages of both 5' and 3' gene traps has been developed (Sivasubbu et al. 2006). The engineered combinational trap consists of the two main cassettes: "mutagenicity" and "gene-finding." In fact, in terms of structure and function, the "mutagenicity" component located at the 5' end of the "gene-breaking" trap represents a classical 5' gene trap. Meanwhile, the "gene-finding" cassette located at the 3' end of the trap structurally represents a poly(A) gene trap, and consists of β-actin promoter driving a reporter sequence, GFP, that is followed by poly(A). However, in contrast to the poly(A) gene trap, the "gene-finding" component functions only as a detection module because the wild type transcript will already has been prematurely terminated by the poly(A) from the "mutagenicity" cassette.

Later, Clark and others (2011) have generated an improved version of a "gene-breaking" transposon – a pGBT-RP2.1 (RP2). A reporter sequence, AUG-less RFP, was introduced into the "mutagenicity" cassette. Furthermore, the whole trap was flanked with *loxP* site-specific recombinase sequences that can be recognized by Cre recombinase resulting in an excision of a gene-breaking transposon from the trapped genetic locus (Clark et al. 2011). This one-step conditional regulation can be used to rescue mutant phenotypes and analyze gene functions in the specific somatic cells or tissues.

1. 3. 4. Generation of the conditional zebrafish alleles

In zebrafish, conditional mutagenesis remains a recent approach. The methodology is constantly being improved via applying different strategies and using different site-specific recombinases. To date, only three research groups have successfully engineered transposon-mediated conditional gene traps and isolated conditional alleles in zebrafish (Clark et al. 2011; Trinh et al. 2011; Ni et al. 2012). Importantly, all conditional manipulations demonstrated were performed at embryonic stages.

In 2011, Clark and colleagues reported the first conditional mutagenesis screen that resulted in a collection of 350 mutant lines. The generated mutations were created using the RP2 vector and can be rescued by two strategies. On the one hand, a temporal inactivation of the RP2 gene trap can be achieved by the early microinjection of the antisense morpholino oligonucleotides targeting a GBT splice acceptor (SA). On the other hand, a permanent excision of the mutagenic cassette can be accomplished via delivery of regular or ligand-inducible Cre recombinase either through the microinjection of mRNA into the embryos or by the expression under the tissue-specific promoter (Clark et al. 2011). The injections of SA morpholino or Cre mRNA enable to turn off a mutation in the whole embryo, while introducing a transgene expressing inducible Cre driven by

the tissue-specific promoter allows for a spatial and temporal permanent rescue of a mutation in the tissue or organ of interest in the embryos or adults. However, in RP2 gene trap lines, mutations cannot be induced after the phenotypic rescue in larvae or adults.

In contrast, two other research groups (Trinh et al. 2011; Ni et al. 2012) have generated conditional gene traps allowing for the induction of the mutation in the trapped alleles. Fraser laboratory (Trinh et al. 2011) engineered a FlipTrap that contains a splice-acceptor followed by a *citrine* fluorescent protein reporter sequence and a splice donor. As a result, upon successful intronic integration, a fusion transcript comprising a full-length wild type transcript that flanks a *citrine* open reading frame (localization depends on the integration site) is made and translated into citrine fusion protein. The locus can be irreversibly mutated via Cre recombinase that induces recombination between heterotypic *loxP* sites resulting in an excision of the *citrine* sequence and an inversion of the *mCherry* cassette followed by poly(A). As a result, the upstream exons of the trapped gene will be fused to the *mCherry* reporter of the FlipTrap, and a truncated mCherry fusion protein produced.

Trinh and colleagues (2011) have isolated 170 FlipTrap lines and tested six of them for conditional manipulations. The trapped loci were successfully mutated in ubiquitous fashion using two strategies: a microinjection of Cre mRNA or an expression of the Cerulean-Cre fusion protein driven by the *β-actin2* promoter. Therefore, the FlipTrap was the first gene trap that has been used to demonstrate a conditional induction of the mutation in zebrafish embryos (Trinh et al. 2011).

Meanwhile, Chen laboratory has adapted a FLEx switch system to create a FLExTrap gene trap (FT1 hereafter) for conditional mutagenesis in zebrafish (Ni et al. 2012). The mutagenic cassette of the FT1 vector contains a splice acceptor followed by *mCherry* fluorescent protein reporter and five tandem copies of poly(A). Upon successful intronic insertion, a fusion transcript encompassing the exons upstream of the integration site fused to *mCherry* reporter sequence is made.

The FT1 mutagenic cassette is flanked by heterotypic *loxP* and *FRT* sites allowing for a stable inversion of the mutagenic sequence via Cre or Flp recombinase, respectively. Therefore, a mutation can be rescued and subsequently induced for the second time.

Ni and colleagues (2012) have generated seven FT1 lines and used one of them to test for conditional regulation. Ubiquitous as well as tissue-specific induction of the mutation was demonstrated in zebrafish embryos. Chen laboratory for the first time has shown that FLEx switch system is effectively functioning in zebrafish and can be employed to generate conditional alleles (Ni et al. 2012).

To summarize, three independent transposon-based gene-trapping strategies have been recently developed and successfully used for zebrafish conditional mutagenesis (Clark et al. 2011; Trinh et al. 2011; Ni et al. 2012). The largest collections of conditional mutants were created with RP2 and FlipTrap vectors Clark et al. 2011; Trinh et al. 2011), while only a pilot screen was run with FT1 trap (Ni et al. 2012). Essentially, all engineered conditional gene traps share several common features. First, the 5' module contains a slice acceptor, reporter sequence and poly(A) serves as mutagen. Second, the site-specific recombinase sites allow for conditional regulation. However, a conditional induction of the mutation can be achieved only with FlipTrap and FT1 traps, and so far was demonstrated only at embryonic stages. Therefore, the next important step in zebrafish conditional mutagenesis would involve mutating a gene in adult tissue or organ of interest.

1. 3. 5. Targeted mutagenesis with CRISPR/Cas9 system

CRISPR/Cas9 system is a relatively novel and highly efficient technique for targeted genome editing that allows for creation of insertions/deletions (indels) and/or insertions of exogenous DNA sequences (Hruscha et al. 2013; Hwang et al. 2013; Jao et al. 2013). The system has been adapted from bacteria immune

response against foreign DNA (Horvath and Barrangou 2010; Wiedenheft et al. 2012). The CRISPR/Ca9 genetic tool includes two main components: a sequence specific single guide RNA (sgRNA) and Cas9 DNA nuclease. Upon entering a nucleus, the sgRNA localizes Cas9 protein to the targeted DNA sequence. Cas9 cleaves both strands of DNA producing a double-strand break that will be repaired either by error-prone non-homologous end joining (insertions or deletions can be introduced into the specific genomic sequences) or homologous recombination (a new genetic information can be inserted into the specific genomic location). Theoretically, CRSIPR/Cas9 technique can be used to create the desired genetic modifications in any eukaryotic organism. The main limitations of the technique remain a possibility of the off-target effects and a requirement for the present of a protospacer-adjacent motif (PAM) downstream of the target sequence (Hruscha et al. 2013; Hwang et al. 2013; Jao et al. 2013).

1. 4. Cardiac-specific Cre drivers for conditional mutagenesis

The Cre/lox-based conditional mutagenesis strategy requires two main components: a "floxed" fragment of targeted gene and a tissue-specific Cre driver (Branda and Dymecki 2004). In order to achieve a successful conditional gene-targeting event, a reliable promoter for Cre recombinase expression is required. Several critical characteristics such as a tissue-specificity, strength, and temporal activity of potential Cre driver need to be considered to ensure that intra-molecular recombination is induced in the cells of interest at particular time (Smith 2011). Recently, several pan-cardiac tamoxifen-inducible Cre drivers have been created and effectively used to study heart regeneration in adult zebrafish (Jopling et al. 2010; Kikuchi et al. 2010, 2011). Three of these driver lines are cardiomyocyte-specific: *cmlc2a-Cre-Ert2* (Jopling et al. 2010), *cmlc2: CreER*, *gata4: ERcreER* (Kikuchi et al. 2010). One line, *tcf21: CreER*, is specific to epicardium (Kikuchi et al. 2011). Moreover, an endocardium- and coronary endothelium-specific

tamoxifen-inducible Cre driver, *kdrl: CreER*, was generated and used to permanently label endothelial cells and study a source of new coronary endothelium in the regenerating zebrafish heart (Zhao et al. 2014). However, none of these lines were available when the research project of this dissertation had started. Therefore, other potential heart-specific promoters were analyzed.

1. 4. 1. *nkx2.5* is a potential cardiac Cre driver for conditional mutagenesis

NK2 homeobox 5, Nkx2.5, is a gene that encodes for an early transcription factor essential for vertebrate heart development and homeostasis (Lyons et al. 1995; Cleaver et al. 1996; Chen and Fishman 1996; Tanaka et al. 1999; Biben et al. 2000; Raya et al. 2003; Wakimoto et al. 2003; Jay et al. 2004; Pashmforoush et al. 2004; Briggs et al. 2008; Targoff et al. 2008; Tu et al. 2009). Mouse was the first vertebrate model organism where *Nkx2.5* expression pattern was examined. In 1993, two research groups (Komuro and Izumo 1993; Lints et al. 1993) published papers describing *Nkx2.5* expression analysis. Both laboratories detected *Nkx2.5* transcripts in the mouse embryos starting from 7.5 days *post coitum* (dpc), an early head-fold stage. Importantly, according to *in vitro* experiments, the onset of *Nkx2.5* expression in differentiating embryonic stem (ES) cells and ES cells-derived embryoid bodies precedes expression of early cardiac markers (Komuro and Izumo 1993; Lints et al. 1993).

Komuro and Izumo (1993) found *Nkx2.5* mRNA specifically in the developing heart myocardium, while Lints and colleagues (1993) also reported expression in other tissues such as pharyngeal floor endoderm, thyroid, spleen primodia, distal part of the developing stomach, lingual myoblasts and differentiated lingual muscles. Later, the similar endogenous expression pattern of the *Nkx2-5* gene was confirmed by analysis of the transgenic mouse embryos that carry bacterial artificial chromosome GFP-*Nkx2-5* (Chi et al. 2003). The major difference from the previous results was the absence of GFP in the tongue, which

can be explained by the existence of specific enhancers outside the tested 120 kb region or by the presence of the inhibitory elements in that sequence (Chi et al. 2003). In adult mouse, *Nkx2.5* is highly expressed in the heart myocardium (Komuro and Izumo 1993; Lints et al. 1993), and weakly – in the tongue and splenic stromal cells (Lints et al. 1993).

Kasahara and others (1998) also examined murine NKX2.5 protein localization. The *NKX2.5* product was present in the heart during all developmental stages and always restricted to the nucleus of the atrial and ventricular cardiomyocytes. Imporatantly, NKX2.5 was not detected in the heart valvular tissue, the endocardium, the epicardium and the coronary vasculature (Kasahara et al. 1998). The similar expression pattern was observed in the adult hearts. Similarly to NKX2.5 mRNA expression data (Lints et al. 1993), besides the cardiac expression, NKX2.5 protein was found localized in the developing tongue, spleen, and distal stomach. In contrast to characterized mRNA expression pattern, NKX2.5 protein was also detected in the cranial skeletal muscles, anterior larynx and liver (Kasahara et al. 1998).

In 1994, Tonissen and colleagues characterized the expression of the frog *XNkx2.5* that is a homolog of murine *Nkx2.5* gene. The first transcripts were detected from an early neurula stage in the presumptive heart mesoderm, and from that time point the *XNkx2.5* remained continuously expressed in the developing heart. However, at later developmental stages cardiac expression decreased and low levels also have appeared in the pharyngeal region and the foregut. Moreover, lower transcript levels were also found in the adult frog heart. Therefore, the *XNkx2.5* expression pattern in the frog is relatively similar to *Nkx2.5* reported in the mouse.

In 1995, Schultheiss and colleagues characterized expression of *cNkx-2.5* in the chick embryo. From the stage 5 *cNkx2.5* mRNA was detected in mesodermal cells that are fated to become myocardium. A year later, another research group (Buchberger et al. 1996) also reported *cNkx2.5* expression the precardiac

mesoderm. According to Buchberger and others (1996), similar to murine *Nkx2.5* and frog *XNkx2.5,* cNKx-2.5 gene is constantly expressed in myocardium of both developing and adult heart. In contrast to the results published by Schultheiss and others (1995), at stage 18 cNKx-2.5 mRNA was also highly abundant in the pharyngeal arches mesenchyme and the anterior intestinal portal (Buchberger et al. 1996). Contrary to the *Nkx2.5* expression described in mice (Lints et al. 1993), in chicken embryos no transcript was detected in the pharyngeal endoderm, thyroid and tongue (Buchberger et al. 1996).

At the same time, two laboratories reported *nkx2.5* expression analysis in zebrafish embryos (Chen and Fishman 1996; Lee et al. 1996). In contrast to other vertebrates studied (Komuro and Izumo 1993; Lints et al. 1993; Tonissen et al. 1994; Buchberger et al. 1996), in zebrafish ubiquitous *nkx2.5* expression was detected before gastrulation (Chen and Fishman 1996). This finding suggests an existence of the maternal contribution of *nkx2.5* transcripts. Meanwhile, the earliest *nkx2.5* expression reported by Breitbart laboratory (Lee et al. 1996) was observed only starting from 5-somite stage (12 hpf) in the cardiac precursors. Interestingly, Chen and Fishman (1996) observed that at the beginning of the gastrulation *nkx2.5* mRNA rapidly becomes restricted to the ventral margin of the zebrafish embryo resulting in a crescent-like shape expression pattern. Importantly, this localization corresponds to the heart precursor cells. As in other vertebrate models analyzed (Komuro and Izumo 1993; Lints et al. 1993; Tonissen et al. 1994; Buchberger et al. 1996), expression of *nkx2.5* continues being expressed during all heart developmental stages in zebrafish (Chen and Fishman, 1996; Lee et al. 1996). In 2003, Raya and colleagues reported that *nkx2.5* is also constantly expressed in adult zebrafish heart.

To conclude, the *nkx2.5* transcription factor is distinguished by its early activity in myocardial precursors that precede many other cardiac markers. These features make the promoter of *nkx2.5* as a potentially useful early pan-myocardial Cre driver that can be used to generate myocardium-specific conditional mutants

or to perform myocardium lineage tracing analysis. However, murine *Nkx2.5* promoter was shown to be complicated and contain multiple regulatory regions that activate or repress gene activity in the specific areas in the heart (Searcy et al. 1998; Reecy et al. 1999). This suggests that most likely a similar complexity of *nkx2.5* promoter exists in other vertebrates. Therefore, in order to use the *nkx2.5* promoter as a pan-cardiac Cre driver, the heart-specific regulatory sequences in a particular model organism need to be characterized.

1. 5. Tbx5 plays a critical role during vertebrate development

T-box transcription factor 5, tbx5, encodes for a key transcriptional regulator that is essential for proper development of the heart and upper limbs in vertebrates (Basson et al. 1997; Li et al. 1997; Horb and Thomsen 1999; Rodriguez- Esteban et al. 1999; Liberatore et al. 2000; Bruneau et al. 2001; Ahn et al. 2002; Garrity et al. 2002; Agarwal et al. 2003; Rallis et al. 2003; Takeuchi et al. 2003a, 2003b). As other members of the T-box gene family, Tbx5 contains a T-box DNA binding and dimerization domain that consists of 180 amino acids residues (Müller and Herrmann 1997) and is highly conserved among vertebrates. In humans, mutations in a single copy of *TBX5* gene result in a Holt-Oram Syndrome (HOS) (Basson et al. 1997; Li et al. 1997) that is an autosomal dominant disorder characterized by congenital cardiac defects and skeletal malformations of the upper limbs (Holt and Oram 1960; Gall et al. 1966; Poznanski et al. 1970). HOS is a relatively rare inherited cardiac disease, occurring in an estimate of one per 100,000 live births (Basson et al. 1997). The de novo *TBX5* mutations had also been reported (Dreßen et al. 2016). Moreover, the reported incidence rate is expected to be higher because it was discovered that somatic mutations of *TBX5* in the developing heart could also cause congenital cardiac septum malformations (Reamon-Buettner and Borlak 2004). It is possible

that other tissues where *TBX5* is expressed might also be affected due to somatic mutations.

1. 5. 1. *tbx5* expression pattern is conserved among vertebrates

Li and colleagues examined *TBX5* mRNA expression pattern in the normal human embryo (1997). At 26 days of gestation transcripts were detected in the primitive atria and sinus venosus of the heart, while at 33 days *TBX5* was also expressed in the buds of the developing forelimbs. Later, in 44 days embryos, *TBX5* mRNA was found in the heart atria and atrial septa, coronary sinus, atrio-ventricular endocardial cushions, and ventricles. In addition, *TBX5* transcripts were also detected in the extra-cardiac tissues such as an anterior thoracic wall, trachea and retina. Later, another research group performed a detailed analysis of TBX5 protein expression in both developing and adult human heart (Hatcher et al. 2000). TBX5 transcription factor was found in all three cardiac layers: the epicardium, myocardium (in the nuclei of all four chambers), and endocardium (only in the left ventricle) (Hatcher et al. 2000). Importantly, the described *TBX5* expression pattern on both mRNA and protein level corresponds to the tissues affected in the patients with HOS.

Expression pattern of *TBX5* orthologs was also studied in different model organisms. In 1996, Chapman and colleagues reported *Tbx5* mRNA localization in the mouse embryo. Transcripts were detected in the allantois (7.5 – 8.5 dpc), sinus venosus (from 8.5 dpc), optic vesicle (at 9.5 dpc), forelimb bud (from 9.5 dpc), and genital papilla (from 11.5 dpc) (Chapman et al. 1996). Moreover, by 12 dpc *Tbx5* mRNA was found in the dorsal region of the neural retina, mesenchyme of the mandibular arch, the lung, mesenchyme surrounding the trachea, the body wall of the thorax overlying cardiac tissues, and in the heart (Chapman et al. 1996). Later, Seidman laboratory performed a thorough analysis of the *Tbx5* expression in the developing murine heart (Bruneau et al. 1999). *Tbx5* mRNA was detected in

the epicardium, sinus venosus, both left and right atrium, left ventricle, and atrio-ventricular valves (Bruneau et al. 1999).

In 1998, several research groups reported an expression pattern of the chick *Tbx-5* gene (Gibson-Brown et al.; Isaac et al.; Ohuchi et al.). The first transcripts of *Tbx-5* were detected from stage 12/13 and were localized in the heart and presumptive wing mesoderm. Interestingly, later a transient *Tbx-5* expression was found in the flank region mesenchyme and the dorsal part of the eye (Gibson-Brown et al. 1998; Isaac et al. 1998; Ohuchi et al. 1998), and was absent at stage 25 (Isaac et al.1998). In contrast, *Tbx-5* remained constantly expressed in the heart and mesoderm of the wing bud (Gibson-Brown et al. 1998; Isaac et al. 1998; Logan et al. 1998; Ohuchi et al. 1998). No *Tbx-5* expression was detected in the apical ectodermal ridge (AER) and ectoderm (Isaac et al. 1998). In addition, Ohuchi and others (1998) reported *Tbx-5* expression in the lung and tracheal mesenchyme at stage 23. Furthermore, Gibson-Brown and others (1998) also detected mRNA expression in the notochord and genital papilla starting from stage 26.

Several laboratories performed a thorough analysis of *cTbx5a* expression dynamics during chick cardiogenesis. Bruneau and colleagues (1999) found that, similarly to mouse, *cTbx5a* mRNA is present in a posterior to an anterior gradient in the developing chick heart. However, in contrast to mouse, *cTbx5a* was also expressed in the right ventricle (Gibson-Brown et al. 1998; Bruneau et al. 1999). After the heart looping, *cTbx5a* was progressively down-regulated in the right ventricle (Gibson-Brown et al. 1998), and from stage 20 cardiac expression pattern resembled the one observed in the developing murine heart (Bruneau et al. 1999). When skeletal elements of the forelimb are starting to form, *cTbx5* is differentially expressed in the forelimb mesenchyme (Logan et al. 1998). At stage 29, the lowest levels of *cTbx5* were observed in the proximal part of the forelimb, while the highest expression was detected between the developing digits (Logan et al. 1998).

The expression pattern of *Tbx5* had also been studied in lower vertebrates, such as frog and zebrafish. In 1999, Horb and Thomsen reported a detailed analysis of *XTbx5* during the development of the frog embryo. The first heart-specific transcripts were detected at the mid-neurula, stage 17, in the bilateral populations of cells corresponding to the cardiac precursors (in the anterior lateral plate mesoderm). The continuous expression in the pre-cardiac mesoderm was observed throughout the migration of the cardiac progenitor fields and their fusion at the midline. *XTbx5* activity was also detected during the later stages of the heart tube formation such as looping and morphogenesis. At stages 35 and 40, *XTbx5* transcripts were detected in the ventricle (endocardium, myocardium, and epicardium), atrium and sinus venosus. No expression was found in the bulbus cordis. Besides cardiac expression, Horb and Thomsen (1999) also detected *XTbx5* transcripts in the dorsal region of the developing eye starting from tail-bud stage 20. Interestingly, by stage 35 the expression became restricted to the retinal stem cell population of the ciliary marginal zone (CMZ).

In 1999, Belmonte's group reported *tbx5a* expression in zebrafish embryos (Tamura et al. 1999). Transcripts were detected in the developing eye specifically in the dorsal optic cup. In addition, *tbx5a* expression was also found in the mesenchyme of pectoral fin buds, at both early and later developmental stages (Tamura et al. 1999). Similarly to Tamura and others (1999), Begemann and Ingham (2000), has also detected *tbx5a* expression in the developing zebrafish eye and pectoral fins. First transcripts were found at 6-7-somite stages in the optic precursors, and later, at 15-20-somite stage *tbx5a* expression was restricted to the posterior part of the neural retina (Begemann and Ingham (2000). Expression was detected in the neuroepithelium at 24 and 36 hpf, and was lost by 48 hpf.

At 6-7-somite stages *tbx5a* is bilaterally expressed in the later plate mesoderm. The expression regions appear in the form of two bilateral stripes (Begemann and Ingham (2000). Cells located in the anterior part of *tbx5a*-expressing stripes contribute to the early cardiac fields, while cells situated in the

posterior regions contribute to the pectoral fin bud. *Tbx5a* remains constantly expressed during cardiogenesis. By 30 hpf, strong expression was detected in the atrium and weaker – in the sinus venosus (Begemann and Ingham (2000). At all stages of the pectoral fin development *tbx5a* expression was restricted to the mesenchyme, and has never been detected in the epidermis (Begemann and Ingham (2000). At 48 hpf *tbx5a* was unevenly expressed in the pectoral fin bud. The strongest *tbx5a* expression was observed in the distal region of the bud, while the weakest expression was located in the proximo-central part. At 3 dpf *tbx5a* expression is uniform. Interestingly, at 5 dpf *tbx5a* is inhibited in the central region of the pectoral fin bud, but remains highly expressed in the mesenchyme of the dorso-ventral boundary (Begemann and Ingham (2000).

In 2010, Albalat and colleagues identified a novel *tbx5a* gene in zebrafish, *tbx5b*. The developmental expression pattern of a characterized paralog of *tbx5a* was detected in the eye and heart of zebrafish embryos. Interestingly, in contrast to *tbx5a,* no expression of *tbx5b* was found in the pectoral fins (Albalat et al. 2010). However, later *in situ hybridization (ISH)* studies demonstrated an existence of a weak Tbx5b protein signal in the developing pectoral fins at 36 hpf (Parrie et al. 2013). According to Albalat and others (2010), the earliest eye-specific *tbx5b* expression was observed at 14 hpf. Meanwhile, the earliest heart-specific signal of *tbx5b* was detected in the bilateral stripes of the lateral plate mesoderm (LPM) at 17 hpf. Moreover, the *in situ* data revealed that both *tbx5* genes exhibit different expression patterns that are partially overlapping. At 18 hpf, *tbx5a* showed broader expression pattern (in both rostral and caudal subsets of cells) as compared to *tbx5b* (only rostral subset of cells). Similarly to *tbx5a,* 27 hpf zebrafish embryos exhibited a posterior-to-anterior gradient of *tbx5b*. From 36 hpf a localization of *tbx5a* and *tbx5b* transcripts in the heart became dissimilar. The former was expressed in both atrial and ventricular regions, and atrioventricular junction, while the later was restricted only to ventricular area (Albalat et al. 2010).

1. 5. 2. *tbx5* function is conserved among vertebrates

In patients with HOS, the upper limb phenotype is fully penetrant, with the left hand being more often affected than the right (Newbury-Ecob et al. 1996). Strikingly, the defects range from minor thumb malformations to shoulder reductions (Holt and Oram 1960; Gall et al. 1996; Newbury-Ecob et al. 1996) or an emergence of the additional carpal bones (Poznanski et al. 1970). As for cardiac phenotypes, the reported penetrance is 95% (Newbury-Ecob et al. 1996). Similar to the upper limbs defects, the severity of the heart malformations varies. The predominant phenotypes are atrial septal defects (ASDs), ventricular septal defects (VSDs), and atrio-ventricular (AV) block (Holt and Oram 1960; Poznanski et al. 1970; Gall et al. 1996; Newbury-Ecob et al. 1996; Basson et al. 1999). Interestingly, several researchers noticed that severity of the phenotype caused by exactly the same mutation increases in the next generations (Newbury-Ecob et al. 1996; Fan et al. 2003b).

In 1999, Basson and others examined clinical data of patients with HOS carrying different *TBX5* mutations and found a correlation between a position of the missense mutations in T-box sequence and clinical phenotype. Amino acid change in the N-terminal part of the T-box domain that interacts with the major groove of the target DNA results in severe cardiac defects, while amino acid alterations in the C-terminal region that binds the minor groove of the target DNA lead to significant forelimb abnormalities. Fan and others (2003a) divided missense mutations in T-box domain of *TBX5* gene into two groups. The first group disrupts the T-box binding to the DNA resulting in the loss of *TBX5* transcriptional activation as well as interactions of TBX5 with Nkx2.5. The second group have no or only medium effect on the T-box and DNA interactions, and, therefore, causing reduction in a synergy between TBX5 and Nkx2.5. Fan and others (2003a) performed a functional analysis of seven missense mutations located in different exons of *TBX5* gene and uncovered three mechanisms that can

be impaired in HOS patients: TBX5 DNA binding and transcriptional activation, TBX5 interaction with Nkx2.5, TBX5 nuclear localization. Basson and others (1999) also proposed that phenotypic variation between HOS patients carrying the same mutation in *TBX5* could be explained by the fact that TBX5 binds DNA as a dimer. Therefore, in individuals heterozygous for the mutations three combinations of dimers can be formed: mutant/ wild type, mutant/ mutant, wild type/ wild type. Another explanation of why HOS patients carrying an identical mutation in *TBX5* exhibit phenotypic variation is the fact that TBX5 protein is a part of a complex regulatory network (D'Aurizio et al. 2016).

The further analysis of the molecular basis underlying the defects observed in human patients with HOS was performed using model organisms. Frog embryo was the first model system in which the loss of function of *Tbx5* was analyzed. In 1999, Horb and Thomsen generated a hormone-inducible dominant-negative repressor of XTbx5. The C-terminal region of XTbx5 was replaced with Drosophila Engrailed transcriptional repressor domain and fused with a glucocorticoid receptor hormone-binding domain. Inhibition of endogenous XTbx5 activity using a dexamethasone-inducible repressor version resulted in either reduced heart or heartless phenotypes that can be rescued by expression of hormone-inducible form of wild-type XTbx5.

Brown and colleagues (2005) performed injections of morpholino against frog *Tbx5* 5'UTR and translation start site. *XTbx5* morphants exhibited pericardial edema, a reduced and un-looped heart, decreased cardiac cell number, no circulation, and abnormal eyes. Brown and others (2005) found that cardiac precursors were specified normally, and their migration was not affected. Moreover, terminal differentiation of cardiomyocytes was normal. Later, Herman and colleagues (2011) discovered that Tbx5 overexpression, in frog embryos as well as in the murine cells, speeds up a terminal differentiation of cardiomyocytes, increase proliferation of cardiac cells, and results in up-regulation of *Nkx2.5, Mef2c, Bmp2,* and endogenous *Tbx5*.

Bruneau and colleagues (2001) generated a mouse model for Holt-Oram Syndrome. The reported death rate in perinatal mice heterozygous knockout (exon3 of *Tbx5* removed) ranged between 10 and 60 %, depending on the genetic background. *Tbx5* heterozygous knockout newborn mice and adults exhibited forelimb phenotype such as phalangeal segment elongation in the digit I and hypoplastic falciformis. The detected cardiac phenotypes included enlarged atria and misshapen (round) ventricles and atrial septal defects (ASDs) (anterior part of the septum was affected) (Bruneau et al. 2001).

Bruneau and others (2001) discovered that haploinsuficiency of *Tbx5* results in the reduction of *atrial natriuretic factor (ANF)* and *connexin40 (cx40)* transcription. Tbx5 synergistically interacts with Nkx2.5 and that cooperation results in an activation of *ANF* and *cx40* promoters. In *Tbx5* heterozygous knockout, *cx40* expression was absent in the developing heart and reduced by 90% in adult heart atria. *ANF* transcript level in embryonic hearts was 50% lower than in wild types. In adult *Tbx5* heterozygous *ANF* cardiac expression level was comparable to the wild type siblings (Bruneau et al. 2001).

In *Tbx5* homozygous knockout embryos, development of all three cardiac layers has been initiated (Bruneau et al. 2001). Nevertheless, linear heart exhibited hypoplastic atria and inflow tract at E8.5. Later, heart did not undergo looping and an atrio-ventricular cushion was not formed. At E9.5 stage, instead of two atria, only one (left) atrium was present. Reduction in *MLC2v, Irx4, Hey2, Nkx2.5, Gata4, ANF,* and *cx40* expression was detected at E8 – 9 stages. The development of homozygous embryos appeared to be arrested at E9, and no embryos survived past E10.5 stage (Bruneau et al. 2001). Agarwal and others (2003) found that *Tbx5a* homozygous knockout embryos lack forelimb buds at E9.5. Importantly, the establishment and patterning of the limb field was not affected (Agarwal et al. 2003). Rallis and colleagues (2003) generated a conditional homozygous knockout and showed that *Tbx5* is required for early development of a forelimb bud.

Several laboratories took advantages of a chicken model organism to study a role of *Tbx5* in vertebrate embryogenesis. It was found that transplantation of wing grafts expressing *Tbx5* into the trunk and leg results in a development of wing-like features (Gibson-Brown et al. 1998b; Isaac et al. 1998; Logan et al. 1998; Ohuchi et al. 1998). Rodriguez-Esteban and colleagues (1999) showed that Tbx5 is a critical regulator of forelimb outgrowth in chick embryo and forms a regulatory loop with Fgf, Wnt and Bmp signaling pathways (Rodriguez-Esteban et al. 1999). Later, Takeuchi and others (2003a) demonstrated that a misexpression of a dominant-negative Tbx5 protein in the prospective wing field causes repression of Wnt and Fgf pathways resulting in a wingless phenotype. At the same time, misexpression of *Tbx5* in the flank induced Wnt and Fgf signaling resulting in a formation of an ectopic wing (Takeuchi et al. 2003a). Importantly, misexpression experiments in the hearts of chicken embryos revealed that *Tbx5* is essential for ventricular septum formation (Takeuchi et al. 2003b). When *Tbx5* was misexpressed ubiquitously, only a single ventricle formed. When a small area of the ventricle was missing expression of *Tbx5*, this region developed into small right ventricle (Takeuchi et al. 2003b).

Zebrafish was another model organism used to uncover a role of *tbx5* in vertebrate development. In 2002, Ahn and colleagues reported that zebrafish *tbx5* morphants completely lack pectoral fin buds. Since *tbx5* is expressed in the lateral plate mesoderm before the emergence of the pectoral fin buds that suggested its important role during the early forelimb developmental stages such as forelimb field specification and/or forelimb induction (Ahn et al. 2002). In order to determine what stages of pectoral fin development are affected in the absence of *tbx5* activity, Ahn and others (2002) analyzed expression of several markers. It was found that the apical ectoderm ridge (AER) (marker – *dlx2*) is not formed and the zone of polarizing activity (ZPA) (marker - *shh*) is not specified in the fin bud of the zebrafish morphants (Ahn et al. 2002). Furthermore, an activity of the fin-specific genes such as *hoxa* and *hoxd* was not detected.

Ahn and colleagues (2002) found that *tbx5* zebrafish morphants exhibit abnormal migration of lateral plate mesodermal cells; instead of forming a cluster, *tbx5a*-expressing cells were dispersed over the pectoral fin field. Importantly, pectoral fin development was rescued by transplantation of wild-type cells into anterior-lateral plate region of *tbx5* morphants. Based on these results, Ahn and others (2002) concluded that *tbx5* functions autonomously to allow for mesenchymal cell movement and condensation resulting in the formation of a pectoral fin bud in zebrafish embryos. Interestingly, injections of lower concentration of *tbx5* morpholino produced a dose-dependent series of pectoral fin phenotypes. This finding suggests that, similarly as in humans (Basson et al. 1999) and mice (Bruneau et al. 2001), zebrafish *tbx5* is a haploinsufficient gene (Ahn et al. 2002). Besides pectoral fin phenotype, *tbx5* morphants showed cardiac defects caused by incomplete looping of the heart. In contrast to wild type larvae in which atrium is positioned dorsally to the ventricle, in 5 dpf *tbx5* morphants both chambers were positioned on the same dorso-ventral level (Ahn et al. 2002). However, in contrast to cardiac looping phenotypes due to *tbx5* deficiency described in mice (Bruneau et al. 2001), the observed heart defect was relatively mild.

At the same time as *tbx5* morpholino phenotype in zebrafish was reported (Ahn et al. 2002), a recessive *tbx5a* mutation isolated in ENU screen was published (Garrity et al. 2002). A *heartstrings (hst)* mutation produced a premature stop codon downstream of T-box DNA binding domain. In comparison to *tbx5* morphants, *hst* homozygotes exhibit more drastic cardiac phenotype and completely lack pectoral fins. Hearts of homozygous *hst* embryos exhibit normal morphology by 24 - 26 hpf. However, at 3 dpf severe cardiac defects can be observed. The severity of the phenotypes varies from not completely looped to absolutely linear heart (Garrity et al. 2002).

Later studies of both *tbx5* paralogs revealed that they have independent functions in zebrafish cardiogenesis and pectoral fin formation (Parrie et al. 2013).

In contrast to *tbx5a*^{hst} mutants, embryos injected with *tbx5b* morpholino showed unaltered expression of cardiac markers, *nppa* and *bmp4*. However, similary to *tbx5a*^{hst} mutants, *tbx5b* morphants displayed abnormal expression of cardiac differentiation markers such as *hand2* and *versican*. Moreover, gene expression analysis of six targets (*tbx5a, tbx5b, nppa, bmp4, hey2, tbx2b*) via qPCR uncovered that gene regulation profiles of both *tbx5* paralogs do not overlap. In addition, it was showed that injections of *tbx5a* and *tbx5b* mRNA partially rescued the cognate cardiac and pectoral fin phenotypes; however, they failed to rescue the paralogous cardiac and pectoral fin defects. Parrie and others (2013) also found that pectoral fin initiation in *tbx5b* morphants is delayed, while pectoral fin outgrowth and patterning is affected.

Chiavacci and others (2012) showed that cardiac defects caused by *tbx5* overexpression in zebrafish can be rescued via down-regulation of Tbx5-modulated microRNA, *miR-218*. Later studies revealed that Tbx5a overexpression significantly increases expression level of five microRNAs: miR-219, miR-190b, miR-19a, miR-7a, miR-7b (Chiavacci et al. 2015). Moreover, both gain and loss of function experiments uncovered that change in Tbx5 expression modulates miR-17-92 cluster, which contains miR-19a. It was demonstrated that miR-19a can partially rescue cardiac and pectoral fin phenotypes in embryos injected with Tbx5 morpholino (Chiavacci et al. 2015).

1. 6. A potential role of Tbx5a in vertebrate heart regeneration

According to published data discussed in the section (1.5.2.), *tbx5a* is absolutely required for vertebrate heart development. Consistent with information previously discussed in section (1.1.4.), genes essential for development are highly expected to be important for regeneration. Therefore, *tbx5a* potentially might play a significant role in zebrafish cardiac regeneration. In addition, several recent studies on stem cell reprogramming (Ieda et al. 2010) and zebrafish heart

regeneration support this assumption (Lepilina et al. 2006; Liu and Stainier 2010; Zhang et al. 2013).

Tbx5 was found to be one of the three transcription factors that are essential for reprogramming postanatal mouse cardiac or dermal fibroblasts into cardiomyocyte-like cells *in vitro* (Ieda et al. 2010). According to *in vivo* studies, *tbx5a* is constantly weakly expressed in the adult zebrafish heart (Raya et al. 2003). However, no significant changes in transcript level were detected at any stage of cardiac regeneration suggesting that either *tbx5a* is reactivated for a very short period of time or it is dispensable for regeneration (Raya et al. 2003). Importantly, Lepilina and colleagues (2006) detected overexpression of *tbx5a* in adult zebrafish ventricle at 5 and 7 days after resection. Similarly, Zhang and others (2013) found that *tbx5a* is re-activated during ventricular regeneration in zebrafish embryos. Moreover, ventricular resection was found to activate epicardium (Lepilina et al. 2006), while *tbx5a* was shown to be important for specification of proepicardium (Liu and Stainier 2010). All these findings suggest that *tbx5a* is a strong candidate for cardiac regeneration in zebrafish.

2. Methods

2. 1. Identification of insertional mutants using iPCR and 5'RACE methods

Candidate gene trapped mutant alleles obtained from the insertional mutagenesis screen in Dr. Balciunas laboratory were identified using two complementary methodologies: inverse Polymerase Chain Reaction (iPCR hereafter) (Hermanson et al. 2004, Clark et al. 2011) and 5' Rapid Amplification of cDNA Ends (5'RACE) (Clark et al. 2004, Clark et al. 2011).

Five dpf F1 embryos were screened and pre-selected for either presence or absence of fluorescent protein (FP hereafter) expression. Distinct pools of 20 FP-positive and 20 FP-negative embryos were frozen at -80°C. For iPCR, the genomic

DNA from the pools of embryos was extracted using a standard protocol (Hermanson et al. 2004). For 5'RACE, the RNA from the pools of embryos was extracted using Absolutely RNA miniprep kit (Agilent Technologies).

The iPCR method consists of three steps: digestion of the genomic DNA by endonucleases, circulization of the digested DNA fragments, amplification of the genomic sequences flanking the gene trap. Extracted genomic DNA was diluted to 0.67 µg/ µl and digested in four different tubes with four distinct enzyme mixtures: N (NlaIII), T (Taq), X (AvrII, NheI, SpeI, XbaI) ir B (BamHI, BgIII, BcII). Digestions containing N, X, or B enzyme combinations were kept at +37°C, while digestions with T were incubated at +65°C. After 4h, 10 µl of the digested DNA from each sample was run on 1% agarose gel. The remaining 10 µl of each digestion were frozen at -20°C.

Upon successful digestion, produced DNA fragments were self-ligated overnight at +4°C. Next day, 5 µl of ligated circular DNA was used as a template for amplification of 5' and 3' ends of the gene trap via PCR1 (total volume = 25 µl) using two sets of primers, respectively: Tol2-F8 (5') (5'-TCAAGTAAGATTC TAGCCAGATAC-3') and B1/5'No1 (5'-CTAGAGATTCTTGTTTAAGCTGTA G-3'), Tol2-R3 (3') (5'-ACTGGGCATCAGCGCAATTCAATT-3') and B1/3'No1 (5'-CAGGGTAATATAACTTCGTATAGCA-3'). Next, 0.5 µl of the obtained PCR1 products were used a template for amplification of 5' and 3' ends of the gene trap via PCR2 (total volume = 25 µl) using two sets of primers, respectively: Tol2-F10 (5') (5'-AAGTGAAAGTACAAGTACTTAGG-3') and B1/5'No2 (5'-TGTATGCTATACGAAGTTATCAGCA-3'), Tol2-R4 (3') (5'-AT AATACTTAAGTACAGTAATCAAG-3') and B1/3'No2 (5'-GCATACATTATA CGAAGTTATCGTT-3'). The primer pairs used for amplification were specific for one of the transposon ends (5' or 3') and faced an opposite direction. This strategy allowed for amplification of the genomic DNA fragment (sequence flanking transposon from either 5' or 3' side) that is located in a cricular DNA molecule also containing one of the gene trap ends.

The products of PCR2 were analyzed using 1% gel electrophoresis. The PCR2 samples obtained from the pools of FP-positive and FP-negative embryos from the same batch (siblings) were loaded in the adjacent wells of the gel. The lanes containing PCR2 products amplified on the DNA of FP-positive and FP-negative siblings were compared. The bands of similar size and intensity indicated the integrations that were not linked to fluorescence. Meanwhile, the bands unique only to "FP-positive" lane suggested a linkage between the integration and fluorescence.

The bands unique to "FP-positive" lane were cut out from the gel, gel-extracted and sent for sequencing with one of the gene trap specific primers, Tol2-F10 (5') or Tol2-R4 (3'). In cases when both the "FP-positive" and "FP-negative" lanes contained a band of the same size, but this band was significantly brighter in the "FP-positive" lane, there was a possibility that the "FP-negative" pool contained at least one of the "FP-positive" embryos. Therefore, such bright band from the "FP-positive" sample was also cut out from the gel, gel-extracted (GeneJET Gel extraction Kit, ThermoFisher Scientific) and sequenced (Genewiz®).

The obtained DNA sequences were blasted using UCSC (University of California, Santa Cruz) and Ensembl (ENS European Molecular Biology Laboratory) genome browsers. If the blasted sequence matched a region in a known or predicted gene, the next step involved analysis of the gene trap direction and reading frame. If the gene trap had integrated in the sense orientation with respect to the trapped gene, and its reading frame was correct, this indicated that at least theoretically Gal4 fussion transcript (that will be translated into Gal4 fussion protein containg a functional Gal4) could be made. In such cases the genotyping primers were designed.

Genotyping primers (5' genomic primer and 3' genomic primer) were created in the 500 bp regions located upstream and downstream of the candidate integration site. Next, the PCR was run on both FP-positive and FP-negative

embryos genomic DNA. Two sets of primers were used: 5' genomic primer and Tol2-F10 (5'), 3' genomic primer and Tol2-R4 (3'). If band of the expected size was present only in "FP-positive" lane, it was cut from the gel, gel-extracted and sequenced with either 5' genomic primer or 3' genomic primer. The obtained sequences were blasted using the genome browser, and hits were analyzed. If the predicted match was found, the exact location of the transposon integration in a particular gene was confirmed.

If iPCR method was not effective in determining the integration of the gene trap, another alternative technique, 5'RACE, was applied. In contrast to iPCR, the 5'RACE method did not permit for the exact identification of the transposon integration site. However, it provided the information about the 5' endogenous exons that are fused with an exogenous Gal4 sequence. The RNA extracted (250 - 500 ng) from pools of FP-positive and FP-negative embryos was used for cDNA synthesis with Superscript™ II Reverse Transcriptase (Invitrogen). The synthesized cDNA was then used as a template for 5'RACE PCR. The PCR1 was run using a primer mix, KJC-002 (5'-AATGGCTTCCGAGACCTGCTGTCCAA GTTCGTACAAAAAAGCAGGC-3') and KJC-003 (5'-AATGGCTTCCGAGAC CTGCTGT-3'), with Gal4-R2 (5'-TTCTTCAGACACTTGGCGCACTTCG-3'). Ten times diluted PCR1 product was used as template for PCR2 with KJC-004 (5'-GAGACCTGCTGTCCAAGTTCGT-3') and Gal4-R3 (5'-TAAGTCGGCAA ATATCGCATGCTTG-3'). The obtained 5'RACE PCR products were run on the gel. The bands unique to "FP-positive" lane were cut from the gel, gel-extracted and sequenced with Gal4-R3.

Upon successful mapping of the gene trap integration site (by either iPCR or 5'RACE technique) that is linked to fluorescent protein, the presence of Gal4 mRNA fusion transcript was confirmed by RT PCR and sequencing. The RNA (250 - 500 ng) extracted from pools of FP-positive and FP-negative embryos was used for cDNA synthesis with SuperScript™ III Reverse Transcriptase (Invitrogen) and random hexamers. One µl of prepared cDNA was used as a

template for PCR with 5' genomic primer (specific to an endogenous exon upstream of the integration site) and Gal4-R3. The samples were run on the gel. The bands were cut out from the gel, gel-purified and sequenced to check for the presence of Gal4-fusion transcript.

2. 2. Testing regeneration of the blood vessels in *fli1b*^{tpl50} mutants

In order to test if *fli1b* gene is required for vascular regeneration of adult zebrafish, a group of not genotyped fish obtained from *fli1b*$^{tpl50/+}$ incross was tail-clipped. Fish were anesthetized in 0.892 mM tricaine solution for exactly 3 min, and placed in a small Petri dish left lateral side up. Five ml of water were added into the dish. The Petri dish was placed under the ZEISS Axio IMAGER.A1 microscope and positioned in a way that would allow for observation of distal part of the caudal fin in the microscope field of view.

The bright field and fluorescent pictures of the upper tip of the distal part of caudal fin (Fig. 9) were taken before amputation (ba hereafter) using NIKON SPOT RT3 camera. Next, approximately 60% of the distal part of fish tail was clipped using small fine scissors. The amputated tissue was frozen, and later used for DNA extraction. The three-primer PCR with two genomic primers, fli1b-int1-F1 (5'-CGTCAACTTCTGCTTTCTTT CG-3') and fli1b-int1-R1 (5'-TAACCACAGGCACTGTCACG-3'), and one gene trap specific primer, Tol2-F10 (5') (5'-AAGTGAAAGTACAAGTACTTAGG-3') (Craig et al. 2015), was run for genotyping adult fish.

The appearance of the regenerating caudal fin and expression of fluorescent protein were examined at four different regeneration stages: 0, 7, 14 and 21 dpa. Each time both bright field and fluorescent pictures of the regenerating tail were taken. In order to ensure that all pictures obtained can be compared in terms of caudal fin size, shape, pigmentation, and fluorescent protein expression (GFP and

RFP), each time the same microscope settings (magnification, exposure time, etc.) were used.

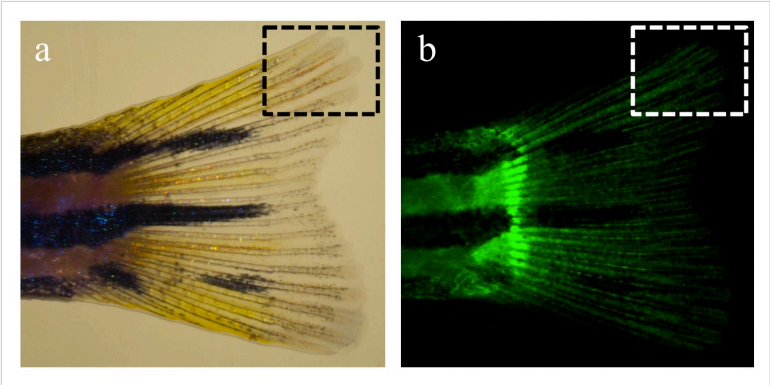

Figure 9. In order to evaluate vascular regeneration in f*li1b*^{tpl50} mutants, both brightfied (a) and fluorescent (b) pictures of regenerating tail were taken. The upper right boxes show the area of the caudal fin that was photographed and analyzed.

2. 3. Molecular cloning of *nkx2.5* promoter and chicken β-globin insulators

Both *-3.3nkx2.5:RFP/INS* and *-6.1nkx2.5:RFP/INS* constructs (containing 4.8 and 7.6 kb promoter regions of *nkx2.5*) used in the dissertation project were previously generated in Dr. Balčiūnas lab (Grajevskaja et al. 2013). The other two constructs, *-6.1nkx2.5:RFP-pp(A)* and *-6.1nkx2.5:RFP-zp(A)*, were cloned during the actual research project (Fig. 10). The *-6.1nkx2.5:RFP-pp(A)* plasmid was generated from *-6.1nkx2.5:RFP/INS* by removing both insulation sequences in a two-step process.

The 5' insulator was cut out from *-6.1nkx2.5:RFP/INS* with *NotI* and *SacI* restriction enzymes. The digestion also resulted in a loss of Tol2 fragment that was subsequently restored from the pDB773 plasmid. The 3' insulator was removed by digestion of the intermediate plasmid pVG1 (*-6.1nkx2.5:RFP/INS* without 5' insulation sequence) with *ApaI* and *BstBI* restriction enzymes.

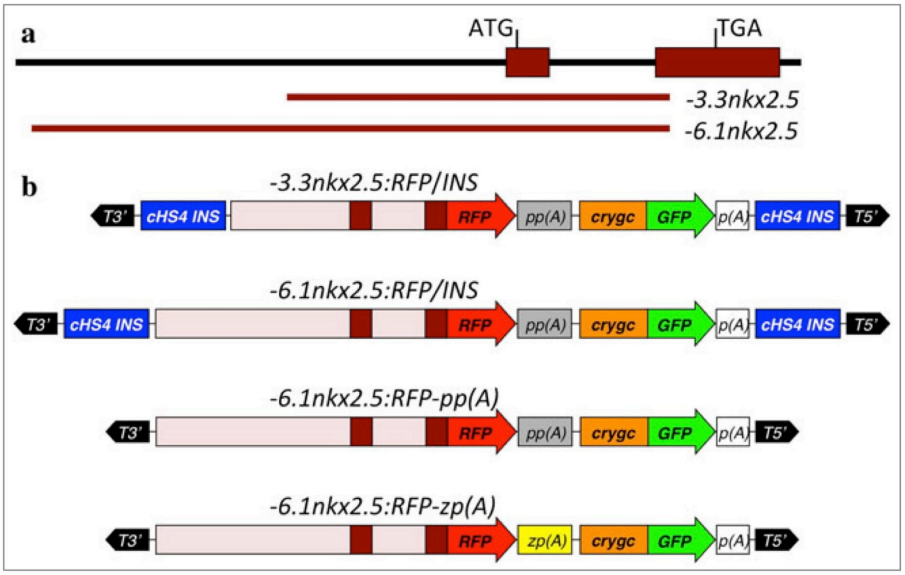

Figure 10. Diagram of *nkx2.5* promoter regions cloned (a) and transgenic constructs generated (b) (Grajevskaja et al. 2013)

The *-6.1nkx2.5:RFP-zp(A)* plasmid was created by removing an ocean pout antifreeze protein polyadenylation sequence *(pp(A))* from *-6.1nkx2.5:RFP-pp(A)*, and replacing it with zebrafish β-actin transcription termination sequence (*zp(A)*) from pDB713 using *AvrII* and *AatII* enzymes (Grajevskaja et al. 2013).

2. 4. Testing a conditional regulation of the *tbx5a* activity in *tbx5a*^{tpl58}

2. 4. 1. Principle of the gene trapping with "Switchblade 1"

A null *tbx5a*^{tpl58} allele was generated through an insertional mutagenesis using a "Switchblade 1" (S1 hereafter) gene trap that was designed by dr. D. Balciunas and cloned by D. Camerota. The S1 gene trap, *Gt(lox71-FRT(-10)-SA-^Gal4-VP16-zpA-FRT(+10)-lox66,crygc:BFP)*, contains a mutagenic cassette and a marker, a blue fluorescent protein (BFP), driven by the lens specific promoter (*crygc*). The mutagenic cassette encompasses splice acceptor (SA), AUG-less Gal4-VP16, and zebrafish transcription termination sequence (zpA) (Fig. 11).

Upon successful integration with a sense orientation of the gene trap into an intron of a gene, upstream exons of the trapped gene are fused with Gal4-VP16 sequence (Fig. 12). The resulting Gal4 fusion transcript is terminated by zpA, and downstream exons of the trapped gene are not expressed. If the gene trap integrates in a correct reading frame, a Gal4 fusion protein is produced.

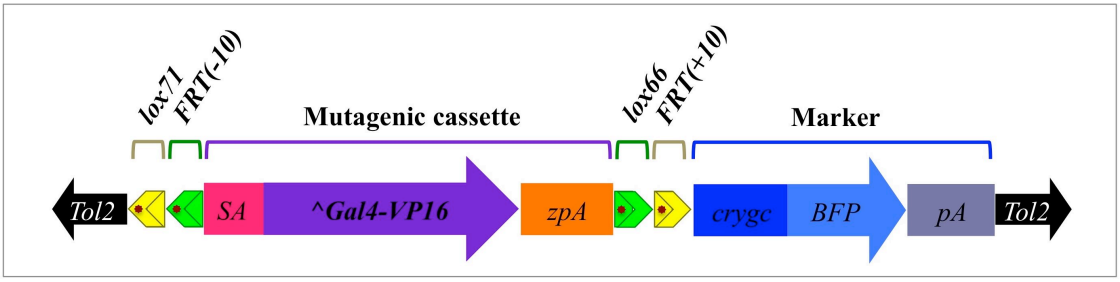

Figure 11. Design of the gene trap "Switchblade 1"

In order to detect Gal4, the gene trap lines are outcrossed to *Tg(crygc:GFP,UAS:RFP)* reporter line (UAS reporter line hereafter) that has a lens specific green fluorescent protein (GFP) marker. When Gal4 fusion protein binds an upstream activating sequence (UAS), it initiates a transcription of a red fluorescent protein (mRFP). Therefore, the detected expression of the mRFP is restricted only to the cells with the promoter of the insertionally mutated gene.

In *tbx5a*^{tpl58} line, the S1 gene trap has randomly integrated into the second intron of *tbx5a* gene. The created insertional allele produces a Tbx5a protein that is truncated after first 48 amino acids (before T-box DNA binding domain) and fused with Gal4-VP16. As a result, every cell with *tbx5a*^{tpl58} mutation lacks a functional copy of *tbx5a*, but only the cells with active *tbx5a* promoter are mRFP-positive.

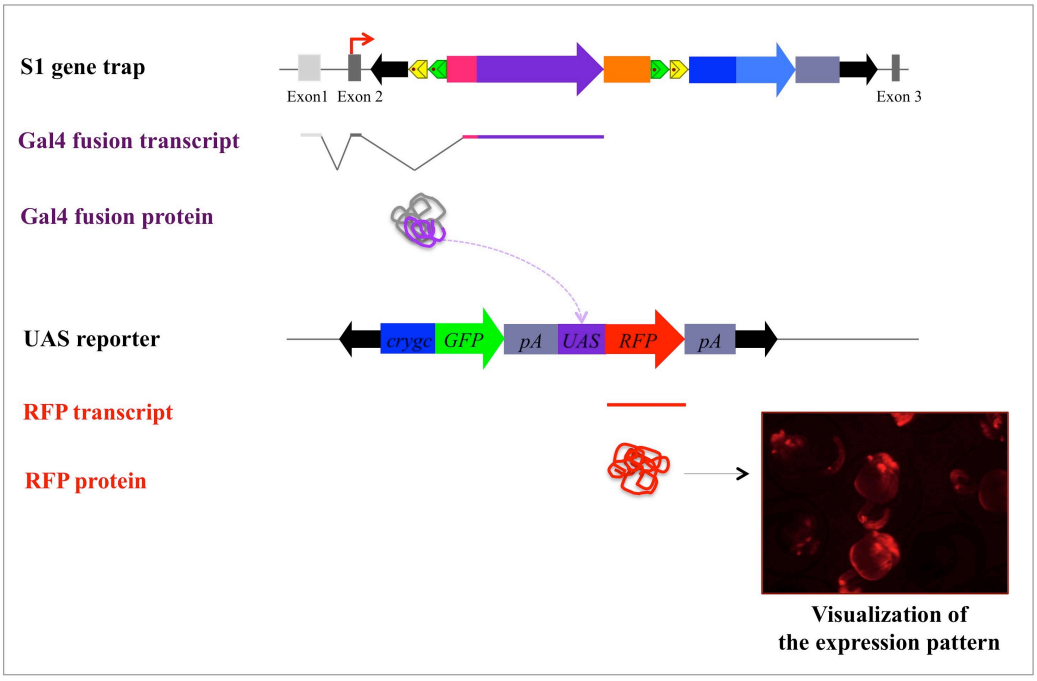

Figure 12. Diagram representing a summary of a successful gene-trapping event with the "Switchblade 1."

2. 4. 2. Conditional manipulations of the "Switchblade 1" gene trap

Insertional mutations generated with S1 gene trap are expected to be fully conditional because a mutagenic cassette is flanked by oppositely oriented modified site-specific recombinase sequences (SSRs): *lox71, FRT(-10)* upstream and *lox66, FRT(+10)* downstream of the cassette (Branda and Dymecki 2004) (Fig. 13). The recognition of these modified *loxP* and *FRT* sites by Cre or Flp recombinases, respectively, is anticipated to induce an intra-molecular recombination reaction between SSRs, resulting in a stable inversion of the mutagenic cassette.

Therefore, theoretically, a mutation generated by S1 gene trap can be switched off, and then, switched on again (Fig. 13). In other words, the activity of the trapped gene can be restored to obtain viable homozygous fish that exhibits no phenotype. Consequently, the trapped locus can be re-mutated in the whole

organism or specifically in a tissue of interest at any time point during development or regeneration.

In order to test if *tbx5a* activity in *tbx5a*^{tpl58} line can be conditionally regulated in a special and temporal manner, *tbx5a*$^{tpl58/+}$ embryos were microinjected with *Flp*^{o} mRNA, and their progeny was either microinjected with *Cre* mRNA or crossed to the heart-specific *CreER*^{T2} driver line.

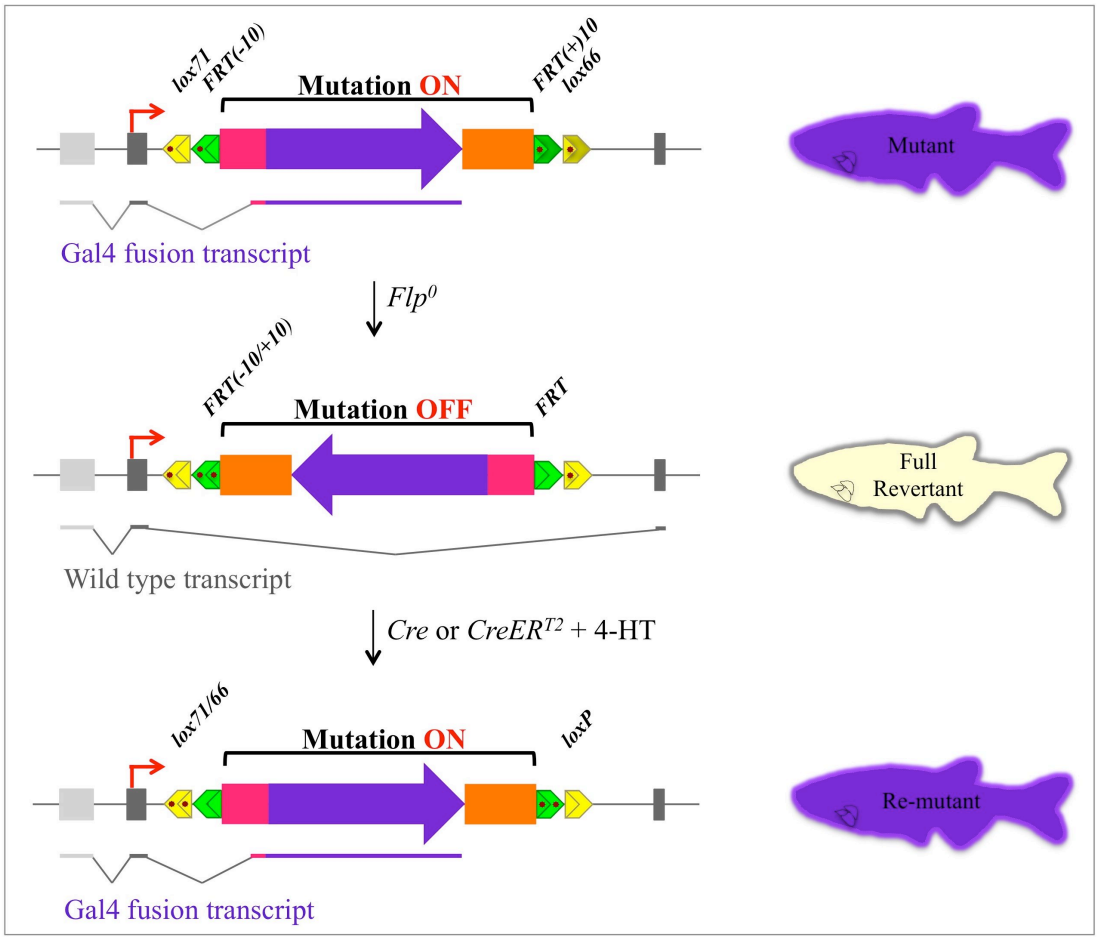

Figure 13. Conditional regulation of the trapped alleles

2. 4. 3. Microinjections of *Flp*^{o} mRNA

Through an *in vitro fertilization (IVF)* (Draper and Moens 2009), *tbx5a*$^{tpl58/+}$ zebrafish were outcrossed to *UAS* reporter line. Obtained 1-cell stage

embryos were microinjected with 75 pg of a codon optimized *Flp (Flp^{o})* mRNA into the yolk. The *Flp^{o}* recombinase activity was expected to induce recombination between *FRT(-10)* and *FRT(+10)* SSRs sites resulting in a stable inversion of a mutagenic cassette. In this way an insertional mutation in *tbx5a* would be turned off (Fig. 13).

Injected embryos (F0) were screened for mRFP expression at 3 dpf. Embryos exhibiting mosaic mRFP and milder pectoral fins phenotype were raised until adulthood. It was expected that individuals with mosaic somatic tissues also have a mosaic germline. At three months age fish were outcrossed with *UAS* reporter line. The embryos were screened for mRFP and scored. A batch that showed the lowest percentage of mRFP-positive embryos was genotyped. The same parent was outcrossed again, and all mRFP-negative embryos with GFP-positive lens were raised until adulthood. Adult fish were genotyped.

2. 4. 4. Genotyping *tbx5a^{tpl58}* line

In order to determine if injections of *Flp^{o}* mRNA resulted in a successful inversion of a mutagenic cassette of the gene trap in *tbx5a^{tpl58}* line, injected embryos were genotyped at both embryonic and adult stages. All injected embryos were screened for GFP expression in the lens and mRFP expression in the heart and pectoral fins at 3 dpf. For genotyping at embryonic stage, mRFP-positive as well as mRFP-negative single embryos were frozen at 5 dpf in 1.5 ml micro centrifuge tubes at -80°C. Single embryo DNA was extracted using a standard protocol (Balciunas, unpublished protocol). For genotyping at adult stage, zebrafish were anesthetized in 0.446 mM MS222 solution (tricaine hereafter) for 3 min. A distal part of the caudal fin was amputated with small scissors and used for DNA extraction.

Single embryo DNA as well as tail-clips DNA was diluted to a final concentration of 100 ng/µl. One µl of the diluted DNA was used as template for a

polymerase chain reaction (PCR). Three-primer PCR was run with two genomic primers (tbx5a-F1 ATCCCCGTCATCGCAGACTACATACATT, tbx5a-R1 TTATCAAGTTTAGCTTACCTCTGGACAG) and one primer from the zpA of a mutagenic cassette (zpA-F2 CATATGAAGGTAGCTAACTGCAA). Generated PCR products were separated using 1% agarose gel electrophoresis. To determine the size of the bands GeneRuler^{TM} DNA ladder was used. A combination of two out of three possible bands was expected in each lane (every lane represents a single embryo or single adult genotype for *tbx5a* locus): 457 bp (wild type *tbx5a* allele (*tbx5a*$^{+}$)), 2303 bp (mutant *tbx5a* allele (*tbx5a*^{tpl58})) and 671 bp (reverted *tbx5a* allele (*tbx5a*^{tpl58R})). Wild type individuals were expected to show a single *tbx5a*$^{+}$ band. Zebrafish heterozygous for *tbx5a*^{tpl58} insertional mutation were expected to have two bands: one *tbx5a*$^{+}$ and one *tbx5a*^{tpl58}. Fish heterozygous for a successful recombination event were expected to show two bands: one *tbx5a*$^{+}$ and one *tbx5a*^{tpl58R}. To confirm genotypes, DNA bands were extracted from the gel and sent for sequencing (Genewiz®).

2. 4. 5. Microinjections of *Cre* mRNA

In order to test if a flipped mutagenic cassette in a reverted *tbx5a* allele, *tbx5a*^{tpl58R}, can be re-inverted, *tbx5a*$^{tpl58R/+}$ were outcrossed to *UAS* reporter line, and obtained embryos at 1-cell stage were injected with 25 pg of *Cre* mRNA into the yolk. Cre recombinase was expected to induce recombination reaction between *lox71* and *lox66* SSRs sites resulting in a stable inversion of a mutagenic cassette. In this way, an insertional mutation in *tbx5a* can be turned on for the second time. Injected embryos (F2) were screened for mRFP at 3 dpf. mRFP expression would indicate a successful re-mutation of *tbx5a*^{tpl58} locus.

2. 4. 6. Testing a specificity of *tnnt2a:CreER^{t2}*

The SSRs sites in S1 gene trap provide a way to control a spatiotemporal expression of the trapped gene. A basic strategy allowing for a regulation of the gene activity in a special manner involves a usage of tissue-specific Flp or Cre drivers that can be generated by cloning a SSR sequence downstream of the tissue-specific promoter. Therefore, an insertional mutation can be turned off or turned on in the tissue or cells of interest. However, studying developmentally essential genes also requires temporal regulation that offers an ability to switch on a mutation in the particular type of tissue or cells in the late developmental stages or in adult organism. That can be achieved by using drug inducible tissue-specific SSR drivers. For example, Cre sequence can be fused with ER sequence that can bind an estrogen analog, drug 4-hydoxytamoxifen (4-HT) (Branda and Dymecki 2004). In the absence of 4-HT, CreER fusion protein will be made in every cell in which a tissue-specific promoter driving CreER is active. However, CreER will be able to translocate into the nucleus only after the binding a 4-HT. In this way, a recombination between SSRs sites will be spatially restricted to the area of the tissue-specific promoter activity and temporarily controlled by the administration of 4-HT.

In order to turn on an insertional mutation in *tbx5a* gene specifically in the heart, a heart-specific CreER driver line, *tnnt2a:CreER,* previously generated in dr. Balciunas lab, was used. To test *tnnt2a:CreER* for specificity, *tnnt2:CreER* heterozygotes from three independent founders were outcrossed to a pDB860 reporter line, *carpβ-actin-loxP-STOP-loxP-GFP-ppA-crygc:RFP-pA* (Fig. 14). Embryos from every batch were separated into two groups at 2 dpf. An experimental group was treated with 0.05 μM TAM, while a control group was incubated with DMSO. All treatments were carried out for 24 h at 28°C in incubator. Incubations were kept in the dark because 4-HT is known to be a light sensitive. Embryos were screened for fluorescence and photographed at 4 dpf.

Both *tnnt2a:CreER* and pDB860 constructs are marked with RFP driven by a lens-specific promoter. Trans-heterozygous embryos in a control group (treated with DMSO) were expected to express only RFP in the lens. In distinction, trans heterozygotes in an experimental group (treated with TAM) were expected to express not only RFP in the lens, but also GFP in the heart if a *tnnt2a* is indeed a heart-specific promoter.

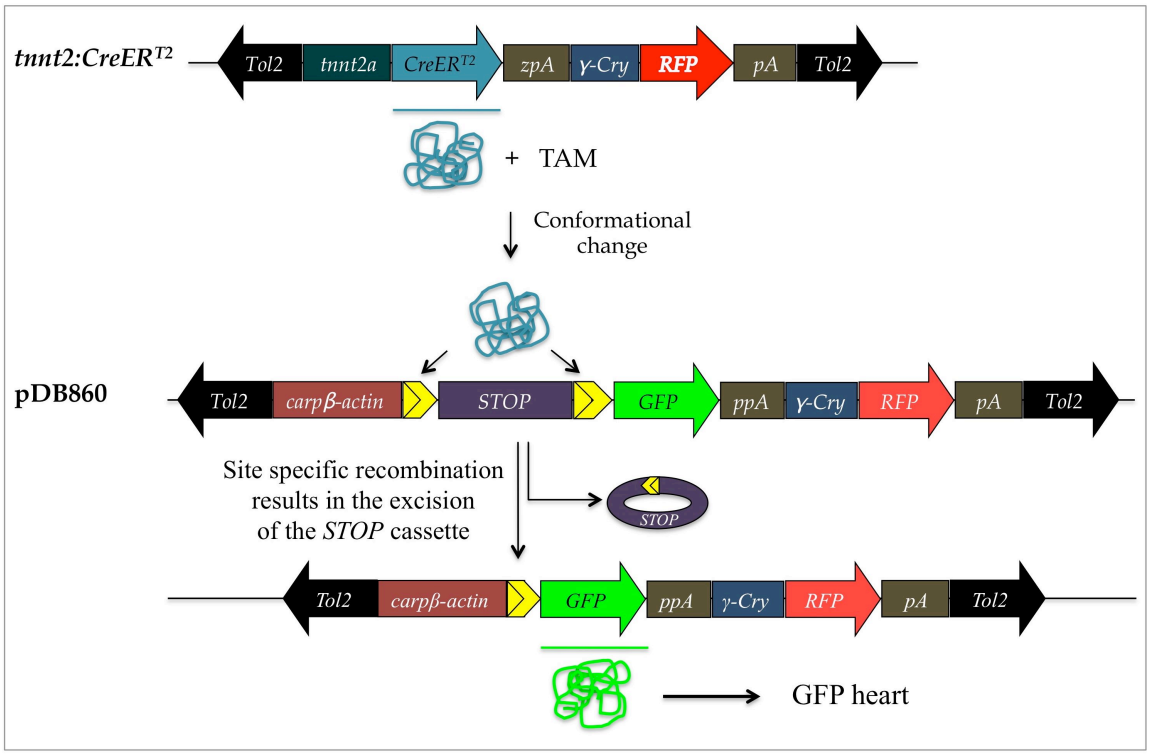

Figure 14. Testing a specificity of *tnnt2a:CreER* line

2. 4. 7. Establishment of the double transgenic lines

In order to generate a conditional system, a heart-specific CreER^{T2} driver line, *tnnt2a:CreER^{T2}*, was outcrossed to a full revertant gene trap line, *tbx5a^{tpl58R}*. Embryos were preselected for RFP/GFP lens and raised. Two months old fish were genotyped for both *tnnt2a:CreER^{T2}* (because RFP expression in the lens was very weak) and *tbx5a^{tpl58R}* alleles. To genotype for *tnnt2a:CreER^{T2}* transgene, a

PCR was run with two primers, mRFP F2 (5'-ATGGCCTCCTCCGAGGACG-3') and SV40 R2 (5'-AACTTCGATGATAATCAGCCATACCA-3'), that in a presence of *tnnt2a:CreER*^{T2} sequence in the examined DNA were expected to give a band. Established *tbx5a*$^{tpl58R/+}$*;tnnt2a:CreER*^{T2} double transgenic lines were outcrossed with *tnnt2a:CreER*^{T2} to generate *tbx5a*$^{tpl58R/tpl58R}$*;tnnt2a:CreER*^{T2} zebrafish. Embryos with RFP/GFP-positive lens were raised and later genotyped.

2. 4. 8. Re-mutation of *tbx5a*^{tpl58R} locus specifically in the heart

In order to re-mutate *tpl58* insertional mutation in the *tbx5a* gene specifically in the heart, both *tbx5a*$^{tpl58R/+}$*;tnnt2a:CreER*^{T2} and *tbx5a*$^{tpl58R/tpl58R}$*;tnnt2a:CreER*^{T2} double transgenic lines were treated with 4-HT. For a re-mutation of the *tbx5a*^{tpl58R} locus specifically in the developing heart, *tbx5a*$^{tpl58R/tpl58R}$*;tnnt2a:CreER*^{T2} were outcrossed with wild type and their progeny at 2 dpf was incubated in 0.5 µM 4-HT solution for 24 h in the dark (Fig. 15). Next day embryos were preselected for mRFP expression in the heart and raised until adulthood. At three-month age three individuals were sacrificed. Hearts were dissected, screened for fluorescence, photographed and fixed in 4 % paraformaldehyde solution (PFA hereafter). Siblings of the dissected fish were later used for regeneration studies.

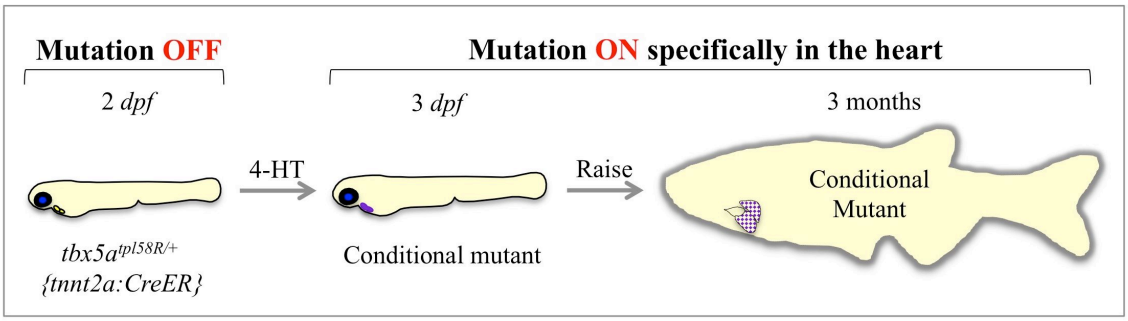

Figure 15. Re-mutation of *tbx5a*^{tpl58R} locus in the developing zebrafish heart.

For a re-mutation of the *tbx5a*^{tpl58R} locus specifically in the adult heart, *tbx5a*$^{tpl58R/+}$;*tnnt2a:CreER*^{T2} and *tbx5a*$^{tpl58R/tpl58R}$;*tnnt2a:CreER*^{T2} adults were incubated separately in 100 ml of the 5 µM 4-HT solution for 24 h (Fig. 16). In total, three incubations for every fish were carried out. To avoid complications that may caused the amount of stress experienced by fish during procedure and to reduce a possible toxicity level, there was made a rest period of 24 h between each incubation.

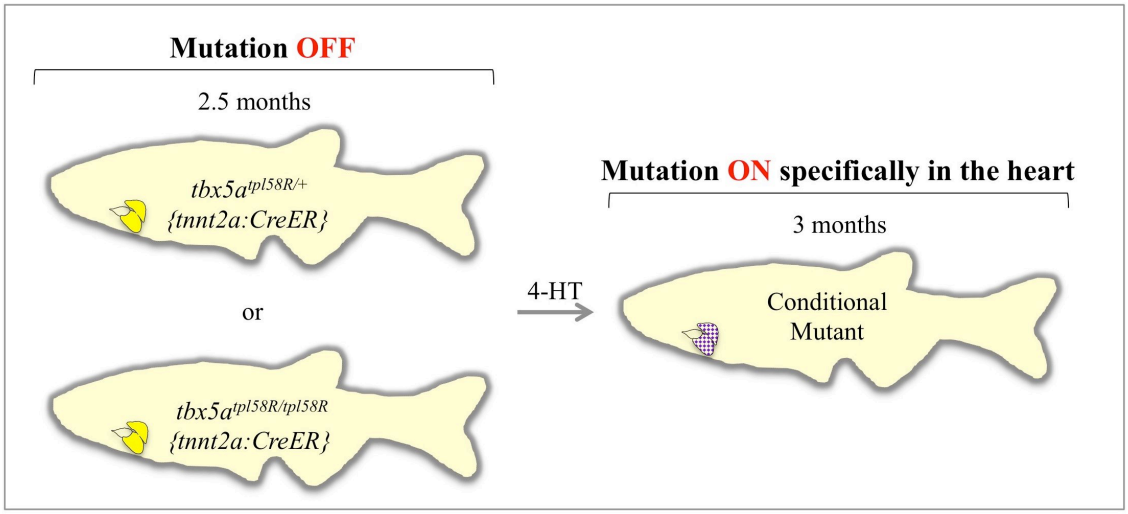

Figure 16. Re-mutation of *tbx5a*^{tpl58R} locus in the adult zebrafish heart.

For a control group, ethanol was used instead of 4-HT. In one week after incubations were completed several fish from both control and experimental group were sacrificed. The dissected hearts were screened for mRFP, photographed, and fixed in 4% pfa. The remaining siblings were later used for heart regeneration experiments.

2. 5. Testing the Heart Regeneration in *tbx5a* Mutants

Heart regeneration experiments were performed in the following lines: *tbx5a* insertional mutant, *tbx5a*$^{tpl58/+}$, *tbx5a* conditional mutants,

tbx5a$^{tpl58R/+}$*;tnnt2a:CreER*^{T2} and *tbx5a*$^{tpl58R/tpl58R}$*;tnnt2a:CreER*^{T2}, and published *tbx5a* ENU mutant, "*heartstrings"* (*tbx5a*^{hst} hereafter) (Garrity et al 2002). The age of all fish used for experiments ranged from three to six months. For a heart muscle injury previously published technique, a partial ventricular resection, was adapted (Poss et al 2002). Fish were sacrificed at 30 days post amputation (dpa hereafter). Dissected hearts were processed, sectioned, stained and analyzed.

2. 5. 1. Partial amputation of the heart ventricle

Fish one by one were anesthetized in 0.892 mM tricaine solution for exactly 3 min. After anesthesia fish was removed from solution and placed in a wet sponge ventral side up. All procedures were performed under NIKON stereomicroscope. Surgery was performed using two pairs of fine forceps and one pair of fine micro-scissors. In the area of heart a small incision was made with scissors. Next, pericardium sac was carefully opened with forceps avoiding any contact with heart. About 20 % of ventricular apex was carefully removed with scissors. After successful partial amputation of the ventricle a strong bleeding from the heart was observed. The bleeding was stopped by applying a small piece of a new KimWipe to the injury site for 5 s. Next, fish was transferred to a recovery tank that was filled with a fresh fish system water and had an additional air supply. It takes approximately from 1 to 5 min for fish to recover after anesthesia. Recovered fish were kept in a 2 L tank (1 - 5 fish in each tank) connected to a main water system.

2. 5. 2. Heart fixation, sectioning and analysis

At 30 dpa fish were euthanized by incubation in 0.892 mM tricaine solution for 15 min. Dead fish were pinned to a sponge. Hearts were carefully dissected using small scissors and forceps, and placed in a small Petri dish in 1x phosphate-

buffered saline (PBS hereafter). Hearts were cleaned from fat and remaining tissues (for example, pericardium) with forceps. Fluorescent (mRFP) as well as bright field pictures were taken on NIKON SMZ1500 microscope using 10x, 25x, and 40x magnifications. Hearts were fixed in 4 % PFA overnight at +4°C. For the next 2 days hearts were washed in 1x PBS (solution was changed 4 -5 times a day) at +4**°C**. Washed hearts were dehydrated in a series of 1xPBS and ethanol dilutions (2 times for 10 min in each solution):

1. 1x PBS
2. 25 % ethanol in 1x PBS
3. 50 % ethanol in 1x PBS
4. 75 % ethanol in 1x PBS
5. 100 % ethanol.

Dehydrated hearts were incubated in Xylenes for 30 min and then transferred into molds filled with melted paraffin at + 56 °C. After positioning of the hearts using forceps and needle, molds with the hearts were returned to the water bath. After 30 min molds with the heart were removed from water and left at room temperature overnight. Next day paraffin squares with the embedded hearts were removed from the molds and attached to the wooden squares. Eight nm hearts were sections were made using a Leitz 1512 Rotary Microtome. A paraffin film containing 3 – 4 heart sections was placed on the surface of double distilled water preheated to + 42 °C. Using a fine forceps and a small paintbrush paraffin film was carefully transferred from water surface on the microscope glass slide. Next, slides were placed on hot top plate preheated to + 42 °C and kept there until all water evaporates from the slide surface. Slides were left at room temperature overnight. Next day slides were transferred into Xylenes. After 24h sections were re-hydrated in a series of ethanol and 1x PBS dilutions (2 times for 15 min in each solution):

1. 100 % ethanol
2. 75 % ethanol in 1x PBS

3. 50 % ethanol in 1x PBS

4. 25 % ethanol in 1x PBS

5. 1x PBS

To detect a myocardial scar tissue, rehydrated heart sections were stained with Picro-Mallory technique (Gonzáles-Rosa et al 2011). Heart muscle was stained red, while collagen deposition indicating a scar was stained blue. Immediately after staining heart sections were quickly dehydrated:

1. 95% ethanol (1 min)

2. 100% ethanol (1 min)

3. Xylenes (2-3 s)

Dehydrated sections were mounted through applying a drop of mounting media on the sections and immediately covering them with a cover slip. Covered sections were left to dry out overnight at room temperature. Next day sections were examined using ZEISS Axio IMAGER.A1 microscope and photographed with NIKON SPOT RT3 camera at 2.5x, 10x and 20x magnifications.

To distinguish cells in the heart, nuclei of the cells were stained with DAPI by incubating cardiac section in standard DAPI solution for 10 min. Stained sections were rinsed with PBS. Sections were mounted with water-based mounting media by applying a drop of the media on section and immediately covering it with a coverslip. Slides were left to dry overnight at room temperature. Following day cardiac sections were examined for mRFP and DAPI on the ZEISS Axio IMAGER.A1 microscope and photographed at 2.5x, 10x and 20x magnifications.

2. 6. Deletion analysis of *tbx5a* enhancer

To perform a functional dissection and characterization of a 2309 bp zebrafish *tbx5a* enhancer sequence (previously identified and cloned in dr. Balciunas lab), 14 plasmids, pVG11 – pVG24, containing different fragments of

the *tbx5a* enhancer upstream of the *hst 70 (heat shock protein 70)* minimal promoter driving mRFP have been cloned (Fig. 17).

To generate pVG11 and pVG12 plasmids containing 744 or 1479 bp deletions in the *tbx5a* enhancer, pBK48 was digested either with NotI and BsrG1 or NotI and NheI restriction enzymes. DNA bands were separated using agarose gel electrophoresis. Fragments (6049 and 5314 bp) were gel-extracted using "Fermentas" DNA extraction kit, blunt digested with 0.5µL of Klenow DNA polymerase I ("New England BioLabs Inc.") and ligated.

To clone pVG13 plasmid comprising a 1602 bp deletion in *tbx5a* regulatory region, pBK48 was digested with SpeI restriction enzyme and ligated. In order to generate pVG14 – pVG16 plasmids containing only 514, 593 or 616 bp regions of *tbx5a* enhancer (Fig. 17), respectively, fragments were PCR amplified from pBK48 using corresponding forward primers with NheI site and reverse primers with BsrGI site. PCR products were run on the agarose gel, extracted, digested with NheI and BsrGI restriction enzymes and ligated into pBK48 vector digested with NheI and BsrGI. Similar strategy was used to make pVG18 – pVG21 plasmids that contain only 308, 290, 529 or 177 bp fragments of *tbx5a* regulatory region, respectively. However, all reverse primers had SpeI restriction site instead of NheI.

To determine what regions in *tbx5a* enhancer could potentially serve as transcription factor (TF) binding sites, *tbx5a* minimal enhancer sequence was examined using TFSEARCH program that is directly connected to TRANSFAC database (Heinemeyer et al 1998). PCR and cloning methods were used to generate deletions in the two candidate TF sites in PVG21 plasmid, PCR and cloning.

In order to clone pVG22 plasmid containing a 10 bp deletion in 177 bp minimal *tbx5a* enhancer, two-step PCR was performed. First, two distinct regions, one upstream and another downstream of the deletion were PCR amplified from pVG21 template. The upstream region was amplified using a forward primer with

NheI site and a reverse primer with 10 bp overhang that corresponds to a region downstream of the deletion. The rest 20 bp of the reverse match a sequence upstream of the deletion. In similar manner, the downstream region was amplified. For second PCR, two PCR products (upstream region and downstream region of the deletion) were diluted to 100 ng/µl, mixed at 1:1 ratio, and 1 µl of solution was used as a template. Amplified fragment was digested with NheI and SpeI and cloned into pBK48 vector digested with the same enzymes.

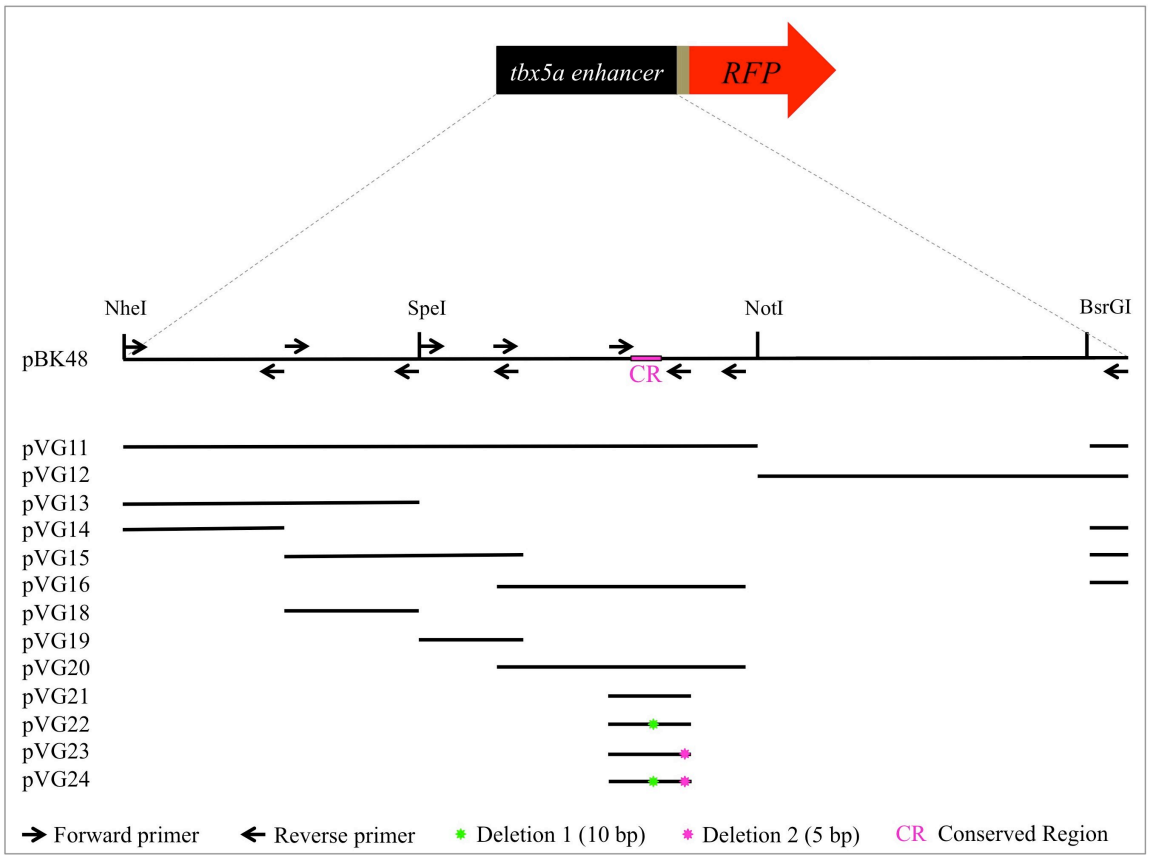

Figure 17. Deletions generated in *tbx5a* enhancer.

All digestions of the PCR products and plasmids were kept for 4h at +37°C. All ligation reactions were performed using "Fermentas" T4 ligase for 2.5h at room temperature. Ligated plasmids were transformed using homemade *Escherichia coli* dH5α competent cells. Single colonies were transferred into a

plastic culture tube with 3 ml of the LB medium containing 3 µl of ampicillin (100 mg/ml stock). Colonies were cultured overnight in the shaking incubator at +37°C. Next day bacteria cultures were centrifuges for 15 min in the centrifuge. The liquid was carefully aspirated, and pellet was left on the bottom of the tube. The cells remaining on the bottom of the tubes were resuspended and plasmids were extracted using alkaline phosphatase miniprep protocol (C. Chen from Zarkower lab, unpublished). Minipreps were tested either by colony PCR or or by digestion with PvuII restriction for 3h at +37°C.PCR products or digested plasmids DNA were run on the gel. For each plasmid, at least three colonies that showed expected band on the gel were cultured. When testing minipreps, one or two that showed expected digestion pattern on the gel were sent for sequencing. Before microinjections, correct plasmids were washed with PB buffer from the Qiagen miniprep kit. Plasmid DNA concentration was measured using spectrophotometer. DNA was diluted to a final concentration of 10 ng/µl. Eight µl of diluted DNA was added to a tube containing 2 µl of 40 ng/µl Tol2 mRNA dilution.

2. 7. Microinjections, Screening and Establishment of the Transgenic Lines

All generated plasmids (8.4 ng/µl) were co-microinjected with Tol2 mRNA (40 ng/µl) into 1-cell wild type zebrafish embryos. Injections were cleaned every day. Three dpf embryos were screened for red or green fluorescent protein expression using NIKON SMZ1500 and ZEISS Axio IMAGER.A1 fluorescent microscopes at magnifications ranging from 2.5x to 5x. Embryos were pre-selected for the brightest fluorescent protein expression and raised until adulthood. Three months old F0 fish were incrossed or outcrossed to generate F1 families. For each construct, at least three F1 lines from different founders have been established. F2 embryos, obtained by outcrossing F1 transgenic lines to wild types, were screened for fluorescence and photographed at 3 dpf using the same settings for all the lines that had to be compared by the expression pattern and/or intensity.

2. 8. Statistical analysis

Statistical analysis of the obtained data was carried out using STATISTICA 13 program. The exact binomial test of goodness-of-fit was used to test the null hypothesis that the number of the observed mRFP-negative (showing no pectoral fin phenotype) (n = 241) and mRFP-positive embryos (exhibiting developmental phenotype of pectoral fins) (n = 290) from *tbx5a*$^{tpl58/+}$ heterozygous outcross fit the theoretical expectations (the number of mRFP-positive embryos is equal to the number of mRFP-negative embryos). The exact binomial test of goodness-of-fit was chosen because sample size was small (less than 1000), and only one nominal variable (morphology of the pectoral fins) was used for analysis.

Table 1. The results obtained from the heart regeneration studies of *tnnt2a:CreER*^{T2}, *tbx5a*$^{tpl58R/tpl58R}$ zebrafish adults were evaluated using statistical analysis (Fisher exact test of independence). A control group (n = 8) was incubated in ethanol solution, and, therefore, had *tbx5a*^{tpl58} mutation turned off. Meanwhile, an experimental group (n = 7) was treated with 5μM 4-HT, which induces *tbx5a*^{tpl58} mutation in cardiomyocytes when *tnnt2a* promoter drives expression of CreER^{T2}. Therefore, at least in some cardiomyocytes of 4-HT treated fish, *tbx5a*^{tpl58} mutation was turned on.

Treatment	**Heart at 30 dpa**		**Total**
	Not regenerated (Scar present)	**Regenerated (Scar absent)**	
EtOH -> *tbx5a*^{tpl58} OFF	0	8	8
4-HT -> *tbx5a*^{tpl58} ON	7	0	7
Total	7	8	15

Moreover, Fisher exact test of independence was applied in order to test the null hypothesis that the presence of heart regeneration defects are independent of the 4-HT inducible *tbx5a*^{tpl58} mutation. Fisher exact test of independence was chosen because sample size was small (n = 15) and two nominal variables (type of

treatment and either presence or absence of heart regeneration phenotype) were used for analysis (Table 1).

3. Results and Discussion

3. 1. Identification of insertional zebrafish mutants

Six out of eight gene trap lines previously recovered from the insertional mutagenesis screen in Dr. Balciunas laboratory were successfully identified using iPCR or 5'RACE methodologies that take an advantage of known gene trap sequence (Table 2). The iPCR technique allows for exact identification of the gene trap integration. In contrast, 5'RACE method only provides the information about the 5' exons upstream of the gene trap integration site. Therefore, designing the primers to determine the exact gene trap location can be problematic, and not always effective. Therefore, genotyping mutants using PCR is not always possible.

Three out of eight mutations (B4-12-2, B1-40A, B4-23-1) were mapped via iPCR method. B4-12-2 line exhibited FP expression in the floor plate, and was found to carry a gene trap in the second intron of the predicted gene, *ENSDART00 000112671*. B1-40-A embryos showed blood-specific FP expression pattern, and were determined to have transposon integration in the first intron of the predicted gene, *ENSDART00000111400*. As for B4-23-1 line, it expressed FP in the vascular system, and the gene trap integration was found to be located in the first intron of the *fli1b* gene (Craig et al. 2015). The *fli1b*^{tpl58} insertional line was later used for angiogenesis, vasculogenesis (Craig et al. 2015) and vascular regeneration studies.

Three lines (B1-31-A, B1-42-1A, B1-45-A) were identified using 5'RACE method. B1-31-A insertional mutants displayed FP expression in vasculature, and were found to have the gene trap integrated into the first intron of the predicted gene, *ENSDART00000114996.* B1-42-1A embryos had FP-positive heart and

somites, and the integration of transposon was mapped in the third intron of the *pdlim7* (*PDZ and LIM domain 7*) gene. Interestingly, Camarata and others (2010) demonstrated that *pdlim7* is co-expressed with *tbx5a* during cardiac and pectoral fin development. Moreover, it was shown that Pdlim7 protein regulates nuclear/ actin cytoskeletal associated localization and transcriptional activity of Tbx5a during cardiac atrioventricular boundary and valve development (Camarata et al. 2010). B1-45-A line exhibited FP expression in the brain, and was determined to have the gene trap integration in the first intron of *smndc1* (*survival motor neuron domain containing 1*) gene.

Table 2. Summary of the identified gene trap lines, their expression patterns, used identification methods, names of the trapped genes, and locations of the mapped gene trap integrations.

Gene trap line	**Expression pattern**	**Identification method**	**Location of integration**	
			Trapped gene ID	**Intron**
B4-12-1	Ubiquitous	5'RACE	Unidentified	Unidentified
B4-12-2	Floor plate	iPCR	*ENSDART 00000112671*	2
B1-31A	Vascular	5'RACE	*ENSDART 00000114996*	1
B1-40A	Blood	iPCR	*ENSDART 00000111400*	1
B1-42-1A	Heart and somits	5'RACE	*pdlim7*	3
B1-45A	Brain	5'RACE	*smndc1*	1
B4-23-1	Vascular	iPCR	*fli1b*	1
B4-24-1	Neural crest	5'RACE	Unidentified	Unidentified

3. 2. Vascular regeneration studies in *fli1b*^{tpl50} insertional mutants

In order to test if *fli1b* function is required for vascular regeneration, a blind experiment was carried out. Fourteen adult fish siblings obtained from the same incross of *fli1b*$^{tpl50/+}$ were tail clipped, and the regeneration process at four different stages was observed and documented.

After the regeneration experiment was completed, the previously amputated and frozen tail-clips were successfully used for DNA extraction. The genotyping results showed that only one out of fourteen fish was homozygous for *fli1b*^{tpl50} mutation (Fig. 18). These data suggested that *fli1b*$^{tpl50/tpl50}$ has reduced survivability as compared to *fli1b*$^{tpl50/+}$.

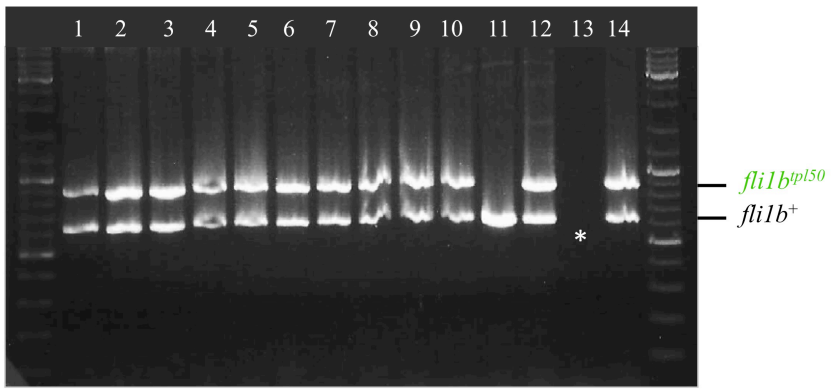

Figure 18. Genotyping results for *fli1b* locus via three-primer PCR. Each lane contains the PCR product amplified on DNA extracted from a single adult fish from the incross of *fli1b*$^{tpl50/+}$.

The examination of the expression of *fli1b*^{tpl50} gene trap allele after caudal fin amputation revealed that GFP is significantly upregulated in vasculature of caudal fin at 7 dpa (Fig. 19). Upregulation of GFP expression was detected in both heterozygotes and homozygotes. The *fli1b*$^{tpl50/tpl50}$ fish died after anesthesia at

7dpa. The GFP expression in *fli1b*$^{tpl50/+}$ was constantly decreasing over time. The significant reduction of fluorescence was observed at 14 dpa, and returned to almost pre-amputation level at 21 dpa (Fig. 19).

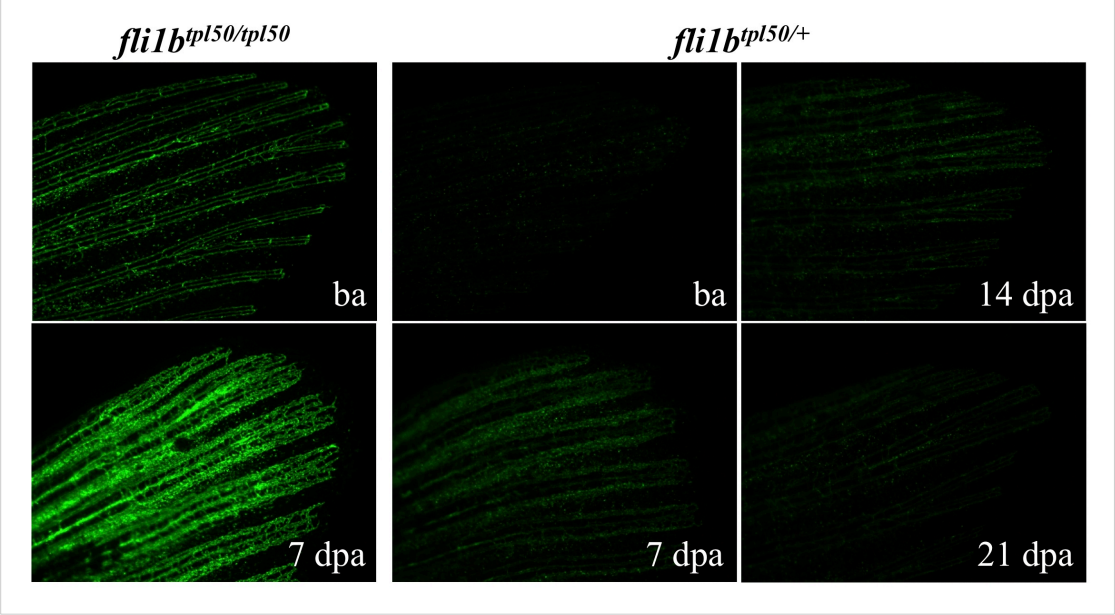

Figure 19. GFP expression changes in vasculature of the regenerating caudal fin in *fli1b*$^{tpl50/tpl50}$ and *fli1b*$^{tpl50/+}$ adult fish. Each picture shows the upper tip of the distal part of regenerating tail.

GFP expression analysis in the regenerating caudal fin of *fli1b*^{tpl50} adult fish also revealed a presence of large number of fluorescence-positive cells in the bloodstream at 7 dpa. There were at least two different types of circulating cells observed. Some cells were small and fast moving, while other cells were large and slow moving. The number of GFP-positive cells significantly decreased at 14 dpa, and further diminished almost to pre-amputation level at 21 dpa. Importantly, before amputation small GFP-positive blood cells were rare, while large GFP-positive cells were not detected. Interestingly, a low number GFP-positive cells was also noticed in 1 dpf *fli1b*^{tpl50} embryos. The small GFP-positive cells observed in the bloodstream during tail regeneration could potentially be circulating

endothelial cells, while the large GFP-positive cells could be macrophages. They may arise either from wound blastema or elsewhere in the body in response to injury.

Despite the notably changing *fli1b* expression pattern during caudal fin regeneration, it was found that *fli1b*$^{tpl50/+}$ adult zebrafish regrew vascular system normally. Tails of *fli1b*$^{tpl50/+}$ seemed to be totally regenerated at 21 dpa, but still had less pigmentation as compared to their pictures taken before the amputation. It is possible that regeneration proceeds normally because *fli1a* gene product compensated for the absence or reduced level of Fli1b protein. In repeat experiments, *fli1b*$^{tpl50/tpl50}$ were found to regenerate fins unevenly (data not shown). The upper part of the caudal fin was regrowing faster than the lower one. However, at 21 dpa the regenerated tails appeared normal.

3. 3. Morphological/ anatomical and genotypic analysis of *tbx5a*^{tpl58} embryos and adults

A detailed phenotypic analysis of zebrafish embryos obtained from an outcross of *tbx5a*$^{tpl58/+}$ with UAS reporter line revealed that *tbx5a*^{tpl58} mutation in *tbx5a* causes haploinsufficiency in zebrafish. Haploinsufficient phenotype was found to be fully penetrant. In comparison to wild type siblings (n = 290), all analyzed *tbx5a*$^{tpl58/+}$ embryos (n = 241), revealed a significant reduction of the pectoral fins at 6 dpf (Fig. 20). The observed *tbx5a* dose-dependent pectoral fin phenotype coincides with previously published defects in zebrafish *tbx5a* morphants (Ahn et al. 2002). Moreover, a negative effect for upper limb development due to the haploinsufficiency of *tbx5a* is also known from the analysis of mice knockouts heterozygous for *Tbx5* (Bruneau et al. 2001) and clinical data about human patients lacking functional copy of *TBX5* (Basson et al. 1999).

The majority (60 %) of all examined *tbx5a*$^{tpl58/+}$ embryos had equally affected pectoral fins. One third of the *tbx5a*$^{tpl58/+}$ (29%) had a left pectoral fin more affected than a right. Only 11 % of the heterozygotes showed more affected right pectoral fin. Importantly, the frequency of the unequally affected pectoral fins in *tbx5a*$^{tpl58/+}$ zebrafish embryos corresponds to the occurrence of the forelimb reduction in humans (Poznanski et al. 1970; Newbury-Ecob et al. 1996). These findings suggest that a role of *tbx5a* gene in both zebrafish and human forelimb development is highly conserved.

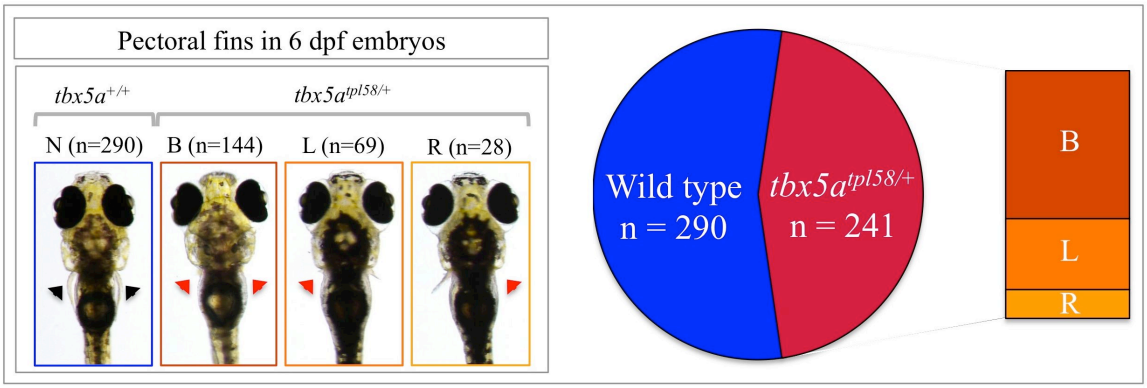

Figure 20. Haploinsufficiency of *tbx5a* in *tbx5a*$^{tpl58/+}$ embryos results in the pectoral fin defects. N – normal pectoral fins, B - both pectoral fins equally affected, L - left pectoral fin more affected, R - right pectoral fin more affected.

The statistical analysis (The exact binomial test of goodness-of-fit) rejected the null hypothesis that the number of the observed mRFP-negative (showing no pectoral fin phenotype) and mRFP-positive embryos (exhibiting developmental phenotype of pectoral fins) from *tbx5a*$^{tpl58/+}$ heterozygous outcross fit the theoretical expectations (the number of mRFP-positive embryos is equal to the number of mRFP-negative embryos). It was determined that the number of embryos exhibiting developmental phenotypes (*tbx5a*$^{tpl58/+}$) is significantly different from a number of embryos showing no phenotype (*tbx5a*$^{+/+}$) ($p = 0.037$). Thus, approximately 17% of *tbx5a*$^{tpl58/+}$ embryos die before 3 dpf. It was noticed

that usually 3 - 5% of *tbx5a*$^{tpl58/+}$ survive until adulthood. In all examined *tbx5a*$^{tpl58/+}$ adults (n = 48), pectoral fins were absent (Fig. 21). Moreover, all hearts dissected from *tpl58* heterozygotes (n = 13) exhibited overt cardiac phenotype: enlarged atrium and misshaped ventricle. The observed heart defects are similar to the cardiac malformations characterized in mice knockouts heterozygous for *Tbx5* (Bruneau et al. 2001). This phenotypic similarity implies for a high conservation level of *tbx5a* function in vertebrate heart development.

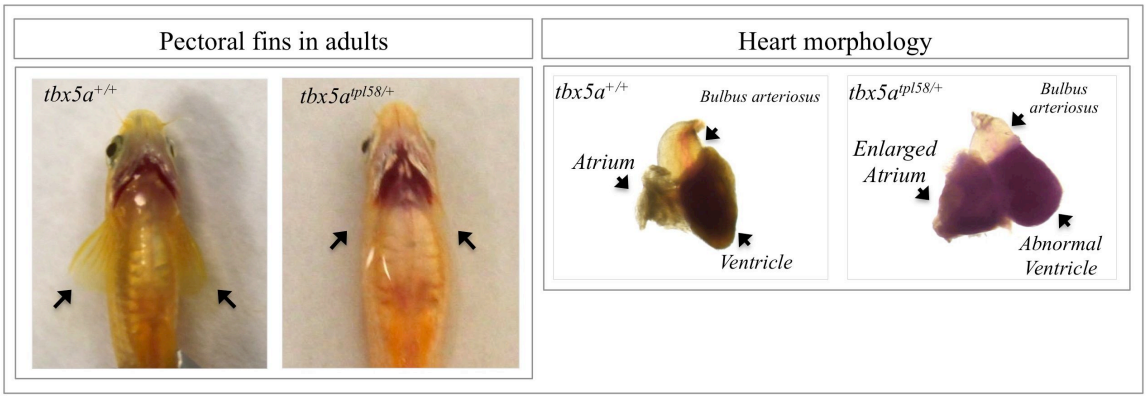

Figure 21. Haploinsufficiency of *tbx5a* in *tbx5a*$^{tpl58/+}$ adults results in the pectoral fin and cardiac defects.

Since *tbx5a* is an essential transcription factor during cardiogenesis, it may also be an important player during cardiac regeneration. In order to test this hypothesis, a partial ventricular resection was performed in *tbx5a*$^{tpl58/+}$ adults. One month after amputation resected ventricles exhibited a significant scar formation. These data suggest that, in zebrafish, haploinsufficieny of *tbx5a* negatively affects cardiac regeneration. On the other hand, since *tbx5a*$^{tpl58/+}$ fish display fully penetrant haploinsufficient cardiac phenotype characterized by abnormal morphology (enlarged atrium and abnormal shape of the ventricle), it is not clear if the observed phenotype is direct or indirect consequence of *tbx5a* haploinsufficiency.

In order to characterize a homozygous phenotype in *tbx5a*^{tpl58} insertional line, *tbx5a*$^{tpl58/+}$ were incrossed through an *in vitro fertilization (IVF)*. Only mRFP-positive embryos were included in analysis. In total, 363 embryos from 6 clutches were examined (Fig. 20). Single embryo genotyping of a clutch containing 27 embryos was performed. Homozygocity for *tbx5a*^{tpl58} mutation of the *tbx5a* gene was found to result in a fully penetrant lethal phenotype. All *tbx5a*$^{tpl58/tpl58}$ homozygous embryos exhibit linear heart and completely lack pectoral fins (Fig. 22). The observed cardiac and pectoral fin defects are highly similar to the previously published phenotypes in *tbx5a* morphants (Ahn et al. 2002) as well as *tbx5a* ENU mutant, *heartstrings* (*tbx5a*^{hst} hereafter) (Garrity et al. 2002). However, the cardiac defects observed in *tbx5a*$^{hst/hst}$ range from mild (edema and non-completely looped heart) to severe (edema and linear heart), while all *tbx5a*$^{tpl58/tpl58}$ always show severe heart phenotype. Since truncated Tbx5a in *tbx5a*^{hst} mutant remains a T-box DNA binding domain, protein may still have some activity. In comparison, Tbx5a-Gal4 fusion protein in *tbx5a*^{tpl58} mutant completely lacks T-box binding domain. Therefore, *tbx5a*^{tpl58} is expected to be a null allele.

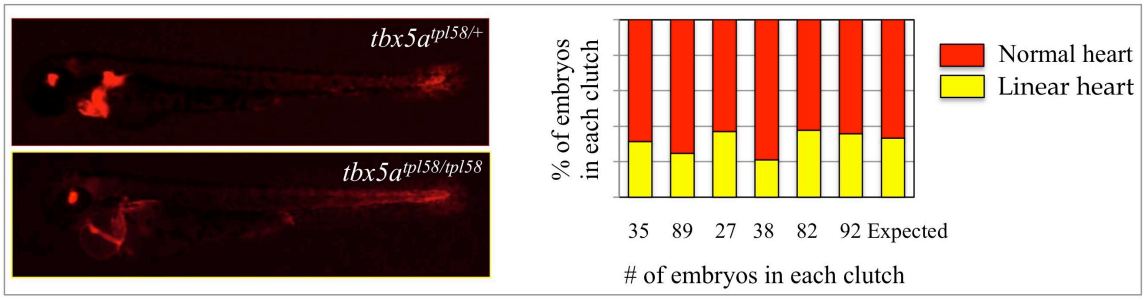

Figure 22. Homozygocity in *tbx5a*^{tpl58} results in a lethal cardiac phenotype.

3. 4. *tbx5a* BAC rescue of the morphological/ anatomical defects in the *tbx5a*^{tpl58} and *tbx5a*^{hst} mutants

In order to rescue mutations in *tbx5a* gene, zebrafish line pKS12, *BAC(tbx3a:YFP;tbx5a)*, previously generated in dr. Balciunas lab was crossed with *tbx5a*$^{hst/+}$ and *tbx5a*$^{tpl58/+}$. The *BAC(tbx3a:YFP;tbx5a)* line carries a bacterial artificial chromosome (BAC) that contains 144155 bp genomic DNA region of zebrafish chromosome 5 that encompasses two entire genes, *tbx3a* and *tbx5a*, and a gene desert upstream and downstream of them (Fig. 23). Interestingly, in all vertebrates, *tbx3* and *tbx5* are always segregating together in a single cluster (Horton et al. 2008). Moreover, both genes are expressed in the developing heart (xx) and forelimbs (Gibson-Brown et al. 1998; Yonei-Tamura et al. 1999; Wang et al. 2014). This suggests that *tbx3* and *tbx5* can potentially possess shared cis-regulatory elements essential for proper development of the heart and forelimbs. Thus, a BAC containing both genes is a potential candidate for rescue experiments. In order to avoid an overexpression of *tbx3a*, *BAC(tbx3a:YFP;tbx5a)* has an insertion of a Venus yellow fluorescent protein (YFP) sequence that is followed by the SV40 transcription termination sequence engineered into the first exon of *tbx3a* gene, 471 bp downstream of ATG (Fig. 23). Therefore, *tbx3a* gene is mutated, and YFP mimics *tbx3a* expression that can be used as a selection marker for the presence of BAC in the genome.

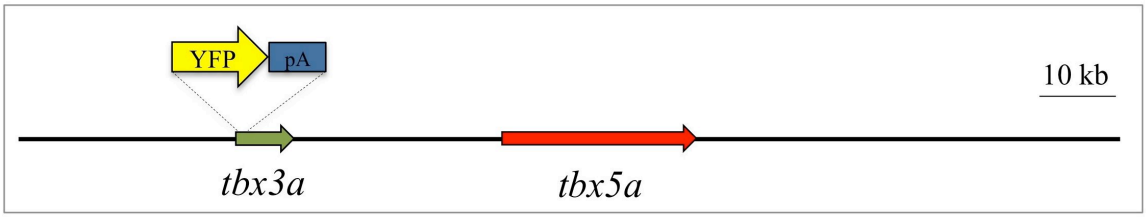

Figure 23. Zebrafish genomic region in *BAC(tbx3a:YFP;tbx5a)*.

In order to test if *BAC(tbx3a:YFP;tbx5a)* can rescue mutations in *tbx5a* gene, *tbx5a*$^{tpl58/+}$*;BAC(tbx3a:YFP;tbx5a)* and *tbx5a*$^{hst/+}$*;BAC(tbx3a:YFP;tbx5a)* trans-heterozygous lines have been established and later outcrossed to *tbx5a*$^{hst/+}$. The obtained progeny was screened for fluorescence at 2 dpf. Phenotypic analysis was performed at 3 dpf and 6 dpf.

Since *hst* mutation is recessive (Garrity et al. 2002), only 25% of embryos from *tbx5a*$^{hst/+}$ incross are expected to exhibit mutant phenotype (linear or not completely looped heart and absence of the pectoral fins). When *tbx5a*$^{hst/+}$*;BAC(tbx3a:YFP;tbx5a)* zebrafish were crossed with *tbx5a*$^{hst/+}$, 78% of embryos (n = 113) displayed no phenotype corresponding with the expectations. However, only 10 % of the progeny (n = 15/145) exhibited the expected homozygous phenotype, while 12% (n =17) had reduced pectoral fins and normal heart. The fact that partial reduction of the pectoral fins is never found in zebrafish heterozygous or homozygous for *tbx5a*^{hst} allele suggests that the observed phenotype is either an outcome of the overexpression of *tbx5a* in wild type embryos or a result of the partial rescue of *hst* mutation. Five embryos were sacrificed for DNA extraction. According to genotyping results, all five embryos were *tbx5a*$^{hst/hst}$. These data indicate that an additional copy of *tbx5a* provided with BAC is sufficient to rescue a phenotype caused by a *heartstrings* mutation in *tbx5a* gene. Interestingly, one from 12 raised embryos survived to adulthood. The *tbx5a*$^{hst/hst}$*;tbx5aBAC(tbx3a:YFP;tbx5a)* adult fish completely lacked pectoral fins and survived for 6 months. Thus, *BAC(tbx3a:YFP;tbx5a)* allele can rescue lethal phenotype in *tbx5a*$^{hst/hst}$ mutants.

In order to test if the same BAC copy that rescues *tbx5a*^{hst} mutation can rescue a phenotype caused by an insertional *tbx5a*^{tpl58} mutation in *tbx5a* gene, *tbx5a*$^{hst/hst}$*;BAC(tbx3a:YFP;tbx5a)* male was crossed through an *IVF* to *tbx5a* $^{tpl58/+}$ female. From previous unpublished observations it is known that when *tbx5a*$^{hst/+}$ is crossed to *tbx5a*$^{tpl58/+}$, 25% of the obtained progeny have linear heart and no pectoral fins indicating that *tbx5a*$^{hst/tpl58}$ embryos exhibit homozygous phenotype

similar to the one described for *tbx5a*$^{hst/hst}$ or *tbx5a*$^{tpl58/tpl58}$. It was found that 3% of embryos (n = 91) obtained from the cross of *tbx5a*$^{hst/hst}$*;BAC(tbx3a:YFP;tbx5a)* with *tbx5a*$^{tpl58/+}$ had a partially rescued heart, but no pectoral fins. However, so far no embryos survived to adulthood.

3. 5. Restoration of normal development by the revertion of *tbx5a*^{tpl58} mutation using Flp^{o} recombinase

In order to test if a mutagenic cassette in *tbx5a*^{tpl58} can be inverted by Flp^{o} recombinase *in vivo*, one-cell stage zebrafish embryos (n = 92) obtained from the outcross of *tbx5a*$^{tpl58/+}$ with UAS reporter line were injected with 75 pg of *Flp*^{o} mRNA. Screening for mRFP expression at 3 dpf revealed that some F0 embryos exhibited somatic mosaicism such as a reduction in mRFP and/or milder pectoral fin phenotype (Fig. 24).

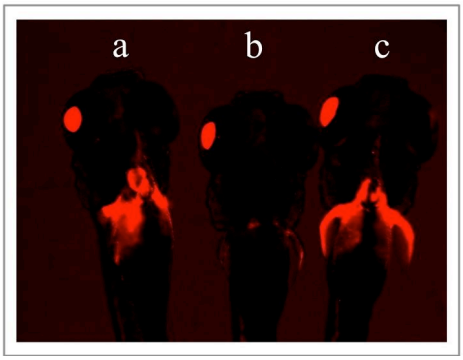

Figure 24. Injections of 75 pg of *Flp*^{o} mRNA into 1-cell stage *tbx5a*$^{tpl58/+}$ result in somatic mosaicism; a –uninjected embryo (control), b – mRFP reduction in the injected embryo, c – milder pectoral fin phenotype in the injected embryo.

All mRFP-positive F0 embryos were raised until maturity. F0 adults that showed milder pectoral fin phenotypes were outcrossed to UAS reporter line. F1 embryos were screened for mRFP and scored. In case if the germline is mosaic for

tbx5a gene trapped allele with a reverted mutagenic cassette, less than 50% of F1 embryos obtained from an outcross are expected to show mRFP expression. One of the F0 females when outcrossed to UAS reporter line gave a clutch that had only 13% of the mRFP-positive embryos. First clutch of F1 embryos was sacrificed for genotyping single embryos. According to genotyping results, 3 out of 16 embryos carried a *tbx5a*^{tpl58} allele with a reverted mutagenic cassette (*tbx5a*^{tpl58R} hereafter) (Fig. 25). Three mRFP-positive embryos were confirmed to be *tbx5a*$^{tpl58/+}$, and 12 embryos were found to be wild type. Interestingly, wild type allele revealed a polymorphism that possibly may or may not affect the type of reduction of the pectoral fins. Genotyping results were confirmed by sequencing four bands: *tbx5a*^{tpl58}, *tbx5a*^{tpl58R} and two wild type bands of different size.

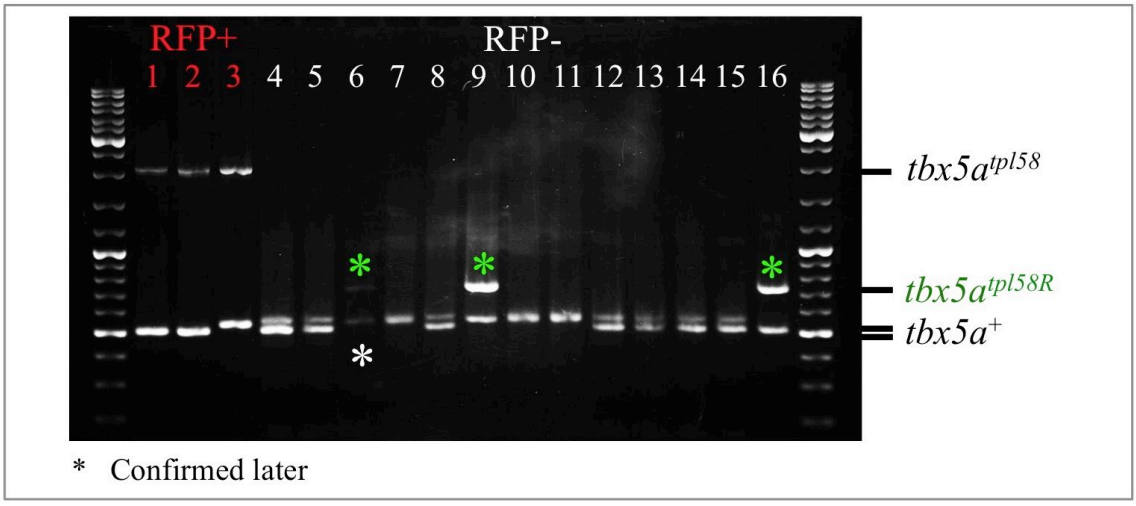

Figure 25. Single F1 embryo genotyping via three-primer PCR: germline mosaicism in *tbx5a*$^{tpl58/+}$ heterozygotes injected with 75 pg of *Flp*^{o} mRNA.

To establish a stable *tbx5a*^{tpl58R} full revertant line, the same F0 female was outcrossed again. Obtained F1 progeny was screened for mRFP, and only mRFP-negative F1 embryos were raised to adulthood. Adult fish were genotyped with three primers PCR. Thereafter, confirmed *tbx5a*$^{tpl58R/+}$ were incrossed to generate

homozygous full revertants. Adults homozygous for *tbx5a*^{tpl58R} did not show any mRFP expression and did not revealed any overt phenotype (Fig. 26).

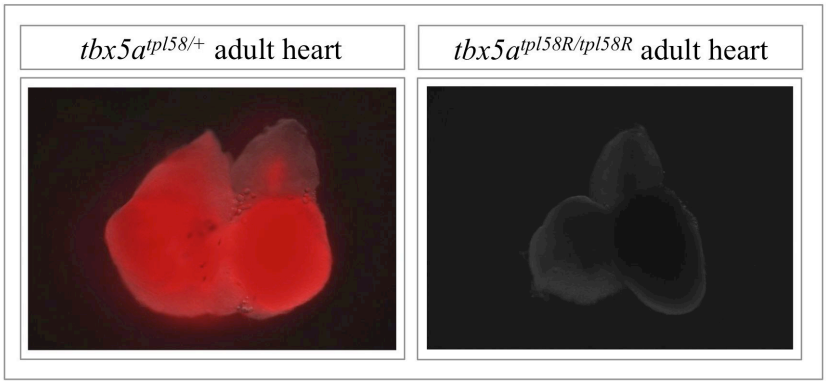

Figure 26. In comparison to *tbx5a*$^{tpl58/+}$ adult heart, full revertant homozygous adult heart exhibits normal morphology and has no mRFP expression, indicating that *tpl58* mutation in *tbx5a* locus is turned off.

3. 6. Analysis of *-3.3nkx2.5* and *-6.1nkx2.5* activity during normal heart development

In vertebrates, expression pattern of the *nkx2.5* gene corresponds to the early cardiac progenitors location (Chen & Fishman, 1996; Lee et al. 1996), and, according to *in vitro* studies, precedes expression of early cardiac markers (Komuro and Izumo 1993; Lints et al. 1993). In zebrafish, *nkx2.5* continuously labels pre-mature cardiomyocardiocytes during all heart developmental stages and remains transcriptionally active in the adult heart (Chen & Fishman, 1996; Raya et al. 2003). These features make the *nkx2.5* promoter a potentially very useful as an early cardiac-specific driver for protein of interest. In order to characterize regulatory DNA regions of *nkx2.5*, two stable transgenic zebrafish lines, -3.3*nkx2.5:RFP-pA/INS* and -6.1*nkx2.5:RFP-pA/INS*, were generated.

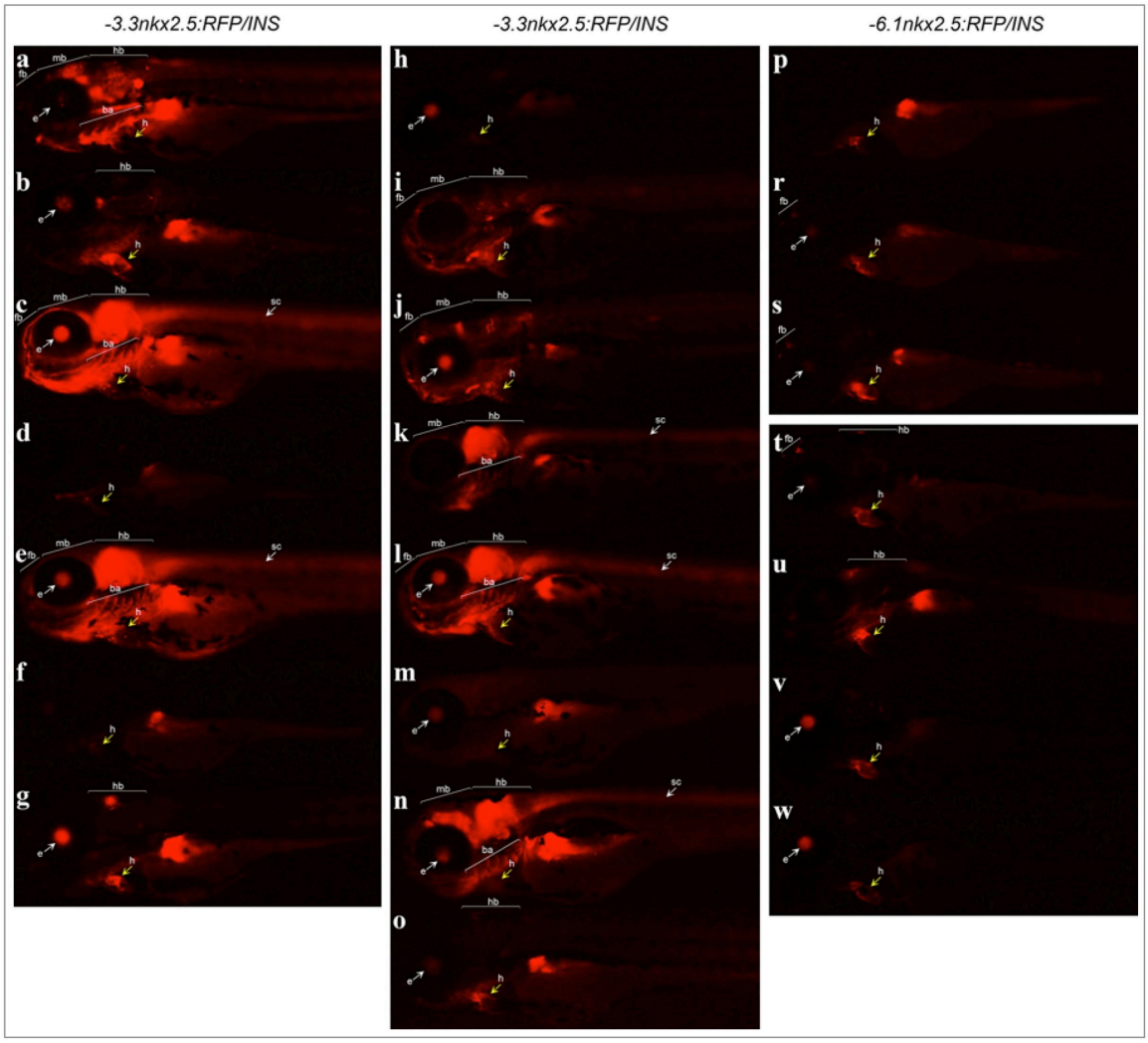

Figure 27. Different mRFP expression patterns in -3.3*nkx2.5:RFP-pA/INS* and -6.1*nkx2.5:RFP-pA/INS* transgenic embryos: a-g F1progeny of -3.3*nkx2.5:RFP-pA/INS* (a parent A; b-d parent B; e-g parent C), h-o F2 progeny of -3.3*nkx2.5:RFP-pA/INS* (h parent A; i-m parent B, n, o parent C), p-s F1 progeny of -6.1*nkx2.5:RFP-pA/INS* (p parent A; r parent B; s parent C), t-w F2 progeny of -6.1*nkx2.5:RFP-pA/INS* (t parent A; u, v parent B, w parent C). A yellow arrow points a heart-specific mRFP. Abbreviations: *ba* branchial arches, *e* eye, *fb* forebrain, *h* heart, *hb* hindbrain, *mb* midbrain, *sc* spinal cord (Grajevskaja et al. 2013).

It was found that both fragments tested are sufficient to activate transcription of mRFP in the embryonic zebrafish heart at 3 dpf (Fig. 27).

Therefore, both genomic regions analyzed contain cardiac-specific enhancers that are active during cardiogenesis. However, in both transgenic lines, mRFP expression was not restricted to the heart, but was also detected in the forebrain, hindbrain, and eye (Fig. 27).

In contrast to -6.1*nkx2.5:RFP-pA/INS*, in -3.3*nkx2.5:RFP-pA/INS* line, mRFP was also found in the branchial arches, midbrain, spinal cord, and pectoral fins. Moreover, in -3.3*nkx2.5:RFP-pA/INS*, ubiquitous mRFP expression was also common, while, in -6.1*nkx2.5:RFP-pA/INS*, ubiquitous patterns were never observed. In contrast to -3.3*nkx2.5:RFP-pA/INS*, -6.1*nkx2.5:RFP-pA/INS* F2 embryos exhibited bright mRFP expression in the heart. Two out of three -6.1*nkx2.5:RFP-pA/INS* lines displayed bright mRFP in both ventricle and bulbus arteriosus (Fig. 27: t, v, w), while one – only in the bulbus arteriosus (Fig. 27:u) (Grajevskaja et al. 2013).

To sum up, from two potential promoter regions of *nkx2.5* gene analyzed, -3.3 kb and -6.1 kb, the longer genomic fragment shows higher cardiac specificity characterized by bright mRFP expression in the heart and low or no mRFP expression in other organs and tissues. The higher variety of the expression patterns in embryos carrying -3.3 kb regulatory sequence suggests that this DNA region is more susceptible to the site position effect (Grajevskaja et al. 2013).

3. 7. Functional analysis of the chicken β-globin insulators in the zebrafish genome during normal cardiogenesis

The susceptibility of the transgenic constructs to enhancers and silencers results in variegation that remains an important obstacle for a precise analysis of the gene expression pattern and intensity. To obtain comparable and reproducible data, a strategy to protect transgene from the endogenous regulatory elements is needed. One of the solutions could be flanking a transgene with insulation elements. The 1.2 kb chicken hypersensitive site-4 insulation sequences (cHS4

hereafter) derived from chicken β-globin locus were previously shown to inhibit spread of heterochromatin and shield from transcriptionally active domains in drosophila and human erythroid cells (Chung et al. 1993). Chung and others (1997) also demonstrated that the 250 bp CpG island of cHS4 provides the main insulating activity.

In order to test if cHS4 insulation sequences can prevent a transgene from the falling under the control of the endogenous regulatory elements, cHS4 insulators were cloned upstream and downstream of the two constructs, -3.3*nkx2.5:RFP-pA* and -6.1*nkx2.5:RFP-pA*. Three independent founders representing at least three independent integrations for every transgenic construct were generated. Outcrosses of F1 families revealed that some lines carry multiple copies of the transgene. In total, from 1 to 5 distinct mRFP expression patterns from a single family have been uncovered (Table 3).

Table 3. Transgenesis and copy number data for all *nkx2.5:mRFP* constructs used (Grajevskaja et al. 2013).

Transgene	F1 family	# of F2 embryos					# of mRFP patterns
		Total #	Lens GFP+	%	Lens GFP−	%	
Tg(CHS4,-3.3nkx2.5:RFP,crygc:GFP,CHS4)	A	32	21	65.62	11	34.38	1
	B	103	97	95.09	5	4.91	5
	C	43	40	93.02	3	6.98	2
	D	68	34	50	34	50	1
Tg(CHS4,-6.1nkx2.5:RFP,crygc:GFP,CHS4)	A	50	35	70	15	30	1
	B	146	107	73.29	39	26.71	2
	C	23	8	34.78	15	65.22	1
Tg(-6.1nkx2.5:RFP-pp(A),crygc:GFP)	A	41	38	92.68	3	7.32	1
	B	28	26	92.86	2	7.14	1
	C	29	26	89.66	3	10.34	2
Tg(-6.1nkx2.5:RFP-zp(A),crygc:GFP)	A	87	45	51.72	42	48.28	1
	B	136	24	17.65	112	82.35	1
	C	34	17	50	17	50	1

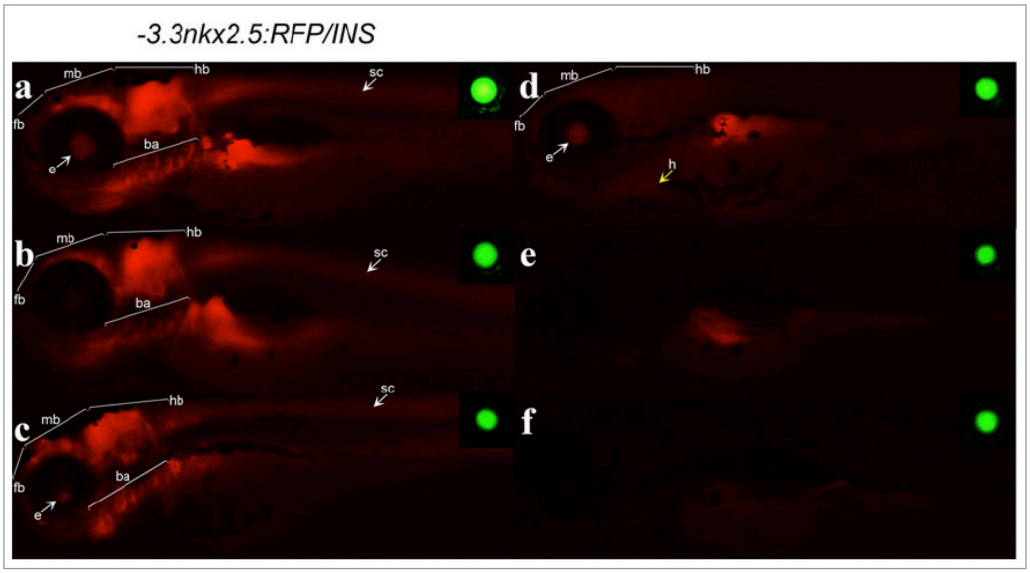

Figure 28. Variegation of mRFP and GFP expression in siblings carrying a single-copy of *-3.3nkx2.5:RFP/INS*. Lens GFP is shown in the upper right corner of each picture. A yellow arrow points to the heart-specific mRFP. *ba* branchial arches, *e* eye, *fb* forebrain, *h* heart, *hb* hindbrain, *mb* midbrain, *sc* spinal cord (Grajevskaja et al. 2013).

As previously mentioned, in -3.3*nkx2.5:RFP-pA/INS*, mRFP expression patterns ranged from highly tissue-specific (restricted to the heart and/or brain) to very ubiquitous (Fig. 28). Most likely the detected patterns mimic the expression of other genes, which enhancers operate in the vicinity of the transgene integration site and by directly activating the core promoter of the *nkx2.5* drive mRFP expression in particular cells. Interestingly, -3.3*nkx2.5:RFP-pA/INS* siblings carrying a single copy of the transgene exhibited different mRFP expression levels that varied from high (Fig. 28: a - c) to very weak (Fig. 28: d - f), and the observed mRFP variegation correlated with the lens-specific GFP expression intensity (Fig. 28). The presence of the diverse expression patterns and highly variable levels of mRFP clearly indicate that regulation of the -3.3*nkx2.5:RFP-pA/INS* transgene expression is affected by its genomic location.

Similarly, the expression of -6.1*nkx2.5:RFP-pA/INS* transgene was also found to be dependent on the genomic position effect. However, in comparison to -3.3*nkx2.5:RFP-pA/INS*, consistent heart-specific expression patterns as well as lower variegation of mRFP were observed (Fig. 28: p - w). This "improvement" suggests that longer *nkx2.5* promoter contains cardiac-specific enhancer(s) and is less susceptible for the site position effect. Importantly, -6.1 kb *nkx2.5:RFP-pA* transgene without insulator sequences showed higher cardiac specificity and lower levels of mRFP expression (Fig. 28). This observation implies that insulator elements not only fail to protect transgenic constructs from the positional effect, but also potentially can contribute to the increased transgene expression.

All together, obtained results indicate that, in contradiction to the expectations, cHS4 insulators cannot be used as a genetic tool to reduce or eliminate chromosomal position effect on the expression of the transgenic constructs in zebrafish. This data contradicts the results published by Bessa and others (2009). The controversial results may be explained by the fact that Bessa and colleagues (2009) performed their experiments in F0 embryos, and flanked the tested promoter sequences with two different insulators, GAB upstream and cHS4 downstream. Strikingly, it was found that cHS4 insulator elements have an opposite effect (induce spread of heterochromatin) on the transgene expression in zebrafish genome. This observation coincides with the published mice data (Emery et al. 2000; Rivella et al. 2000; Yannaki et al. 2002; Yao et al. 2003; Rincon-Arano et al. 2007; Yahata et al. 2007; Ochiai et al. 2011; Sharma et al. 2012; Emery et al. 2013; Uchida et al. 2013).

3. 8. *tnnt2a* promoter can be used as a heart-specific CreER^{T2} driver

In principle, to achieve a heart-specific re-mutation of *tbx5a* in *tbx5a*^{tpl58R} zebrafish at a particular time point, a strong cardiac-specific promoter that could successfully drive a 4-HT inducible Cre is required. For this purpose, a

tnnt2a:CreER^{T2} transgenic line was previously generated in dr. Balciunas lab. To test a specificity of generated CreER^{T2} driver, *tnnt2a:CreER^{T2}* heterozygotes were outcrossed to pDB860 reporter line. Their 2 dpf progeny was separated into two groups: experimental and control. An experimental group was treated for 24h with 0.1μM tamoxifen (TAM hereafter) that is converted by liver to its active metabolite, 4-HT (Holmes and Liticker 2005). At the same time, a control group was treated with DMSO. Next day embryos were screened for RFP in the lens and GFP expression in any part of the body.

Table 4. Heart-specific GFP expression in the progeny of *tnnt2a:CreER^{T2}* and pDB860 cross at 3 dpf.

Results / Genotype	Expected outcome, %	RFP lens	GFP heart (TAM-induced)	Observed outcome, %
tnnt2a:CreER^{T2};pDB860	25	+	+	29.7
tnnt2a:CreER^{T2}	25	+	-	28.4
pDB860	25	+	-	24.3
Wild type	25	-	-	17.6

According to the screening results, 29.7 % of embryos treated with TAM exhibited bright GFP-positive hearts at 3 dpf (Table 4). Since GFP expression was detected in the heart and nowhere else that implies that an activity of *tnnt2a* promoter is restricted to the heart (Fig. 29). These results collaborate with previously published *in situ* hybridization data for *tnnt2* gene expression analysis in zebrafish embryos (Hsiao et al. 2003).

Unlike an experimental group, control embryos did not show any GFP expression in the heart (Fig. 29), meaning that CreER^{T2} protein can translocate from the cytoplasm to the nucleus only after conformational change induced by 4-HT. Therefore, *tnnt2a* CreER^{T2} driver is not leaky and can potentially be used to invert a mutagenic cassette specifically in the cardiac tissue of *tbx5a^{tpl58R}* zebrafish resulting in a re-mutaion of *tbx5a* gene only in the heart.

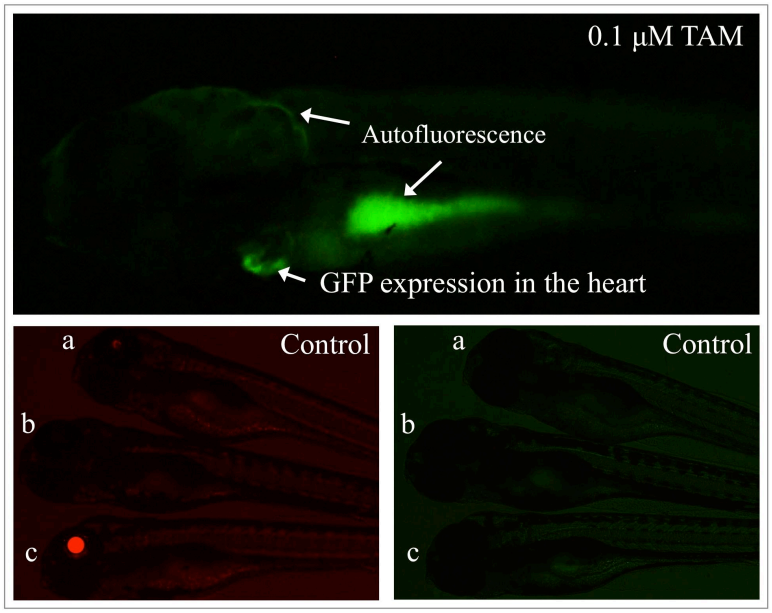

Figure 29. Testing *tnnt2a:CreERT2* for specificity. In TAM treated embryos GFP was detected specifically in the heart. Weak autofluorescence was observed in the head and strong autofluorescence was detected in the yolk. Control embryos treated with DMSO did not exhibit any GFP. a - *tnnt2a:CreERT2*, b – wild type, c – pDB860 or *tnnt2a:CreERT2;* pDB860.

3. 9. Conditional re-mutation of *tbx5a*^{tpl58R} locus specifically in the heart of the zebrafish embryos and adults

In order to determine if *tbx5a*^{tpl58R} locus can be re-mutated specifically in the embryonic zebrafish heart, *tbx5a*$^{tpl58R/tpl58R}$ fish were outcrossed to *tnnt2a:CreER*^{T2}, and obtained embryos were screened for fluorescence at 2 dpf. No mRFP expression was detected suggesting that a CreER^{T2} driver at least at that period in development is not leaky. The same day embryos were transferred into 0.5 µM 4-HT solution and kept there for 24 h in the dark. Next day embryos were screened for mRFP. It was found that an insertional *tbx5a*^{tpl58R} mutation was successfully re-mutated specifically in the heart of the *tbx5a*$^{tpl58R/+}$ zebrafish

embryo (Fig. 30a). All embryos with mRFP-positive hearts were raised to adulthood. At three months three adult fish were sacrificed, their heart dissected and screened for mRFP. All examined hearts were mRFP-positive suggesting that at least some cardiomyocytes that lack one functional copy of *tbx5a* persist in the heart during development. Moreover, although mRFP-positive cardiomyocytes remained during heart formation, the organ formed normally (Fig. 30b).

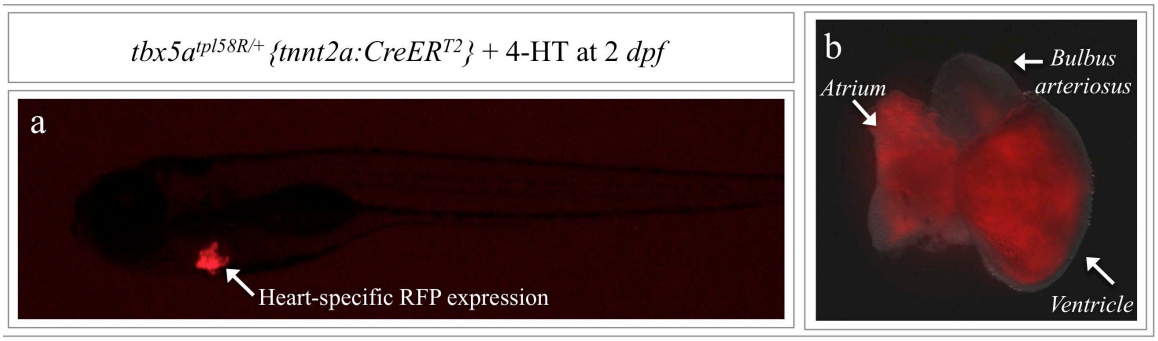

Figure 30. Re-mutation of *tbx5a* locus in the developing zebrafish heart: a – 4-HT induced heart-specific mRFP expression indicates a successful reversion of the mutagenic cassette in $tbx5a^{tpl58R}$; b – although cells re-mutated in embryo were not eliminated during cardiogenesis, adult heart morphology is normal.

To test if in a similar fashion $tbx5a^{tpl58R}$ mutation can be re-mutated heart-specifically in the adult zebrafsh, $tbx5a^{tpl58R/+}$;*tnnt2a:CreER*^{T2} and $tbx5a^{tpl58R/tpl58R}$; *tnnt2a:CreER*^{T2} double transgenic lines were established. Adult fish were incubated in 80 ml of 5µM 4-HT solution three times for 24 h. One week after the last incubation three fish were sacrificed. Dissected hearts were found to be mRFP-positive indicating that *tbx5a* can be successfully re-mutated in the adult zebrafish. These results are highly important because they demonstrate the first conditional induction of the mutation in the adult zebrafish and provide a way to test a role of the developmentally essential gene, *tbx5a*, in the heart regeneration.

3. 10. Cardiac regeneration studies in *tbx5a*^{tpl58R};*tnnt2a:CreER*^{T2} conditional mutants

For testing a role of *tbx5a* during adult zebrafish heart regeneration, *tbx5a*^{tpl58R} locus was re-mutated either in the embryonic or adult heart. To induce *tbx5a*^{tpl58} mutation specifically in the developing heart, 2 dpf embryos obtained from *tbx5a*$^{tpl58R/+}$;*tnnt2a:CreER*^{T2} outcross were treated with 4-HT, and pre-selected for mRFP at 3 dpf. To turn on *tbx5a*^{tpl58} mutation specifically in the adult heart, 2.5 months *tbx5a*$^{tpl58R/+}$;*tnnt2a:CreER*^{T2} and *tbx5a*$^{tpl58R/tpl58R}$;*tnnt2a:CreER*^{T2} double transgenic fish were incubated in 4-HT. In all cases, partial ventricular resection (Poss et al. 2002) was performed in 3 months old conditional mutants, and fish were sacrificed at 30 dpa.

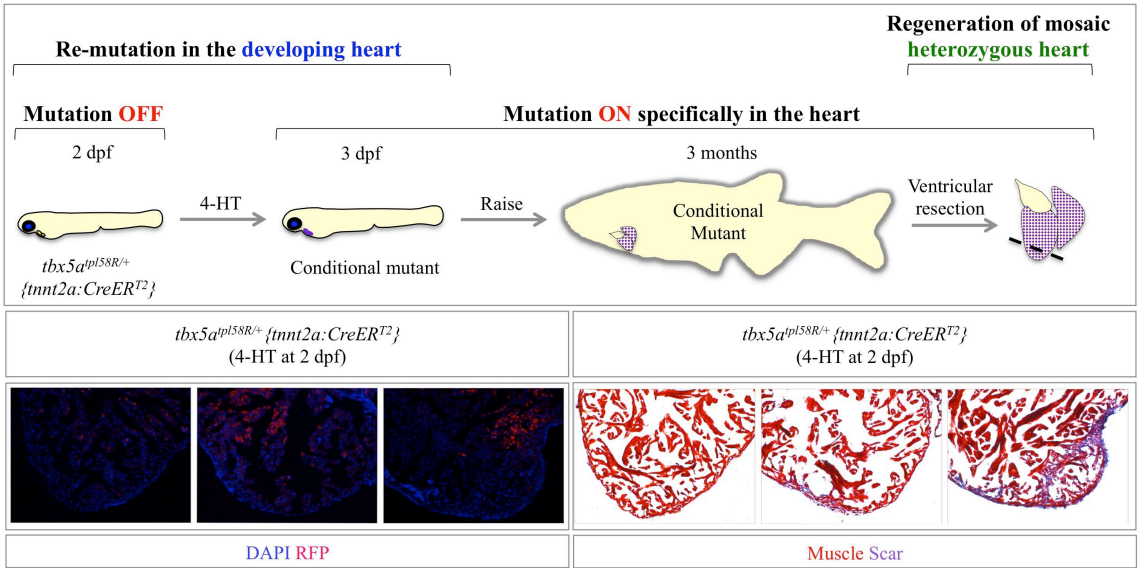

Figure 31. Heart sections of 30 dpa *tbx5a*$^{tpl58R/+}$;*tnnt2a:CreER*^{T2} adults that were treated with 4-HT at 2 dpf: a, c – normally regenerated ventricle; b, e – mild defects; c, f – severe scarring. Sections: a-c DAPI staining, d - f Picro-Mallory staining.

Five out of 7 hearts of *tbx5a*$^{tpl58R/+}$;*tnnt2a:CreER*^{T2} fish that were incubated in 4-HT as embryos showed impaired regeneration (Fig. 31). The severity of the observed regenerative phenotypes varied. Three hearts exhibited some deposition of collagen in the area of injury, while two hearts showed significant scar formation at the ventricular apex. The variation of phenotypes detected can be explained by the fact that the hearts were mosaic for the reverted *tbx5a*^{tpl58R} mutation (Fig. 31). The presence of regeneration phenotype in these mosaic ventricles suggests that *tbx5a* is important for heart regeneration. However, since *tbx5a*^{tpl58} mutation was induced during cardiogenesis, a possibility that the observed regeneration phenotype is an indirect consequence of *tbx5a* deficiency cannot be excluded.

In order to exclude a possibility of cardiac developmental defects being caused by *tbx5a* deficiency, *tbx5a*^{tpl58} mutation was induced in the adult *tbx5a*$^{tpl58R/+}$;*tnnt2a:CreER*^{T2} and *tbx5a*$^{tpl58R/tpl58R}$;*tnnt2a:CreER*^{T2} hearts. In comparison to ethanol treated *tbx5a*$^{tpl58R/tpl58R}$;*tnnt2a:CreER*^{T2} controls (n = 7) that completely regenerated partially resected ventricles, *tbx5a*$^{tpl58R/+}$;*tnnt2a:CreER*^{T2} incubated with 4-HT (n = 2) showed mild regenerative defects such as minor collagen deposition and abnormal shape of the ventricular apex. Meanwhile, *tbx5a*$^{tpl58R/tpl58R}$;*tnnt2a:CreER*^{T2} treated with 4-HT (n = 8) failed to regenerate partially amputated ventricles and exhibited severe cardiac regeneration defects such as a significant scar formation and misshaped ventricular apex (Fig. 32).

Statistical analysis (Fisher exact test of independence) showed that the null hypothesis, which states that the presence of heart regeneration defects is independent of 4-HT inducible *tbx5a*^{tpl58} mutation, could be rejected. The obtained results ($p = 0.002$) revealed that the ratio of the observed heart regeneration phenotypes is significantly different for fish treated with EtOH (mutation OFF) and 4-HT (mutation ON) (Table 5). Therefore, *tbx5a* is required for heart regeneration in *tnnt2a:CreER*^{T2}, *tbx5a*$^{tpl58R/tpl58R}$ adults.

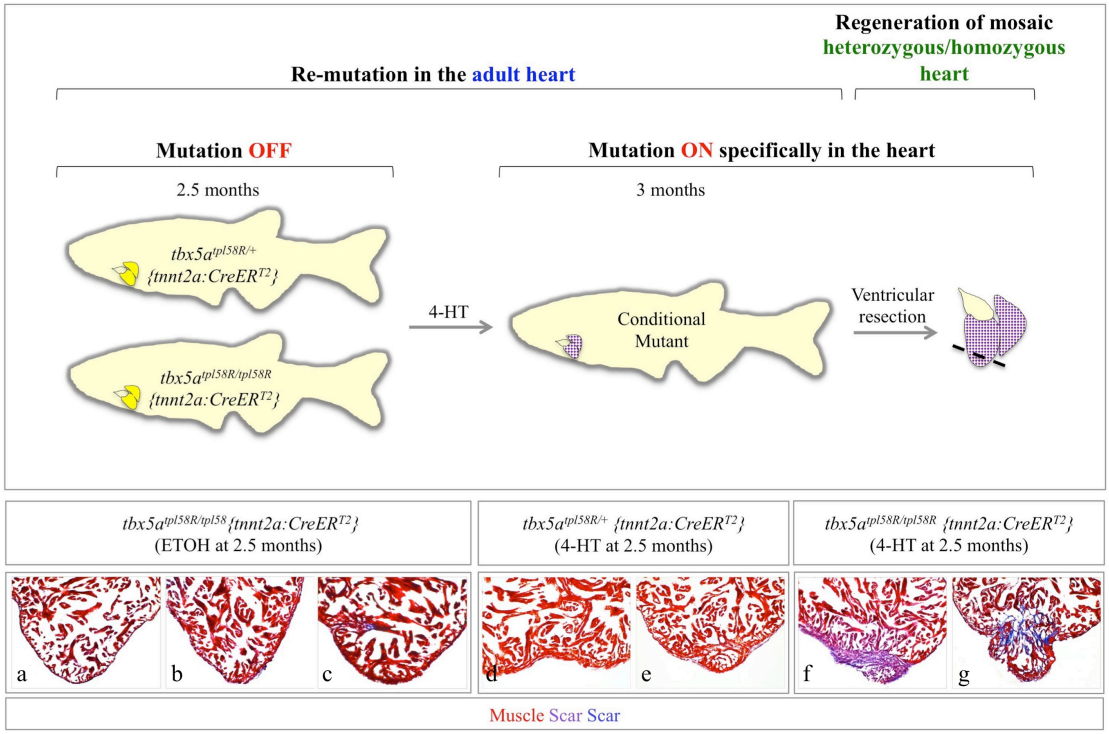

Figure 32. Picro-Mallory stained 30 dpa heart sections of *tbx5a* conditional mutants treated either with ethanol (control) or 4-HT at 2.5 month age: a - c – normally regenerated ventricles; d, e – mild defects; f – severe scar, g – severe scar and misshaped ventricular apex.

Table 5. Summary of the statistical analysis (Fisher exact test of independence) performed on the heart regeneration data obtained from *tbx5a*$^{tpl58R/tpl58R}$; *tnnt2a:CreER*^{T} adults treated either with ethanol (control group) or 4-HT (experimental group) at 2.5 month.

	Not regenerated ventricle (scar present)	Regenerated ventricle (scar absent)	Row Totals
Frequencies, EtOH (mutation OFF)	0	8	8
Percent of total	0.000%	53.333%	53.333%
Frequencies, 4-HT (mutation ON)	7	0	7
Percent of total	46.667%	0.000%	46.667%
Column totals	7	8	15
Percent of total	46.667%	53.333%	
Fisher exact p, one-tailed		p= .0002	
two-tailed		p= .0002	

Performed regeneration experiments in *tbx5a* conditional mutants revealed that *tbx5a* is critical for zebrafish cardiac regeneration. The first conditional induction of the mutation in adult fish as well as successful application of the conditional mutant to test a role of developmentally essential gene, *tbx5a*, in regeneration provides an important contribution to the regeneration studies in vertebrate organisms.

3. 11. Characterization of a novel *tbx5a* minimal enhancer in zebrafish *in vivo*

Transcriptional enhancers also known as cis-regulatory modules or genomic regulatory elements are DNA sequences that precisely coordinate spatial and temporal expression of the transcription factors in vertebrate development and disease. In humans, mutations in enhancer sequences are known to result in 'enhanceropathies' (Smith and Shilatifard 2014). For example, Smemo and colleagues (2012) have identified a single nucleotide polymorphism in a non-coding region upstream of *TBX5* gene that results in cardiac defects associated with Holt-Oram syndrome. However, there are many regulatory elements that still remain undiscovered.

Location of the enhancers in the genome can be predicted using a variety of approaches that include analyzing motifs and conservation, regulator binding, chromatin accessibility, histone modification and enhancer-promoter interactions (reviewed in Shlyueva et al. 2014). Analysis of epigenetic signatures such as DNA methylation sites was previously used in dr. Balciunas lab to uncover a genomic regulatory element of *tbx5a* gene. A hypothesized enhancer was confirmed by injecting zebrafish embryos with a plasmid containing a potential enhancer cloned upstream of the minimal *heatshock (hsp* hereafter*)* promoter driving mRFP.

In order to determine a minimal DNA sequence that can act as a heart-specific enhancer, previously discovered 2309 bp *tbx5a* regulatory region that is located 15677 kb upstream of *tbx5a* transcription start site was dissected into

smaller regions and cloned in front of mRFP into enhancer testing vector, pBK48 (Fig. 33). Ten plasmids were generated and injected into wild type zebrafish embryos (n = 741). At 3 dpf embryos were preselected for mRFP expression. In total, 474 out of 613 embryos (77.3%) showed mRFP expression.

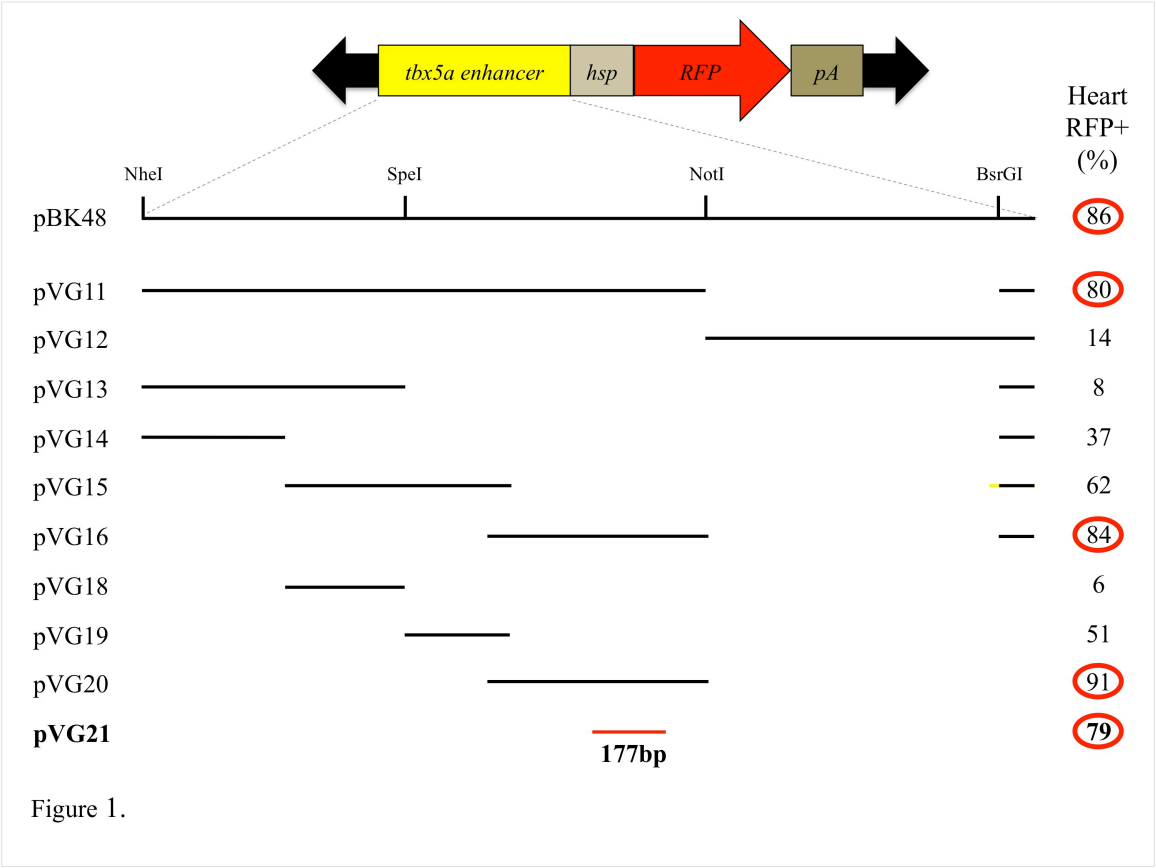

Figure 33. Fragments of *tbx5a* enhancer tested for regulatory activity *in vivo*.

The highest number of embryos with mRFP-positive heart (91%) was obtained upon injection of pVG20 plasmid (Fig. 33). However, mRFP in pVG20 F0 larvae was not restricted to the heart, but it was also detected in the somites. In contrast, F0 embryos injected with pVG21 plasmid showed a heart-specific mRFP expression, and no mRFP in the somites (Fig. 34). In addition, the fluorescence in pVG21 F0 was also found in the lens.

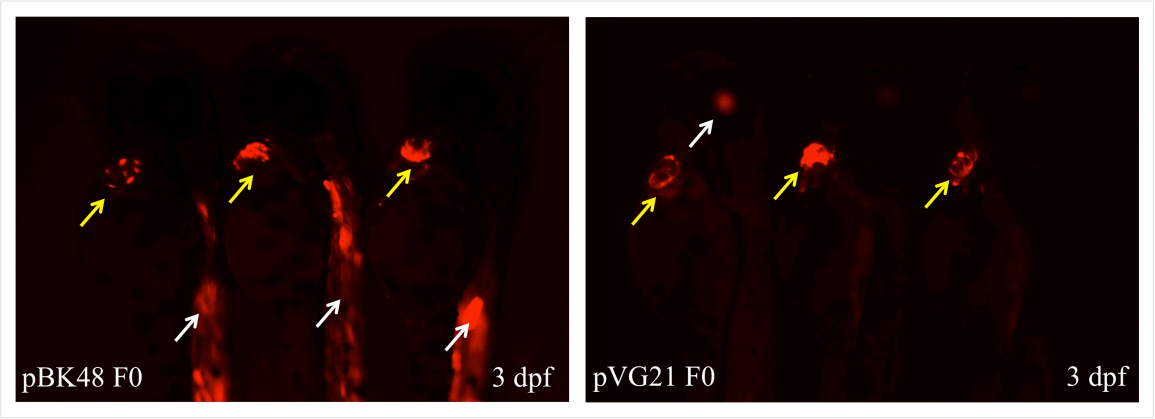

Figure 34. mRFP expression in 3 dpf larvae injected with pBK48 (2309 bp *tbx5a* enhancer sequence) and pVG21 (177 bp *tbx5a* enhancer sequence). A yellow arrow points to a heart-specific mRFP. A white arrow indicates ectopic mRFP expression in the eye and somites.

The observed mRFP expression in the eye is expected to be a result of *hsp* minimal promoter leakage because the embryos injected with enhancer-less are known to exhibit similar mRFP expression in the eye. Therefore, it was concluded that 177 bp region of *tbx5a* enhancer in pVG21 plasmid is sufficient to drive mRFP specifically in the heart of 3 dpf zebrafish embryos (Fig. 34).

Figure 35. A minimal heart-specific *tbx5a* enhancer activates mRFP expression in the developing zebrafish heart. A yellow arrow points to a ventricle-specific mRFP. Since mRFP expression in the atrium is very weak, it was not recorded in a picture.

The analysis of pVG21 F1 embryos confirmed the preliminary results obtained from the pVG21 F0 larvae. It was found that F1 embryos carrying a minimal *tbx5a* enhancer exhibit mRFP expression in the heart. Importantly, mRFP fluorescence in the ventricle was significantly brighter than in the atrium (n = 89) (Fig. 35). Similar mRFP expression pattern was detected in the adult pVG21 F1 zebrafish hearts (n = 3) (Fig. 36).

Interestingly, the uncovered *tbx5a* minimal regulatory element contains a 24 bp genomic region (gtgtgtgatgtgattgttagcaga) that is conserved among fish. Thereby, the data suggest that an identified minimal *tbx5a* enhancer may play an important role in zebrafish heart development and/or regeneration.

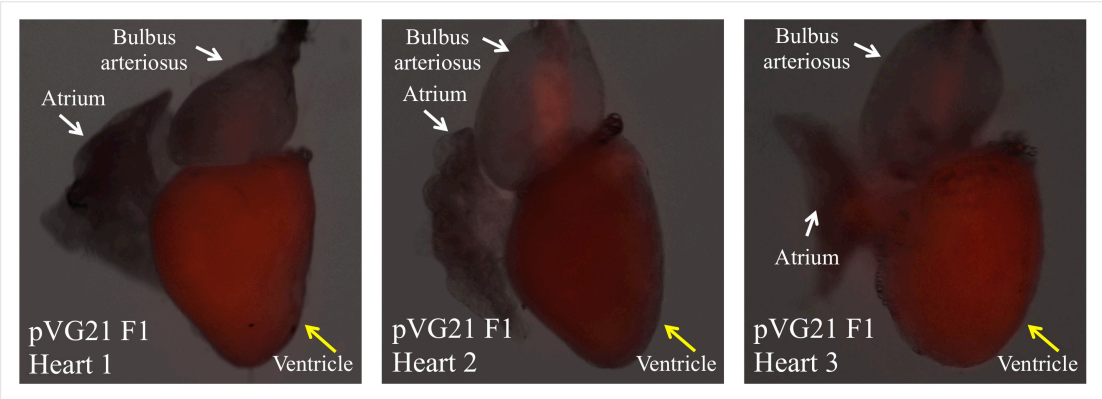

Figure 36. A minimal heart-specific *tbx5a* enhancer activates mRFP expression in the adult zebrafish heart. A yellow arrow points to mRFP expression in a ventricle. A white arrow indicates mRFP in atrium and bulbus arteriosus. The mRFP fluorescence in a bulbus arteriosus is expected to be an autofluorescence, and it's source is blood.

3. 12. Functional analysis of the transcription factors binding sites in *tbx5a* minimal enhancer *in vivo*

To determine what transcription factors could potentially bind to *tbx5a* minimal enhancer, a 177 bp sequence was blasted in TFSEARCH program that is

directly connected to TRANSFAC database (Heinemeyer et al 1998). According to the search results, at least two genomic regions can serve as a potential binding site. A first set of overlapping motifs located in a conserved region of *tbx5a* minimal enhancer can be bound by Sox-5, Gata-1 and/ or Pbx1 transcription factors. The second region located downstream of the conserved sequence can potentially serve as a binding site for Gata-2, Evi-1, Gata-X and/ or Mzf1 transcription factors.

In order to check if the revealed candidate transcription factor sites are important for driving mRFP transcription specifically in the heart, 10 and 5 bp deletions have been introduced into the first and second potential binding sites, respectively. Plasmids containing first (pVG22), second (pVG23) or both deletions (pVG24) were injected into zebrafish embryos. It was found that in the presence of the first or second deletion separately, a number of embryos with mRFP-positive heart increased from 79 to 92 and 99 %, respectively. However, the observed heart-specific mRFP expression was weaker. In case when both deletions were present, a number of embryos exhibiting mRFP-positive hearts decreased dramatically, from 79 to 27 %, suggesting that the presence of both potential binding sites is critical for the activation of *tbx5a* minimal enhancer specifically in the heart during zebrafish development. However, when a region containing a set of overlapping motifs that can be bound by Sox-5, Gata-1 and/ or Pbx1 transcription factors was mutated using CRISPR/ Cas9 technique (Burg et al. 2016), mRFP expression in the developing hearts of F1 embryos significantly decreased (data not shown). This indicates that a potential transcription binding site that was also tested in pVG22 might play an important role in the regulation of *tbx5a* activity during zebrafish cardiogenesis.

Conclusions

1. Six insertional gene trap lines were successfully characterized using iPCR and 5'RACE methods. The gene trap integrations were detected in six different genes: *fli1b, pdlim7, smndc1, ENSDART00000112671, ENSDART00000114996,* and *ENSDART00000111400.*
2. Regeneration of the blood vessels in *fli1b*^{tpl50} insertional zebrafish mutant proceeds normally. However, the observation that GFP driven by a gene trapped *fli1b*^{tpl50} allele is overexpressed in the blood vessels and some circulating cells at 7 dpa suggests that *fli1b* might be important for regeneration of vascular system, but it's role is most likely compensated by it's paralog *fli1a.*
3. Both *-3.3nkx2.5* and *-6.1nkx2.5* promoter regions contain heart-specific enhancers that are capable of activating reporter expression at 3 dpf zebrafish embryos during normal heart development. However, both *nkx2.5* promoter fragments can not be used as a heart-specific Cre driver because they also drive ectopic mRFP expression in other tissues such as eye, brain, and branchial arches.
4. Chicken β-globin insulation sequences fail to protect *-3.3nkx2.5:RFP/INS* and *-6.1nkx2.5:RFP/INS* transgenes from chromosomal position effect in *D. rerio* genome during normal cardiogenesis. As a result, embryos carrying the transgene integration in the same or different genomic locations exhibit variable expression patterns, intensity and variegation.
5. Incubation of *tbx5a*^{tpl58R}*;tnnt2a:CreER*^{T2} embryos and adults in 4-hydroxytamoxifen induces a recombination event between *lox71* and *lox66* sites, inverts the gene trap mutagenic cassette, and results in a successful re-mutation of *tbx5a*^{tpl58R} locus specifically in the heart. Therefore, it has been shown for the first time that loss of function mutation can be induced not only in embryos, but also in adult fish.

6. *tbx5a*^{tpl58R}*;tnnt2a:CreER*^{T2} conditional zebrafish mutants with hearts mosaic for *tbx5a*$^{tpl58R/tpl58R}$, *tbx5a*$^{tpl58R/tpl58}$, and *tbx5a*$^{tpl58/tpl58}$ cardiomyocytes exhibit severe regeneration phenotypes such as significant scar and misshaped ventricle. The detected cardiac regeneration defects indicate that *tbx5a* plays a critical role in zebrafish heart regeneration process.
7. A minimal 177 bp *tbx5a* enhancer, which is located over 15 kilobases upstream of the *tbx5a* gene, drives a heart-specific mRFP expression in the developing and adult zebrafish. The observed *tbx5a* enhancer activity suggests that this regulatory sequence might play a role in controlling *tbx5a* gene during cardiogenesis, homeostasis, and heart regeneration.

References

Agarwal P, Wylie JN, Galceran J, Arkhitko O, Li C, Deng C, Grosschedl R, Bruneau BG. 2003. Tbx5 is essential for forelimb bud initiation following patterning of the limb field in the mouse embryo. *Development*. 130(3):623-33.

Ahn DG, Kourakis MJ, Rohde LA, Silver LM, Ho RK. 2002. T-box gene tbx5 is essential for formation of the pectoral limb bud. *Nature*. 417(6890):754-8.

Albalat R, Baquero M, Minguillón C. 2010. Identification and characterisation of the developmental expression pattern of *tbx5b*, a novel *tbx5* gene in zebrafish. *Gene Expr. Patterns*. 10(1): 24-30.

Amsterdam A, Burgess S, Golling G, Chen W, Sun Z, Townsend K, Farrington S, Haldi M, Hopkins N. 1999. A large-scale insertional mutagenesis screen in zebrafish. *Genes Dev*. 13(20):2713-24.

Amsterdam A. 2003. Insertional mutagenesis in zebrafish. *Dev Dyn*. 228(3):523-34.

Amsterdam A, Hopkins N. 2004. Retroviral-mediated insertional mutagenesis in zebrafish. *Methods Cell Biol*. 77:3-20.

Amsterdam A, Hopkins N. 2006. Mutagenesis strategies in zebrafish for identifying genes involved in development and disease. *Trends Genet*. 22(9):473-8.

Balciunas D, Wangensteen KJ, Wilber A, Bell J, Geurts A, Sivasubbu S, Wang X, Hackett PB, Largaespada DA, McIvor RS, Ekker SC. 2006. Harnessing a high cargo-capacity transposon for genetic applications in vertebrates. *PLoS Genet*. 2(11):e169.

Bakkers J. 2011. Zebrafish as a model to study cardiac development and human cardiac disease. *Cardiovasc Res*. 91(2):279-88.

Basson CT, Huang T, Lin RC, Bachinsky DR, Weremowicz S, Vaglio A, Bruzzone R, Quadrelli R, Lerone M, Romeo G, Silengo M, Pereira A,

Krieger J, Mesquita SF, Kamisago M, Morton CC, Pierpont ME, Müller CW, Seidman JG, Seidman CE. 1999. Different TBX5 interactions in heart and limb defined by Holt-Oram syndrome mutations. *Proc Natl Acad Sci U S A*. 96(6):2919-24.

Becker T, Wullimann MF, Becker CG, Bernhardt RR, Schachner M. 1997. Axonal regrowth after spinal cord transection in adult zebrafish. *J Comp Neurol* 377: 577-595.

Becker CG, Becker T. 2002. Repellent guidance of regenerating optic axons by chondroitin sulfate glycosaminoglycans in zebrafish. *J Neurosci.* 22(3):842-53.

Begemann G, Ingham PW. 2000. Developmental regulation of Tbx5 in zebrafish embryogenesis. *Mech Dev*. 90(2):299-304.

Beis D, Bartman T, Jin SW, Scott IC, D'Amico LA, Ober EA, Verkade H, Frantsve J, Field HA, Wehman A, Baier H, Tallafuss A, Bally-Cuif L, Chen JN, Stainier DY, Jungblut B. 2005. Genetic and cellular analyses of zebrafish atrioventricular cushion and valve development. *Development.* 132(18):4193-204. Epub 2005 Aug 17.

Bernhardt RR, Tongiorgi E, Anzini P, Schachner M. 1996. Increased expression of specific recognition molecules by retinal ganglion cells and by optic pathway glia accompanies the successful regeneration of retinal axons in adult zebrafish. *J Comp Neurol*. 376(2):253-64.

Bessa J, Tena JJ, de la Calle-Mustienes E, Fernández-Miñán A, Naranjo S, Fernández A, Montoliu L, Akalin A, Lenhard B, Casares F, Gómez-Skarmeta JL. 2009. Zebrafish enhancer detection (ZED) vector: a new tool to facilitate transgenesis and the functional analysis of cis-regulatory regions in zebrafish. *Dev Dyn.* 238(9):2409-17.

Biben C, Weber R, Kesteven S, Stanley E, McDonald L, Elliott DA, Barnett L, Köentgen F, Robb L, Feneley M, Harvey RP. 2000. Cardiac Septal and

Valvular Dysmorphogenesis in Mice Heterozygous for Mutations in the Homeobox Gene *Nkx2-5*. *Circulation Research*. 87: 888-895.

Blum N, Begemann G. 2012. Retinoic acid signaling controls the formation, proliferation and survival of the blastema during adult zebrafish fin regeneration. *Development*. 139(1):107-16.

Brand T. 2003. Heart development: molecular insights into cardiac specification and early morphogenesis. 2003. *Dev Biol*. 258(1):1-19.

Branda CS and Dymecki SM. 2004. Talking about a revolution: The impact of site-specific recombinases on genetic analyses in mice. *Dev Cell.* 6(1):7-28.

Briggs LE, Takeda M, Cuadra AE, Wakimoto H, Marks MH, Walker AJ, Seki T, Oh SP, Lu JT, Sumners C, Raizada MK, Horikoshi N, Weinberg EO, Yasui K, Ikeda Y, Chien KR, Kasahara H. 2008. Perinatal loss of Nkx2-5 results in rapid conduction and contraction defects. *Circ Res*. 103(6):580-90.

Brown DD, Martz SN, Binder O, Goetz SC, Price BM, Smith JC, Conlon FL. 2005. Tbx5 and Tbx20 act synergistically to control vertebrate heart morphogenesis. *Development*. 132(3):553-63.

Bruneau BG, Logan M, Davis N, Levi T, Tabin CJ, Seidman JG, Seidman CE. 1999. Chamber-specific cardiac expression of Tbx5 and heart defects in Holt-Oram syndrome. *Dev Biol*. 211(1):100-8.

Bruneau BG, Nemer G, Schmitt JP, Charron F, Robitaille L, Caron S, Conner DA, Gessler M, Nemer M, Seidman CE, Seidman JG. 2001. A murine model of Holt-Oram syndrome defines roles of the T-box transcription factor Tbx5 in cardiogenesis and disease. *Cell*. 106(6):709-21.

Bruneau BG. 2002. Transcriptional regulation of vertebrate cardiac morphogenesis. *Circ Res*. 90(5):509-19.

Buchberger A, Pabst O, Brand T, Seidl K, Arnold HH. 1996. Chick NKx-2.3 represents a novel family member of vertebrate homologues to the Drosophila homeobox gene tinman: differential expression of cNKx-2.3 and cNKx-2.5 during heart and gut development. *Mech Dev*. 56(1-2):151-

63.

Burg, L., Zhang, K., Bonawitz, T., Grajevskaja, V., Bellipanni, G., Waring, R., Balciunas, D. 2016. Internal epitope tagging informed by relative lack of sequence conservation. *Sci. Rep.* 6: 36986.

Camarata T, Krcmery J, Snyder D, Park S, Topczewski J, Simon HG. 2010. Pdlim7 (LMP4) regulation of Tbx5 specifies zebrafish heart atrio-ventricular boundary and valve formation. *Dev. Biol.* 337(2): 233-245.

Chablais F, Veit J, Rainer G, Jaźwińska A. 2011. The zebrafish heart regenerates after cryoinjury-induced myocardial infarction. *BMC Dev Biol*. 11:21.

Chablais F, Jaźwińska A. 2012. Induction of myocardial infarction in adult zebrafish using cryoinjury. *J Vis Exp.* (62): 3666.

Chapman DL, Garvey N, Hancock S, Alexiou M, Agulnik SI, Gibson-Brown JJ, Cebra-Thomas J, Bollag RJ, Silver LM, Papaioannou VE. 1996. Expression of the T-box family genes, Tbx1-Tbx5, during early mouse development. *Dev Dyn*. 206(4):379-90.

Chen J, Fishman M. C. 1996. Zebrafish *tinman* homolog demarcates the heart field and initiates myocardial differentiation. *Development*. 122, 3809-3816.

Chen W, Burgess S, Golling G, Amsterdam A, Hopkins N. 2002. High-throughput selection of retrovirus producer cell lines leads to markedly improved efficiency of germ line-transmissible insertions in zebra fish. *J Virol*. 76(5):2192-8.

Chi X, Zhang S., Yu W., DeMayo F. J., Rosenberg S. M., Schwartz R. J. 2003. Expression of *Nkx2-5*-GFP Bacterial Artificial Chromosome Transgenic Mice Closely Resembles Endogenous *Nkx2-5* Gene Activity. *Genesis*. 35: 220-226.

Chiavacci E, Dolfi L, Verduci L, Meghini F, Gestri G, Evangelista AM, Wilson SW, Cremisi F, Pitto L. 2012. MicroRNA 218 Mediates the Effects of Tbx5a Over-Expression on Zebrafish Heart Development. *PLoS One.* 7(11): e50536.

Chiavacci E, D'Aurizio R, Guzzolino E, Russo F, Baumgart M, Groth M, Mariani L, D'Onofrio M, Arisi I, Pellegrini M, Cellerino A, Cremisi F, Pitto L. 2015. MicroRNA 19a replacement partially rescues fin and cardiac defects in zebrafish model of Holt Oram syndrome. *Sci. Rep*. 5: 18240.

Choi WY, Poss KD. 2012. Cardiac regeneration. Curr Top *Dev Biol*. 100:319-44.

Choi WY, Gemberling M, Wang J, Holdway JE, Shen MC, Karlstrom RO, Poss KD. 2013. In vivo monitoring of cardiomyocyte proliferation to identify chemical modifiers of heart regeneration. *Development*. 140(3):660-6.

Chung J. H, Whiteley M, Felsenfeld G. 1993. A 5'Element of the Chicken b-Globin Domain Serves as an Insulator in Human Erythroid Cells and Protects against Position Effect in Drosophila. *Cell.* 74: 505-514.

Chung J. H, Bell A. C, Felsenfeld G. 1997. Characterization of the chicken beta-globin insulator. *Proc Natl Acad Sci USA*. 94 (2): 575-580.

Clark KJ, Geurts AM, Bell JB, Hackett PB. 2004. Transposon vectors for gene-trap insertional mutagenesis in vertebrates. *Genesis*. 39(4):225-33.

Clark KJ, Balciunas D, Pogoda HM, Ding Y, Westcot SE, Bedell VM, Greenwood TM, Urban MD, Skuster KJ, Petzold AM, Ni J, Nielsen AL, Patowary A, Scaria V, Sivasubbu S, Xu X, Hammerschmidt M, Ekker SC. 2011. In vivo protein trapping produces a functional expression codex of the vertebrate proteome. *Nat Methods*. 8(6):506-15.

Cleaver OB, Patterson KD, Krieg PA. 1996. Overexpression of the *tinman*-related genes *XNkx-2.5* and *XNkx-2.3* in *Xenopus* embryos results in myocardial hyperplasia. *Development*. 122: 3549-3556.

Craig MP, Grajevskaja V, Liao HK, Balciuniene J, Ekker SC, Park JS, Essner JJ, Balciunas D, Sumanas S. 2015. Etv2 and Fli1b Function Together as Key Regulators of Vasculogenesis and Angiogenesis. Arterioscler. *Thromb. Vasc. Biol*. 35(4): 865-76.

D'Aurizio R, Russo F, Chiavacci E, Baumgart M, Groth M, D'Onofrio M, Arisi I, Rainaldi G, Pitto L, Pellegrini M. 2016. Discovering miRNA Regulatory

Networks in Holt-Oram Syndrome Using a Zebrafish Model. *Front Bioeng Biotechnol*. 4:60.

Davidson AE, Balciunas D, Mohn D, Shaffer J, Hermanson S, Sivasubbu S, Cliff MP, Hackett PB, Ekker SC. 2003. Efficient gene delivery and gene expression in zebrafish using the Sleeping Beauty transposon. *Dev Biol*. 263(2):191-202.

De Preux Charles A-S, Bise T, Baier F, Marro J, Jaźwińska A. 2016. Distinct effects of inflammation on preconditioning and regeneration of the adult zebrafish heart. *Open Biology*. 6(7):160102.

Doyon Y, McCammon JM, Miller JC, Faraji F, Ngo C, Katibah GE, Amora R, Hocking TD, Zhang L, Rebar EJ, Gregory PD, Urnov FD, Amacher SL. 2008. Heritable targeted gene disruption in zebrafish using designed zinc-finger nucleases. *Nat Biotechnol*. 26(6):702-8.

Draper BW, Moens CB. 2009. A high-throughput method for zebrafish sperm cryopreservation and in vitro fertilization. *J Vis Exp*. (29):1395.

Dreßen M, Lahm H, Lahm A, et al. A novel de novo *TBX5* mutation in a patient with Holt–Oram syndrome leading to a dramatically reduced biological function. 2016. *Molecular Genetics & Genomic Medicine*. 4(5):557-567.

Driever W, Solnica-Krezel L, Schier AF, Neuhauss SC, Malicki J, Stemple DL, Stainier DY, Zwartkruis F, Abdelilah S, Rangini Z, Belak J, Boggs C. 1996. A genetic screen for mutations affecting embryogenesis in zebrafish. *Development*. 123:37-46.

Eid H, Larson DM, Springhorn JP, Attawia MA, Nayak RC, Smith TW, Kelly RA. 1992. Role of epicardial mesothelial cells in the modification of phenotype and function of adult rat ventricular myocytes in primary coculture. *Circ Res*. 71(1):40-50.

Emery DW, Yannaki E, Tubb J, Nishino T, Li Q, Stamatoyannopoulos G. 2000. A chromatin insulator protects retrovirus vectors from chromosomal position effects. *Proc Natl Acad Sci U S A*. 97(16):9150-5.

Ennis DG. 2001. Mutagenesis. *Encyclopedia of Life Sciences*. Nature Publishing Group. 1-8.

Fadool JM, Hartl DL, Dowling JE. 1998. Transposition of the mariner element from Drosophila mauritiana in zebrafish. *Proc Natl Acad Sci U S A*. 95(9):5182-6.

Fan C, Liu M, Wang Q. 2003a. Functional analysis of TBX5 missense mutations associated with Holt-Oram syndrome. *J Biol Chem*. 278(10):8780-5.

Fan C, Duhagon MA, Oberti C, Chen S, Hiroi Y, Komuro I, Duhagon PI, Canessa R, Wang Q. 2003b. Novel TBX5 mutations and molecular mechanism for Holt-Oram syndrome. *J Med Genet*. 40(3):e29.

Fang Y, Gupta V, Karra R, Holdway JE, Kikuchi K, Poss KD. Translational profiling of cardiomyocytes identifies an early Jak1/Stat3 injury response required for zebrafish heart regeneration. 2013. *Proc Natl Acad Sci USA*. 110(33):13416-21.

Gaiano N, Amsterdam A, Kawakami K, Allende M, Becker T, Hopkins N. 1996. Insertional mutagenesis and rapid cloning of essential genes in zebrafish. *Nature*. 383(6603):829-32.

Gall JC Jr, Stern AM, Cohen MM, Adams MS, Davidson RT. 1966. Holt-Oram syndrome: clinical and genetic study of a large family. *Am J Hum Genet*. 18(2):187-200.

Garrity DM, Childs S, Fishman MC. 2002. The heartstrings mutation in zebrafish causes heart/fin Tbx5 deficiency syndrome. *Development*. 129(19):4635-45.

Gemberling M, Bailey TJ, Hyde DR, Poss KD. 2013. The zebrafish as a model for complex tissue regeneration. *Trends Genet.* 29(11):611-20.

Gemberling M, Karra R, Dickson AL, Poss KD. 2015. Nrg1 is an injury-induced cardiomyocyte mitogen for the endogenous heart regeneration program in zebrafish. *Elife*. 4. doi: 10.7554/eLife.05871.

Golling G, Amsterdam A, Sun Z, Antonelli M, Maldonado E, Chen W, Burgess S,

Haldi M, Artzt K, Farrington S, Lin SY, Nissen RM, Hopkins N. 2002. Insertional mutagenesis in zebrafish rapidly identifies genes essential for early vertebrate development. *Nat Genet*. 31(2):135-40.

González-Rosa JM, Martín V, Peralta M, Torres M, Mercader N. 2011. Extensive scar formation and regression during heart regeneration after cryoinjury in zebrafish. *Development*. (9):1663-74.

González-Rosa JM, Mercader N. 2012. Cryoinjury as a myocardial infarction model for the study of cardiac regeneration in the zebrafish. *Nat Protoc.* 7(4):782-8.

Gibson-Brown JJ, I Agulnik S, Silver LM, Papaioannou VE. 1998. Expression of T-box genes Tbx2-Tbx5 during chick organogenesis. *Mech Dev*. 74(1-2):165-9.

Grajevskaja V, Balciuniene J, Balciunas D. 2013. Chicken β-globin insulators fail to shield the nkx2.5 promoter from integration site effects in zebrafish. *Mol Genet Genomics*. 288(12):717-25.

Gu H, Marth JD, Orban PC, Mossmann H, Rajewsky K. 1994. Deletion of a DNA polymerase beta gene segment in T cells using cell type-specific gene targeting. *Science.* 265(5168):103-6.

Gupta V, Poss KD. 2012. Clonally dominant cardiomyocytes direct heart morphogenesis. *Nature.* 484(7395):479-84.

Gupta V, Gemberling M, Karra R, Rosenfeld GE, Evans T, Poss KD. 2013. An injury-responsive gata4 program shapes the zebrafish cardiac ventricle. *Curr Biol.* 23(13):1221-7.

Haffter P, Nüsslein-Volhard C. 1996. Large scale genetics in a small vertebrate, the zebrafish. *Int J Dev Biol*. 40(1):221-7.

Hatcher CJ, Goldstein MM, Mah CS, Delia CS, Basson CT. 2000. Identification and localization of TBX5 transcription factor during human cardiac morphogenesis. *Dev Dyn*. 219(1):90-5.

Heinemeyer T, Wingender E, Reuter I, Hermjakob H, Kel AE, Kel OV, Ignatieva

EV, Ananko EA, Podkolodnaya OA, Kolpakov FA, Podkolodny NL, Kolchanov NA. 1998. Databases on Transcriptional Regulation: TRANSFAC, TRRD, and COMPEL. *Nucleic Acids Res*. 26, 364-370.

Hermanson S, Davidson AE, Sivasubbu S, Balciunas D, Ekker SC. 2004. Sleeping Beauty transposon for efficient gene delivery. *Methods Cell Biol.* 77:349-362.

Holmes FA, Liticker JD. 2005. Pharmacogenomics of tamoxifen in a nutshell-and who broke the nutcracker? *J Oncol Pract*. 1(4):155-9.

Holt M, Oram S. 1960. Familial heart disease with skeletal malformations. *Br Heart J.* 22:236-42.

Horb ME, Thomsen GH. 1999. Tbx5 is essential for heart development. *Development*. 126(8):1739-51.

Horton AC, Mahadevan NR, Minguillon C, Osoegawa K, Rokhsar DS, Ruvinsky I, de Jong PJ, Logan MP, Gibson-Brown JJ. 2008. Conservation of linkage and evolution of developmental function within the Tbx2/3/4/5 subfamily of T-box genes: implications for the origin of vertebrate limbs. *Dev Genes Evol.* 218(11-12):613-28.

Horvath P, Barrangou R. 2010. CRISPR/Cas, the immune system of bacteria and archaea. *Science*. 327(5962):167-70.

Hruscha A, Krawitz P, Rechenberg A, Heinrich V, Hecht J, Haass C, Schmid B. 2013. Efficient CRISPR/Cas9 genome editing with low off-target effects in zebrafish. *Development*. 140(24):4982-7.

Hsiao CD, Tsai WY, Horng LS, Tsai HJ. 2003. Molecular structure and developmental expression of three muscle-type troponin T genes in zebrafish. *Dev Dyn*. 227(2):266-79.

Hu N, Sedmera D, Yost HJ, Clark EB. 2000. Structure and function of the developing zebrafish heart. *Anat Rec*. 260(2):148-57.

Huang P, Zhu Z, Lin S, Zhang B. 2012. Reverse genetic approaches in zebrafish. *J Genet Genomics*. 39(9):421-33.

Huang Y, Harrison MR, Osorio A, Kim J, Baugh A, Duan C, Sucov HM, Lien CL. 2013. Igf Signaling is Required for Cardiomyocyte Proliferation during Zebrafish Heart Development and Regeneration. *PLoS One*. 8(6):e67266.

Hwang WY, Fu Y, Reyon D, Maeder ML, Kaini P, Sander JD, Joung JK, Peterson RT, Yeh JR. 2013. Heritable and precise zebrafish genome editing using a CRISPR-Cas system. *PLoS One*. 8(7):e68708.

Ieda M, Fu JD, Delgado-Olguin P, Vedantham V, Hayashi Y, Bruneau BG, Srivastava D. 2010. Direct reprogramming of fibroblasts into functional cardiomyocytes by defined factors. *Cell*. 142(3):375-86.

Isaac A, Rodriguez-Esteban C, Ryan A, Altabef M, Tsukui T, Patel K, Tickle C, Izpisúa-Belmonte JC. 1998. Tbx genes and limb identity in chick embryo development. *Development*. 125(10):1867-75.

Itou J, Oishi I, Kawakami H, Glass TJ, Richter J, Johnson A, Lund TC, Kawakami Y. 2012. Migration of cardiomyocytes is essential for heart regeneration in zebrafish. *Development.* 139(22):4133-42.

Ivics Z, Hackett PB, Plasterk RH, Izsvák Z. 1997. Molecular reconstruction of Sleeping Beauty, a Tc1-like transposon from fish, and its transposition in human cells. *Cell*. 91(4):501-10.

Jao LE, Wente SR, Chen W. 2013. Efficient multiplex biallelic zebrafish genome editing using a CRISPR nuclease system. *Proc Natl Acad Sci U S A*. 110(34):13904-9.

Jay PY, Harris BS, Maguire CT, Buerger A, Wakimoto H, Tanaka M, Kupershmidt S, Roden DM, Schultheiss TM, O'Brien TX, Gourdie RG, Berul CI, Izumo S. 2004. Nkx2-5 mutation causes anatomic hypoplasia of the cardiac conduction system. *J Clin Invest*. 113(8):1130-7.

Johnson SL, Weston JA. 1995. Temperature-sensitive mutations that cause stage-specific defects in Zebrafish fin regeneration. *Genetics*. 141(4):1583-95.

Jopling C, Sleep E, Raya M, Martí M, Raya A, Izpisúa Belmonte JC. 2010. Zebrafish heart regeneration occurs by cardiomyocyte dedifferentiation and proliferation. *Nature*. 464(7288):606-9.

Jopling C, Suñé G, Faucherre A, Fabregat C, Izpisua Belmonte JC. 2012a. Hypoxia induces myocardial regeneration in zebrafish. *Circulation.* 126(25):3017-27.

Jopling C, Suñe G, Morera C, Izpisua Belmonte JC. 2012b. p38α MAPK regulates myocardial regeneration in zebrafish. *Cell Cycle.* 11(6):1195-201.

Kasahara H., Bartunkova S., Schinke M., Tanaka M., Izumo S. 1998. Cardiac and Extracardiac Expression of Csx/Nkx2.5 Homeodomain Protein. *Circulation Research*, 82:936-946.

Kawakami K, Koga A, Hori H, Shima A. 1998. Excision of the tol2 transposable element of the medaka fish, Oryzias latipes, in zebrafish, Danio rerio. *Gene*. 225(1-2):17-22.

Kawakami K, Shima A. 1999. Identification of the Tol2 transposase of the medaka fish Oryzias latipes that catalyzes excision of a nonautonomous Tol2 element in zebrafish Danio rerio. *Gene*. 240(1):239-44.

Kawakami K, Shima A, Kawakami N. 2000. Identification of a functional transposase of the Tol2 element, an Ac-like element from the Japanese medaka fish, and its transposition in the zebrafish germ lineage. *Proc Natl Acad Sci U S A*. 97(21):11403-8.

Kawakami K, Takeda H, Kawakami N, Kobayashi M, Matsuda N, Mishina M. 2004. A transposon-mediated gene trap approach identifies developmentally regulated genes in zebrafish. *Dev Cell.* 7(1):133-44.

Kawakami Y, Rodriguez Esteban C, Raya M, Kawakami H, Martí M, Dubova I, Izpisúa Belmonte JC. 2006. Wnt/beta-catenin signaling regulates vertebrate limb regeneration. *Genes Dev*. 20(23):3232-7.

Kikuchi K, Holdway JE, Werdich AA, Anderson RM, Fang Y, Egnaczyk GF, Evans T, Macrae CA, Stainier DY, Poss KD. 2010. Primary contribution to

zebrafish heart regeneration by gata4(+) cardiomyocytes. *Nature*. 464(7288):601-5.

Kikuchi K, Gupta V, Wang J, Holdway JE, Wills AA, Fang Y, Poss KD. 2011a. tcf21+ epicardial cells adopt non-myocardial fates during zebrafish heart development and regeneration. *Development*. 138(14):2895-902.

Kikuchi K, Holdway JE, Major RJ, Blum N, Dahn RD, Begemann G, Poss KD. 2011b. Retinoic acid production by endocardium and epicardium is an injury response essential for zebrafish heart regeneration. *Dev Cell*. 20(3):397-404.

Kim J, Wu Q, Zhang Y, Wiens KM, Huang Y, Rubin N, Shimada H, Handin RI, Chao MY, Tuan TL, Starnes VA, Lien CL. 2010. PDGF signaling is required for epicardial function and blood vessel formation in regenerating zebrafish hearts. *Proc Natl Acad Sci U S A*. 107(40):17206-10.

Komuro I, Izumo S. 1993. *Csx*: A murine homeobox-containing gene specifically expressed in the developing heart. *Developmental Biology*. 90:8145-8149.

Kwan KM. 2002. Conditional alleles in mice: practical considerations for tissue-specific knockouts. *Genesis*. 32(2):49-62.

Lee KH, Xu Q, Breitbart RE. 1996. A new *tinman*-Related Gene, *nkx2.7*, Anticipates the Expression of *nkx2.5* and *nkx2.3* in Zebrafish Heart and Pharyngeal Endoderm. *Developmental Biology,* 180:722-731.

Lepilina A, Coon AN, Kikuchi K, Holdway JE, Roberts RW, Burns CG, Poss KD. 2006. A dynamic epicardial injury response supports progenitor cell activity during zebrafish heart regeneration. 127(3):607-19.

Li QY, Newbury-Ecob RA, Terrett JA, Wilson DI, Curtis AR, Yi CH, Gebuhr T, Bullen PJ, Robson SC, Strachan T, Bonnet D, Lyonnet S, Young ID, Raeburn JA, Buckler AJ, Law DJ, Brook JD. 1997. Holt-Oram syndrome is caused by mutations in TBX5, a member of the Brachyury (T) gene family. *Nat Genet*. 15(1):21-9.

Liberatore CM, Searcy-Schrick RD, Yutzey KE. 2000. Ventricular expression of tbx5 inhibits normal heart chamber development. *Dev Biol*. 223(1):169-80.

Lien CL, Schebesta M, Makino S, Weber GJ, Keating MT. 2006. Gene expression analysis of zebrafish heart regeneration. *PLoS Biol.* 4(8):e260.

Lints T. J., Parson L. M., Hartley L., Lyons I., Harvey R. P. 1993. *Nkx2-5*: a novel murine homeobox gene expressed in early heart progenitor cells and their myogenic descendants. *Development.* 119, 419-431.

Liu J, Stainier DY. 2010. Tbx5 and Bmp signaling are essential for proepicardium specification in zebrafish. *Circ Res*.;106(12):1818-28.

Logan M, Simon HG, Tabin C. 1998. Differential regulation of T-box and homeobox transcription factors suggests roles in controlling chick limb-type identity. *Development*. 125(15):2825-35.

Lohr JL, Yost HJ. 2000. Vertebrate model systems in the study of early heart development: Xenopus and zebrafish. Am J Med *Genet*. 97(4):248-57.

López-Schier H, Hudspeth AJ. 2006. A two-step mechanism underlies the planar polarization of regenerating sensory hair cells. *Proc Natl Acad Sci U S A*. 103(49):18615-20.

Lyons I, Parson LM, Hartley L, Li R, Andrew JE, Robb L, Harvey RP. 1995. Myogenic and morphogenic defects in the heart tubes of murine embryos lacking the homeo box gene *Nkx2-5*. *Genes Dev*. 9: 1654-1666.

Marín-Juez R, Marass M, Gauvrit S, Rossi A, Lai SL, Materna SC, Black BL, Stainier DY. 2016. Fast revascularization of the injured area is essential to support zebrafish heart regeneration. *Proc Natl Acad Sci USA*. 4;113(40):11237-11242.

Martin P, Leibovich SJ. 2005. Inflammatory cells during wound repair: the good, the bad and the ugly. *Trends Cell Biol.* 15(11):599-607.

Martin RT, Bartman T. 2009. Analysis of heart valve development in larval zebrafish. *Dev Dyn.* 238(7):1796-802.

Meng S, Ryu S, Zhao B, Zhang DQ, Driever W, McMahon DG. 2008. Targeting retinal dopaminergic neurons in tyrosine hydroxylase-driven green fluorescent protein transgenic zebrafish. *Mol Vis*. 14:2475-83.

Menke AL, Spitsbergen JM, Wolterbeek AP, Woutersen RA. 2011. Normal anatomy and histology of the adult zebrafish. *Toxicol Pathol.* 39(5):759-75.

Milan DJ, Giokas AC, Serluca FC, Peterson RT, MacRae CA. 2006. Notch1b and neuregulin are required for specification of central cardiac conduction tissue. Development. 133(6):1125-32.

Müller CW, Herrmann BG. 1997. Crystallographic structure of the T domain-DNA complex of the Brachyury transcription factor. *Nature*. 389(6653):884-8.

Mullins MC, Hammerschmidt M, Haffter P, Nüsslein-Volhard C. 1994. Large-scale mutagenesis in the zebrafish: in search of genes controlling development in a vertebrate. *Curr Biol*. 4(3):189-202.

Newbury-Ecob RA, Leanage R, Raeburn JA, Young ID. 1996. Holt-Oram syndrome: a clinical genetic study. *J Med Genet*. 33(4):300-7.

Ni J, Clark KJ, Fahrenkrug SC, Ekker SC. 2008. Transposon tools hopping in vertebrates. *Brief Funct Genomic Proteomic*. 7(6):444-53.

Ni TT, Lu J, Zhu M, Maddison LA, Boyd KL, Huskey L, Ju B, Hesselson D, Zhong TP, Page-McCaw PS, Stainier DY, Chen W. 2012. Conditional control of gene function by an invertible gene trap in zebrafish. *Proc Natl Acad Sci U S A.*109(38):15389-94.

Ochiai H, Harashima H, Kamiya H. 2011. Effects of insulator cHS4 on transgene expression from plasmid DNA in a positive feedback system. *Journal of Bioscience and Bioengineering.* 112(5): 432-434.

Ohuchi H, Takeuchi J, Yoshioka H, Ishimaru Y, Ogura K, Takahashi N, Ogura T, Noji S. 1998. Correlation of wing-leg identity in ectopic FGF-induced chimeric limbs with the differential expression of chick Tbx5 and Tbx4. *Development*. 125(1):51-60.

Parinov S, Kondrichin I, Korzh V, Emelyanov A. 2000. Tol2 transposon-mediated enhancer trap to identify developmentally regulated zebrafish genes in vivo. *Dev Dyn*. 231(2):449-59.

Parrie LE, Renfrew EM, Vander WA, Mueller RL, Garrity DM. 2013. Zebrafish tbx5 paralogs demonstrate independent essential requirements in cardiac and pectoral fin development. *Dev. Dyn.* 242(5): 485-502.

Pashmforoush M, Lu JT, Chen H, Amand TS, Kondo R, Pradervand S, Evans SM, Clark B, Feramisco JR, Giles W, Ho SY, Benson DW, Silberbach M, Shou W, Chien KR. 2004. Nkx2-5 pathways and congenital heart disease; loss of ventricular myocyte lineage specification leads to progressive cardiomyopathy and complete heart block. *Cell*. 117(3):373-86.

Patton EE, Zon LI. 2001. The art and design of genetic screens: zebrafish. *Nat Rev Genet.* 2(12):956-66.

Poss KD, Wilson LG, Keating MT. 2002. Heart regeneration in zebrafish. *Science*. 298(5601):2188-90.

Poznanski AK, Gall JC Jr, Stern AM. 1970. Skeletal manifestations of the Holt-Oram syndrome. *Radiology*. 94(1):45-53.

Rajewsky K, Gu H, Kühn R, Betz UA, Müller W, Roes J, Schwenk F. 1996. Conditional gene targeting. *J Clin Invest.* 98(3):600-3.

Rallis C, Bruneau BG, Del Buono J, Seidman CE, Seidman JG, Nissim S, Tabin CJ, Logan MP. 2003. Tbx5 is required for forelimb bud formation and continued outgrowth. *Development*. 130(12):2741-51.

Ranzani M, Annunziato S, Adams DJ, Montini E. 2013. Cancer gene discovery: exploiting insertional mutagenesis. *Mol Cancer Res*. 11(10):1141-58.

Raya A, Koth CM, Büscher D, Kawakami Y, Itoh T, Raya RM, Sternik G, Tsai HJ, Rodríguez-Esteban C, Izpisúa-Belmonte JC. 2003. Activation of Notch signaling pathway precedes heart regeneration in zebrafish. *Proc Natl Acad Sci U S A.* 100 Suppl 1:11889-95.

Raya A, Consiglio A, Kawakami Y, Rodriguez-Esteban C, Izpisúa-Belmonte JC. 2004. The zebrafish as a model of heart regeneration. *Cloning Stem Cells*. 6(4):345-51.

Raz E, van Luenen HG, Schaerringer B, Plasterk RH, Driever W. 1998. Transposition of the nematode Caenorhabditis elegans Tc3 element in the zebrafish Danio rerio. *Curr Biol*. 8(2):82-8.

Reamon-Buettner SM, Borlak J. 2004. TBX5 mutations in non-Holt-Oram syndrome (HOS) malformed hearts. *Hum Mutat*. 24(1):104.

Reecy JM, Li X, Yamada M, DeMayo FJ, Newman CS, Harvey RP, Schwartz RJ. 1999. Identification of upstream regulatory regions in the heart-expressed homeobox gene Nkx2-5. *Development*. 126(4):839-49.

Reiter JF, Verkade H, Stainier DY. 2001. Bmp2b and Oep promote early myocardial differentiation through their regulation of gata5. *Dev Biol*. 2001 Jun 15;234(2):330-8.

Rincón-Arano H, Furlan-Magaril M, Recillas-Targa F. 2007. Protection against telomeric position effects by the chicken cHS4 beta-globin insulator. *Proc Natl Acad Sci U S A*. 104(35):14044-9.

Rivella S, Callegari J A, May C, Tan C W, Sadelain M. 2000. The cHS4 insulator increases the probability of retroviral expression at random chromosomal sites. *Journal of Virology*. 74(10):4679-4687.

Rodriguez-Esteban C, Tsukui T, Yonei S, Magallon J, Tamura K, Izpisua Belmonte JC. 1999. The T-box genes Tbx4 and Tbx5 regulate limb outgrowth and identity. *Nature*. 398(6730):814-8.

Roger VL, Go AS, Lloyd-Jones DM, Benjamin EJ, Berry JD, Borden WB, Bravata DM, Dai S, Ford ES, Fox CS, Fullerton HJ, Gillespie C, Hailpern SM, Heit JA, Howard VJ, Kissela BM, Kittner SJ, Lackland DT, Lichtman JH, Lisabeth LD, Makuc DM, Marcus GM, Marelli A, Matchar DB, Moy CS, Mozaffarian D, Mussolino ME, Nichol G, Paynter NP, Soliman EZ, Sorlie PD, Sotoodehnia N, Turan TN, Virani SS, Wong ND, Woo D,

Turner MB; American Heart Association Statistics Committee and Stroke Statistics Subcommittee. 2012. Heart disease and stroke statistics--2012 update: a report from the American Heart Association. *Circulation*. 125(1):e2-e220.

Russell WL, Kelly EM, Hunsicker PR, Bangham JW, Maddux SC, Phipps EL. 1979. Specific-locus test shows ethylnitrosourea to be the most potent mutagen in the mouse. *Proc Natl Acad Sci U S A*. 76(11):5818-9.

Sadler KC, Krahn KN, Gaur NA, Ukomadu C. 2007. Liver growth in the embryo and during liver regeneration in zebrafish requires the cell cycle regulator, uhrf1. *Proc Natl Acad Sci U S A.* 104(5):1570-5.

Sander JD, Cade L, Khayter C, Reyon D, Peterson RT, Joung JK, Yeh JR. 2011. Targeted gene disruption in somatic zebrafish cells using engineered TALENs. *Nat Biotechnol.* 29(8):697-8.

Schindler YL, Garske KM, Wang J, Firulli BA, Firulli AB, Poss KD, Yelon D. 2014. Hand2 elevates cardiomyocyte production during zebrafish heart development and regeneration. *Development.* 141(16):3112-22.

Schnabel K, Wu CC, Kurth T, Weidinger G. 2011. Regeneration of cryoinjury induced necrotic heart lesions in zebrafish is associated with epicardial activation and cardiomyocyte proliferation. *PLoS One*. 6(4):e18503.

Schultheiss TM, Xydas S, Lassar AB. 1995. Induction of avian cardiac myogenesis by anterior endoderm. *Development*. 121(12):4203-14.

Scott I C, Yelon D. 2010. Cardiac Development in the Zebrafish. Heart Evolution. Heart Development and Regeneration. *Elsvier Inc.* 103-120.

Searcy RD, Vincent EB, Liberatore CM, Yutzey KE. 1998. A GATA-dependent *nkx-2.5* regulatory element activates early cardiac gene expression in transgenic mice. *Development.* 125:4461-4470.

Sharma N, Hollensen AK, Bak RO, Staunstrup NH, Schroder, Mikkelsen JG. 2012. The impact of cHS4 Insulators on DNA Transposon Vector

Mobilization and Silencing in Retinal Pigment Epithelium Cells. *PloS ONE*, 7(10):e48421.

Shlyueva D, Stampfel G, Stark A. 2014. Transcriptional enhancers: from properties to genome-wide predictions. *Nat Rev Genet* 15(4):272-86.

Sivasubbu S, Balciunas D, Davidson AE, Pickart MA, Hermanson SB, Wangensteen KJ, Wolbrink DC, Ekker SC. 2006. Gene-breaking transposon mutagenesis reveals an essential role for histone H2afza in zebrafish larval development. *Mech Dev*. 123(7):513-29.

Sleep E, Boué S, Jopling C, Raya M, Raya A, Izpisua Belmonte JC. 2010. Transcriptomics approach to investigate zebrafish heart regeneration. *J Cardiovasc Med.* 11(5):369-80.

Smemo S, Campos LC, Moskowitz IP, Krieger JE, Pereira AC, Nobrega MA. 2012. Regulatory variation in a TBX5 enhancer leads to isolated congenital heart disease. *Hum Mol Genet*. 21(14):3255-63.

Smith A, Avaron F, Guay D, Padhi BK, Akimenko MA. 2006. Inhibition of BMP signaling during zebrafish fin regeneration disrupts fin growth and scleroblasts differentiation and function. *Dev Biol*. 299(2):438-54.

Smith L. 2011. Good planning and serendipity: exploiting the Cre/Lox system in the testis. *Reproduction*. 141(2):151-61.

Smith E, Shilatifard A. 2014. Enhancer biology and enhanceropathies. *Nat Struct Mol Biol.* 21(3):210-9.

Solnica-Krezel L, Schier AF, Driever W. 1994. Efficient recovery of ENU-induced mutations from the zebrafish germline. *Genetics*. 136(4):1401-20.

Srivastava D. 2006. Genetic regulation of cardiogenesis and congenital heart disease. *Annu Rev Pathol*.1:199-213.

Stainier DY. 2001. Zebrafish genetics and vertebrate heart formation. *Nat Rev Genet.* 2(1):39-48.

Streisinger G, Walker C, Dower N, Knauber D, Singer F. 1981. Production of clones of homozygous diploid zebra fish (Brachydanio rerio). *Nature*. 291(5813):293-6.

Tada M, Heisenberg CP. 2012. Convergent extension: using collective cell migration and cell intercalation to shape embryos. *Development*. 139(21):3897-904.

Takeuchi JK, Ohgi M, Koshiba-Takeuchi K, Shiratori H, Sakaki I, Ogura K, Saijoh Y, Ogura T. 2003a. Tbx5 specifies the left/right ventricles and ventricular septum position during cardiogenesis. *Development*. 130(24):5953-64.

Takeuchi JK, Koshiba-Takeuchi K, Suzuki T, Kamimura M, Ogura K, Ogura T. 2003b. Tbx5 and Tbx4 trigger limb initiation through activation of the Wnt/Fgf signaling cascade. *Development.* 130(12):2729-39.

Tamura K, Yonei-Tamura S, Izpisúa Belmonte JC. 1999. Differential expression of Tbx4 and Tbx5 in Zebrafish fin buds. *Mech Dev*. 87(1-2):181-4.

Tanaka M, Chen Z, Bartunkova S, Yamasaki N, Izumo S. 1999. The cardiac homeobox gene *Csx/Nkx2.5* lies genetically upstream of multiple genes essential for heart development. *Development.* 126:1269-1280.

Targoff KL, Schell T, Yelon D. 2008. Nkx genes regulate heart tube extension and exert differential effects on ventricular and atrial cell number. *Dev Biol*. 322(2):314-21.

Thomas KR, Capecchi MR. 1987. Site-directed mutagenesis by gene targeting in mouse embryo-derived stem cells. *Cell*. 51(3):503-12.

To WS, Midwood KS. 2011. Plasma and cellular fibronectin: distinct and independent functions during tissue repair. *Fibrogenesis Tissue Repair*. 4:21.

Tonissen KF, Drysdale TA, Lints TJ, Harvey RP, Krieg PA. 1994. XNkx-2.5, a Xenopus gene related to Nkx-2.5 and tinman: evidence for a conserved role in cardiac development. *Dev Biol*. 162(1):325-8.

Trinh A, Hochgreb T, Graham M, Wu D, Ruf-Zamojski F, Jayasena CS, Saxena A, Hawk R, Gonzalez-Serricchio A, Dixson A, Chow E, Gonzales C, Leung HY, Solomon I, Bronner-Fraser M, Megason SG, Fraser SE. 2011. A versatile gene trap to visualize and interrogate the function of the vertebrate proteome. *Genes Dev*. 25(21):2306-20.

Tu CT, Yang TC, Tsai HJ. 2009. Nkx2.7 and Nkx2.5 function redundantly and are required for cardiac morphogenesis of zebrafish embryos. *PLoS One*. 4(1):e4249.

Trinh LA, Stainier DY. 2004. Fibronectin regulates epithelial organization during myocardial migration in zebrafish. *Dev Cell*. 6(3):371-82.

Uchida N, Hanawa H, Yamamoto M, Shimada T. 2013. The chicken hypersensitivity site 4 core insulator blocks promoter interference in lentiviral vectors. *Hum Gene Ther Methods*. 24(2):117-24.

Wakimoto H, Kasahara H, Maguire CT, Moskowitz IP, Izumo S, Berul CI. 2003. Cardiac electrophysiological phenotypes in postnatal expression of Nkx2.5 transgenic mice. *Genesis*. 37(3):144-50.

Walsh EC, Stainier DY. 2001. UDP-glucose dehydrogenase required for cardiac valve formation in zebrafish. *Science*. 293(5535):1670-3.

Wang J, Panáková D, Kikuchi K, Holdway JE, Gemberling M, Burris JS, Singh SP, Dickson AL, Lin YF, Sabeh MK, Werdich AA, Yelon D, Macrae CA, Poss KD. 2011. The regenerative capacity of zebrafish reverses cardiac failure caused by genetic cardiomyocyte depletion. *Development*. 138(16):3421-30.

Wang J, Karra R, Dickson AL, Poss KD. 2013. Fibronectin is deposited by injury-activated epicardial cells and is necessary for zebrafish heart regeneration. *Dev Biol.* 382(2):427-35.

Wang Z, Dai M, Wang Y, Cooper KL, Zhu T, Dong D, Zhang J, Zhang S. 2014. Unique expression patterns of multiple key genes associated with the evolution of mammalian flight. *Proc Biol Sci*. 281(1783):20133133.

Weeke-Klimp A, Bax NA, Bellu AR, Winter EM, Vrolijk J, Plantinga J, Maas S, Brinker M, Mahtab EA, Gittenberger-de Groot AC, van Luyn MJ, Harmsen MC, Lie-Venema H. 2010. Epicardium-derived cells enhance proliferation, cellular maturation and alignment of cardiomyocytes. *J Mol Cell Cardiol*. 49(4):606-16.

Wiedenheft B, Sternberg SH, Doudna JA. 2012. RNA-guided genetic silencing systems in bacteria and archaea. *Nature*. 482(7385):331-8.

Wienholds E, Schulte-Merker S, Walderich B, Plasterk RH. 2002. Target-selected inactivation of the zebrafish rag1 gene. *Science*. 297(5578):99-102.

Yahata K, Maeshima K, Sone T, Ando T, Okabe M, Imamoto N, Imamoto F. 2007. cHS4 insulator-mediated alleviation of promoter interference during cell-based expression of tandemly associated transgenes. *J Mol Biol.* 374(3):580-90.

Yannaki E, Tubb J, Aker M, Stamatoyannopoulos G, Emery D W. 2002. Topological constraints governing the use of the chicken HS4 chromatin insulators in oncoretrovirus vectors. Molecular Therapy 5:589-598.

Yao S, Osborne CS,Bharadwaj RP, Pasceri P, Sukonnik T, Pannell D, Recillas-Targa F, West AG, Ellis J. 2003. Retrovirus silencer blocking by the cHS4 insulator is CTCF independent. *Nucleic Acids Research.* 31(18): 5317-5323.

Yelon D, Ticho B, Halpern ME, Ruvinsky I, Ho RK, Silver LM, Stainier DY. 2000. The bHLH transcription factor hand2 plays parallel roles in zebrafish heart and pectoral fin development. *Development.* 127(12):2573-82.

Yin VP, Lepilina A, Smith A, Poss KD. 2012. Regulation of zebrafish heart regeneration by miR-133. *Dev Biol*. 365(2):319-27.

Yonei-Tamura S, Tamura K, Tsukui T, Izpisúa Belmonte JC. 1999. Spatially and temporally-restricted expression of two T-box genes during zebrafish embryogenesis. *Mech Dev*. 80(2):219-21.

Zhang R, Han P, Yang H, Ouyang K, Lee D, Lin YF, Ocorr K, Kang G, Chen J, Stainier DY, Yelon D, Chi NC. 2013. *Nature*. 498(7455):497-501.

Zhao L, Borikova AL, Ben-Yair R, Guner-Ataman B, MacRae CA, Lee RT, Burns CG, Burns CE. 2014. Notch signaling regulates cardiomyocyte proliferation during zebrafish heart regeneration. *Proc Natl Sci USA*. 111(4):1403-8.

Xiao Y, Gao M, Gao L, Zhao Y, Hong Q, Li Z, Yao J, Cheng H, Zhou R. 2016. Directed Differentiation of Zebrafish Pluripotent Embryonic Cells to Functional Cardiomyocytes. *Stem Cell Reports*. Sep 13;7(3):370-82.